Yearbook

2015

Institute of Technical Physics and Materials Science

http://www.mfa.kfki.hu/

Hungarian Academy of Sciences
Centre for Energy Research

Institute of Technical Physics and Materials Science

Director: Prof. István Bársony, corr. member of HAS

Address: Konkoly-Thege Miklós út 29-33,
H-1121 Budapest, Hungary
Postal: P.O.Box 49, H-1525 Budapest, Hungary
Phone: +36-1-392 2225
Fax: +36-1-392 2226
E-mail: info@mfa.kfki.hu
URL: http://www.mfa.kfki.hu/

MTA EK MFA Yearbook 2015

Editor: Csaba S. Daróczi
Published by: MTA EK MFA, Budapest, Hungary, 2015

CONTENT

DIRECTOR'S FOREWORD

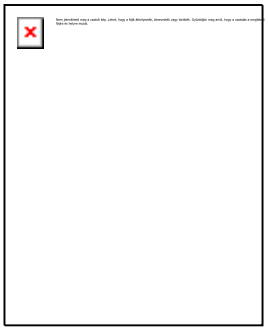

Struggling to survive a difficult year of adaptation… the Institute of Technical Physics and Materials Science in 2015 completed the first year as administratively part of the Centre for Energy Research (EK). We can call ourselves fortunate because of the timely escape from the large centralised organisation of the Research Centre for Natural Sciences (TTK), which in 2015 effectively was declared bankrupt, reporting a huge loss of funds due to mismanagement and bad operation. The long-sought decision of the Presidium of the HAS to detach MFA from that Centre in 2014 meant at the same time to integrate MFA administratively into the current Centre (EK) operating on the KFKI Campus. Based on the experience of a year of marriage we can summarise: this integration became a multicultural approach. The predecessor of the EK centre was established as an engineering-type backup of the Hungarian nuclear power plant in Paks, maintaining special skills and stand-by R&D services next to training activities. "Academic type research", according to the criteria of which the performance of MFA is evaluated in the research network of the HAS, was only a minor part of the EK centre's activity, which drastically changed with the forced integration of MFA. This imbalance is also expressed in the number and qualifications of researchers in fission-related and materials research. The difference in types of activities, or research cultures, obviously requires a different administrative treatment. While the nuclear-type projects mostly have mid-term financing stability owing to well-funded engineering development contracts, materials research at MFA has to collect its funding from a large number of international and national collaborative projects prone to severe EC restrictions in reporting and accounting. While the large experimental nuclear facility historically enjoys substantial dedicated funding from the HAS for its operation as a European research facility, the large microtechnology infrastructure of MFA receives no central subsidy whatsoever. Therefore, the latter research activity requires large flexibility in management and administration to cope with the chronic lack of resources, to create motivation for the researchers to initiate projects and partnerships in research consortia and industrial collaborations.

So far, just the opposite happened as it turned out. The expected „unification of standards and regulations" (in research and administratively, e.g. wage levels, bonuses, etc.) in both parts of the expanded centre was not even attempted. Instead, the director-general and the administrative director, bearing full responsibility for the operation of the centre, did not delegate any, even minor, responsibility and competencies for the director of MFA. As everything requires the signature of the director-general and, more importantly, the approval of the financial director, the MFA director's function became just symbolic in this atmosphere of distrust. The

centre management did not consider it important to involve the research leaders of the institute in strategic or operative decisions; so far, even upon request, no regular information is being provided about the financial situation in individual projects, support received, scheduling of MFA procurements, payment of bills, liquidity of the institute as a whole despite many promises. In order to signal these anomalies to the elected leaders of the Academy, in summer 2015 one of our department leaders volunteered to submit a formal application for the position of the director-general, in which he openly criticised the malfunctioning of the management. The Presidium, however, prolonged the assignment of the present director-general for another five years.

Even in these difficult circumstances MFA in 2015 again recorded a successful year, marked by excellent scientific results and accomplishments, as presented in this booklet.

We only can hope that the survey and fine-tuning of the current centralised research network announced by the President of the HAS will result in a more democratic, transparent and efficient regime in the research centres. The advocated restoration of most of the "freedom of action" enjoyed still five years ago, is hopefully going to ease the life of the new MFA leadership under my successor.

When becoming the director of the at that time independent Research Institute for Technical Physics and Materials Science in 2004 I had a clear vision about the midterm research strategy and goals and how to achieve them. In my application for the assignment I built upon the SWOT analysis of the Institute and defined the major priorities for materials research at MFA: *a complete nanoscience and –technology focus; more opening towards biology to enhance multi-disciplinarity; improve the scientific qualification of researchers; and drastically reverse the age-distribution of the staff.*

After twelve years one can state with satisfaction that most of those targets could be achieved. Although the socio-economic landscape world-wide, in the country and within the Academy changed a lot, MFA had a prosperous decade, before having been forced under centralised administrations. The Institute still works under the Quality assurance system ISO 9000-2008. The annual MFA Yearbooks published in English document the history of development of „MFA as a research community" (available in print and electronically at http://www.mfa.kfki.hu/hu/yearbook).
The scientific part is a summary of most important research results from the previous year, as presented at the end of January each year on the annual „scientific reporting day" of MFA, where the opinion of external reviewers - mainly from prospective co-operating institutions - is also asked for. The Yearbooks also give an account of successful initiatives, like the "**MFA Summer School**" for high school children from the Carpathian Basin, team-building events like the yearly „**MFA-Day**", the "**Christmas celebration"**, and the raising of awareness for our research in different popular actions, which in the meantime were adopted also by others. These occasions

provided the forum for motivation of our staff by handing out the **„MFA Prize" in three categories** and the **"MFA Prize for Excellent Research Support"**, as well as the title "**Professor emeritus instituti**" for our retired scientific advisors. Whenever it was possible, colleagues of our institute were promoted and recommended for distinction by the HAS and by various national awards.

Just to mention a few representative figures from the last 12 years:

At least **8 new laboratories** were built for the novel research activities started, and all the other laboratories and working cabinets were completely renovated, the furniture replaced and modernised, and the research equipment updated depending on availability of resources. MFA successfully guided **47 students to the degree of Ph.D.** with **23 more on the way**, the title of **Dr. of HAS (D.Sc.) was achieved by 15 of our colleagues,** and **two became corresponding members of the HAS**! These achievements earned for our institute respect and appreciation in the academic community expressed also by the **Széchenyi Prize** awarded to the director in 2015. **MFA as mosaic-word became a brand not only in Hungary, but also Europe-wide in our field of activity**. What is most important, it constitutes **a solid scientific base for the future of research of functional materials in Hungary**.

When relinquishing the director's function, held for over 12 years, in the summer 2016, I have to thank all of my co-workers, especially my fellow research leaders, for their excellent collaboration. I wish the new generation mastery in all future challenges with bright new ideas and initiatives, by maintaining the MFA team spirit I was fortunate to experience.

Budapest, March 1st, 2015

István Bársony

GENERAL INFORMATION

Organisation of MFA

Director	- ***István BÁRSONY***

Scientific Departments	
Nanostructures Department	- *László Péter BIRÓ*
Thin film physics Department	- *Béla PÉCZ*
Complex Systems Department	- *György SZABÓ*
Photonics Department	- *Miklós FRIED*
Microtechnology Department	- *Gábor BATTISTIG*
Lendület group - NanoBioSensorics	- *Róbert HORVÁTH*
Lendület group - 2D Materials	- *Levente TAPASZTÓ*

Directly supervised functions	
Head of Scientific Advisory Council	- *János LÁBÁR*
Scientific secretary, projects and PR	- *Krisztina SZAKOLCZAI*
Quality control, MTMT, REAL admin	- *Andrea BOLGÁR*
Technical support	- *Károly BODNÁR*
Deputy financial group leader	- *Zsuzsa KELEMEN*
Informatics	- *Gergely TAMÁS*
Technology transfer (IPR)	- *Antal GASPARICS*

Key Financial Figures

The turnover realised by the institute in the last 12 years provides a good overview about the evolution of the economical-societal circumstances around research and development at an academic research institute, reflected by the composition of the source of income, and the changes therein: the decrease of the central subsidies, the role of international grants prone to the periodicity in the European Commission's and project support schemes, the situation in the domestic R&D financing (largely bound to the EU cohesion- and structural funds), and the contract research - characteristic for the industrial landscape in the country.

Until 2012 MFA was operating as an independent entity with a staff of 130, including completely independent, but competent administration. All decisions were taken in reasonable time and there was considerable freedom of decision granted to the director having full responsibility for his decisions. *The integration wave in the research network of the HAS started from 2012.*We lost our independence becoming part of the 650 strong Research Centre for Natural Sciences (TTK). The increasing costs of central administration meant parallel an operation of larger inertia, leading to the drop in the performance of the same scientific staff. The decision of the Presidium of the HAS taking MFA out of TTK and forcing it to integrate into the Centre for Energy Research (EK) saved us from suffering by the bankruptcy of TTK, which became obvious by early 2016. In the new host centre from 2015, due to the non-transparent decision making and inefficient handling of our administration did not improve much on our financial situation. By the lack of communication and information flow, not to speak about the absence of trust as well as delegation of competencies and responsibilities we do not have even access to authentic figures; the data for 2015 are based upon our own estimates.

MTA EK MFA 2015 Budget Totals in Million HUF

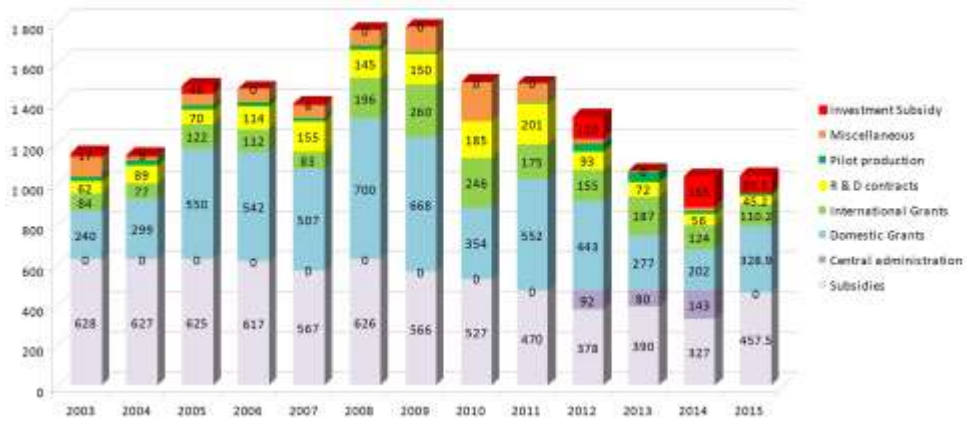

MTA EK MFA 2015 restoration and investment spendings in Million HUF

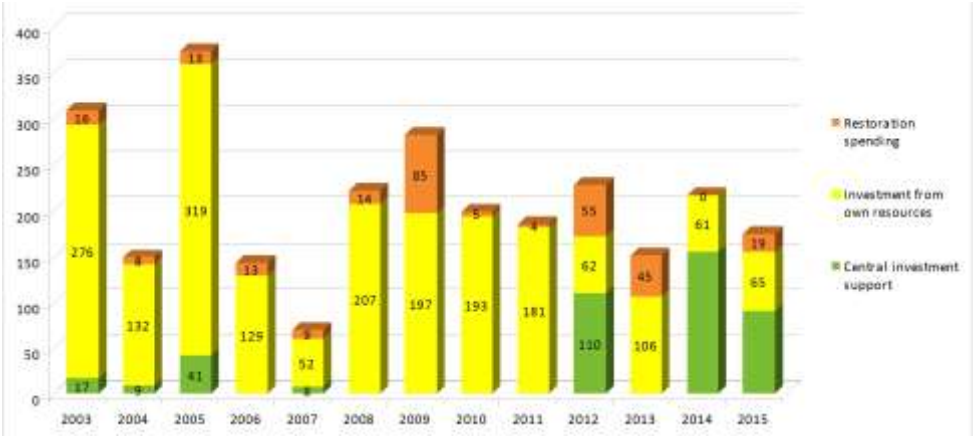

We are confident that *the 2015 figures reflect only a fraction of the performance, MFA would be able to offer*, provided a the young colleagues could be motivated to enter more international and national collaborations, submit more proposals, and risk much more endeavours with the industry.

Publications & Citations

Regarding scientific output, MFA produced a yearly average of 95-100 publications, while continuously improving the record for citations.

MFA and its predecessors' publications

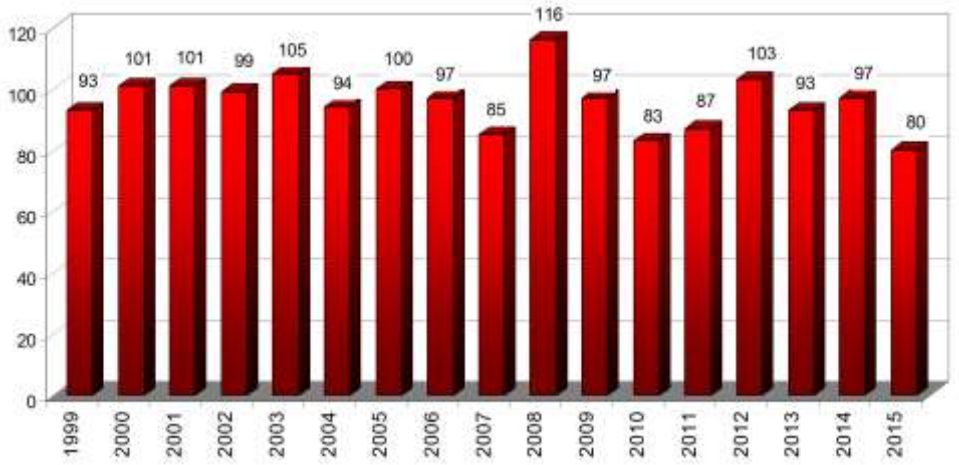

This was the case also in 2015, albeit the number of published papers in the calendar year dropped to 80. This is on one hand caused by submission and evaluation delays; on the other hand it reflects the complex administration problems we were prone to. There is a remarkable trend to go for publications in higher profile periodicals hoping for further significant improvement in the number of citations.

MFA and its predecessors' citations

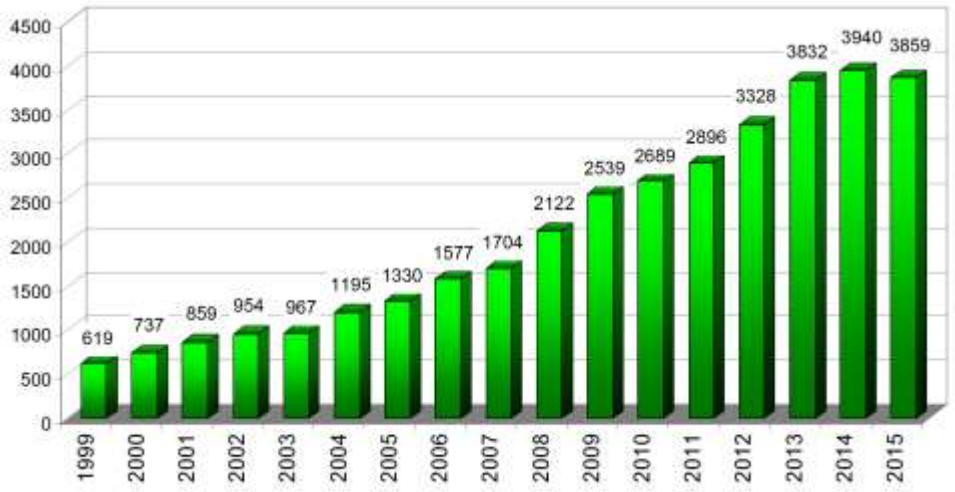

Awards & Distinctions

	**BÁRSONY, István**	Széchenyi Prize by the President of Hungary Distinguished Honorary Professorship by the National Institute of Technology, Toyama College, Japan
	**SZABÓ, György**	Commander's Cross, Order of Merit of the Republic of Hungary
	**DÜCSŐ,Csaba**	Knight's Cross, Order of Merit of the Republic of Hungary
	**LOHNER, Tivadar**	ELFT Medal of the Roland Eötvös Physical Society
	**BARNA, B. Péter**	R. F. Bunshah Award of the International Conference on Metallurgical Coatings and Thin Films for his lifetime achievements
	**VONDERVISZT, Ferenc**	Golden Prize of the Veszprém Chapter of the Hungarian Academy of Sciences
	**SZOLNOKI, Attila**	„Outstanding Referee” award from Physica A
	**FÜRJES, Péter**	MedinProt Synergy Research Program (2014-2015) award

	**BALÁZSI, Katalin**	Bolyai Plaquette of the Hungarian Academy of Sciences
	**HORVÁTH, Róbert**	MFA Prize (Researcher)
	**LUKÁCS, István Endre**	MFA Prize (Postdoctoral)
	**OLÁH, Nikolett**	MFA Prize (Ph.D. student)
	**ILLÉS, Levente**	MFA Prize for Excellent Science Support
	**MENYHÁRD, Miklós**	Prof. Emeritus of the Hungarian Academy of Sciences
	**GAÁL, István**	Professor Emeritus Instituti MTA EK MFA
	**SZENTPÁLI, Béla**	Professor Emeritus Instituti MTA EK MFA
	Sotomi ISHIHARA	MFA prize for fostering a fruitful co-operation between KOSEN Toyama College and MFA in various fields of S&T
	Stefan LUBY	MFA prize for promoting the co-operation between our institute and the institutes of the Slovak Academy of Sciences

HIGHLIGHTS

Wafer-scale integration of piezoelectric nanowires

(EU FP7 collaborative project 611019: PiezoMAT[1])

I. E. Lukács, N.Q. Khánh, R. Erdélyi, Zs. Baji, G. Battistig, and J. Volk

The EU project PiezoMAT proposes new technologies of high-resolution fingerprint sensors based on a matrix of interconnected piezoelectric nanowires (NWs). One of the three targeted chip concepts was realized by the MFA team. Here the integrated free standing vertical NWs are contacted individually at their stock with two metal wires to detect piezoelectricity induced signals between tensed and compressed sides of the NWs upon bending. As it was found by finite element analysis a nearly constant positive/negative stress is built up in the outer/inner side of the NW upon bending it by a lateral loading force directing to its tip (Figs. 1a and b). In contrast, the induced piezoelectric potential has a strong maximum at the bottom of the NW (Fig. 1c). The aim of this sensor concept is to detect this enhanced electrical signal with a pair of metal electrodes contacting the opposite sides of the NWs at their roots. Moreover, with an array of vertically integrated NWs, the distribution of the loading force can also be detected at a very high (>5000 dpi) lateral resolution.

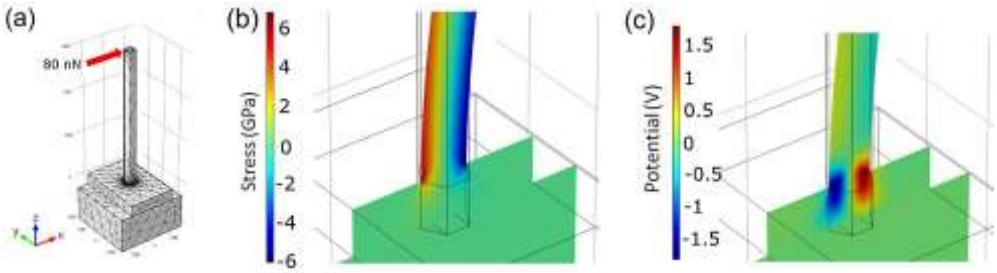

Figure 1 *Finite element analysis of NW/seed layer/substrate assembly showing the ideal meshing by triangular elements (a), cross-section of the* τ_{zz} *component of the mechanical stress (b), and the electric potential distribution (c) for the bottom part of the bent NW at a loading force of 80 nN.*

The optimization of the fabrication procedure was carried out through three stages, at first on small (10 mm × 10 mm) sapphire dices, then on 3" sapphire wafer, and at last on 3" Si wafer. The aim of the sapphire wafer is to realize 'ideal' monocrystalline ZnO NWs on epitaxial ZnO seed layer, whereas that of the Si wafer is to demonstrate

[1] FP7-ICT-2013-10- 611019 - High-resolution fingerprint sensing with vertical piezoelectric nanowire matrices (PiezoMAT), www.piezomat.eu

and test the feasibility of the process on standard Si technology. The optimized process flow consists of more than 25 technological steps, including five electron beam lithography (EBL) alignments. Hence the new Raith 150 EBL system of MFA (Fig. 2), enabling wafer scale processing of sub-20 nm sized patterns, played an essential role in this project. The fabrication process of the wafer had several challenges to be solved, such as the accurate (<50 nm) alignment of the EBL patterns; high quality metal lift-off process after EBL and photolithography; sample charging during EBL; mesa etching of ZnO seed layer; as well as the protection of ZnO mesa island against unwanted etchings.

Figure 2 *Raith 150 electron beam lithography system enabling nanopatterning of full wafers up to 6"-diameter.The system was successfully installed this year in the clean room of MEMS department and is being used in several projects.*

The processed 3" Si wafer holds several chips (Fig. 3a) each of them having an active sensor array of 8 × 8 individually contacted NWs in the center (Fig. 3b). Due to the

high quality ZnO seed layer deposited at the University of Leipzig (ULEI) the ZnO crystals show an excellent c-axis orientation even on the non-lattice matched SiO_2 covered Si wafer. Nevertheless these NW transducers are polycrystalline (Fig. 3d) in contrast to the ones grown on epitaxial ZnO/sapphire substrate (Fig. 3c). High resolution SEM images revealed that the piezocrystals were positioned to the readout contacts with sub-50 nm precision throughout the whole wafer (Fig. 3e).

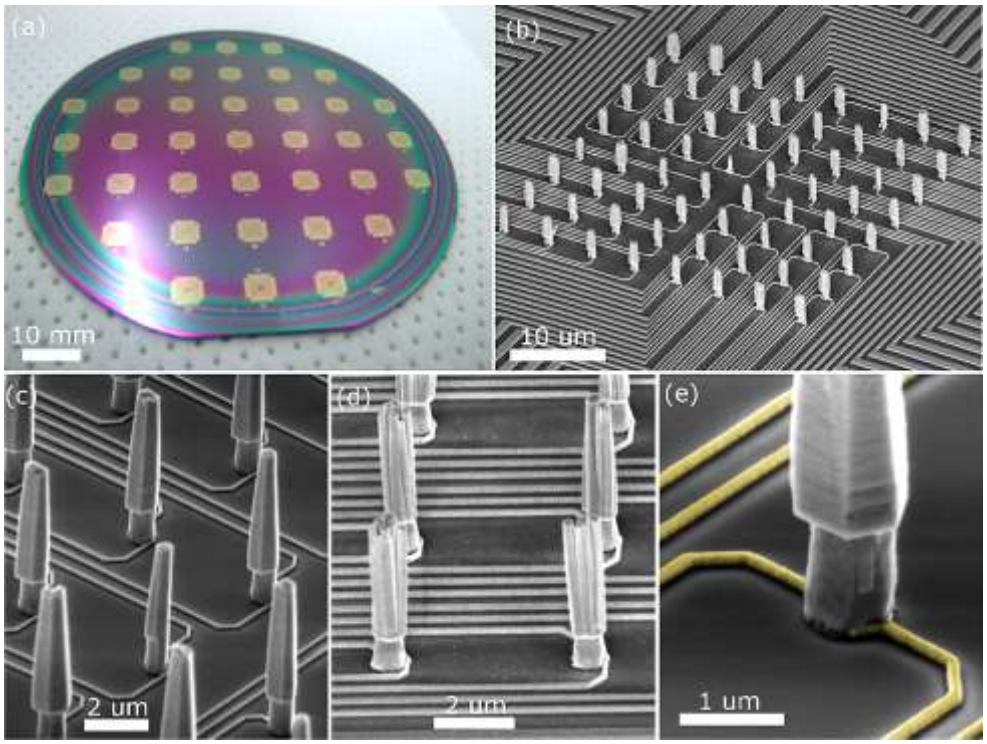

Figure 3 *On-chip integrated piezoelectric NWs. (a): Photo of Si wafer with NW chips, (b): SEM image of the 8 × 8 NW array, (c and d, respectively): comparison of contacted ZnO NWs grown on sapphire and Si substrate, (e): high magnification SEM image of the contacted ZnO crystal where the read-out Au electrical lines are colored with yellow.*

The electrical connections were verified by current-voltage (I-V) measurements using a probe station and negligible crosstalk was found between the separate circuits. The integrated NW chips are thus ready for the electromechanical characterizations which will be carried out in two main steps. At first bending experiments will be done on individual ZnO crystals with AFM and SEM micromanipulator tips in a highly controlled way. It will be followed by parallel detection when the whole array is imprinted with a soft stamp mimicking finger-print detection. Beside the targeted goal of PiezoMAT project, the fabricated chips are planned to be used for other purposes as well (e.g. for in-vitro cell monitoring), where very low lateral forces (1-1000 nN), and small movements are to be monitored in high resolution (>5000 dpi).

Nanoparticle assemblies

D. Zámbó, Sz. Pothorszky, E. Gergely-Fülöp, N. Nagy, and A. Deák

One of the core concept of our work is connected to colloid chemistry, which is essentially the foundation for bottom-up prepared nanostructured, self-assembled systems and processes where nanoscale objects are involved. Our group is engaged in research projects targeting the manipulation and assembly of nanoscale building blocks, with envisaged applications in the field of sensorics (SERS), biomedicine (MRI), energy harvesting (thermoelectrics) and lighting (LEDs). Our activity focuses on both physical and chemical aspects of nanoparticle systems. We rely on state-of-the-art wet chemical synthetic procedure to produce nanoparticles with outstanding uniformity. Physico-chemical and structural characterization of the particles and their structures is also carried out relying on various techniques (TEM, SEM, DLS, various spectroscopy techniques). Computer simulations are also essential part of our activity, boundary and finite element methods are implemented for the simulation of the frequency dependent optical or thermal properties of the nanosystems.

1. Colloidal template based nanostructures

Interfacial assembly of micron and sub-micron particle has been used to produce high quality mono- and multilayers on various substrates using the Langmuir-Blodgett method, that allows the preparation of macroscopic samples (Fig. 1a). These samples are used by us and several other groups at the institute as well to implement different nanostructuring strategies. In a recent work it was demonstrated that such a structure can enable preparation of plasmonic crystal monolayers (Fig. 1b). When a monolayer of template particles is partially replicated in a polymer film and uniformly coated with gold, incident angle and wavelength dependent spectral features (absorption bands) arise (Fig. 1c). The bands are associated with excitation of localized and propagating plasmon modes at the surface, that is, high local electromagnetic fields are generated in the near-field of these structures. This in turn could be used in sensing

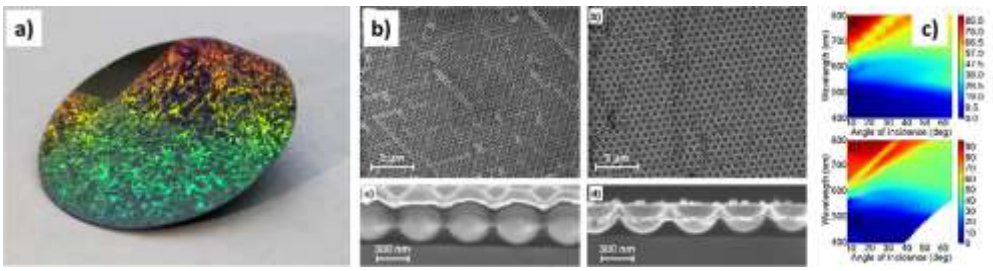

Figure 1 *(a): 3" wafer covered by two partially overlapping (rotated by 90°) monolayer of 500 nm polystyrene particles. (b): Plasmonic crystal prepared by the partial immersion and/or removal of the template layer. (c): Measured (top) and simulated (bottom) Incident angle and wavelength dependent reflection spectrum. The angle-dispersive absorption band can be associated with the propagating Bragg plasmon mode.*

and energy harvesting applications to boost the absorption of optically active species, leading to higher sensitivity or improved photon energy conversion efficiency, respectively.

These template monolayers, on the other hand, can also be used as a template to direct the assembly of smaller sized nanoparticles. When a solution of nanoparticles is drop casted over the monolayer and allowed to dry, necklace-like structures can be obtained (Fig. 2). The process relies on the delicate interplay between colloidal and capillary interactions. Additionally, control over the dewetting of such a high pattern-density impregnated structure is also desirable for the successful implementation of such a massively parallel directed assembly of the nanoparticles. Thanks to the plasmonic properties of the assembled nanoparticles, their necklace structure support coupled plasmon modes, that can be exploited for the enhancement of the Raman scattering signal of analytes.

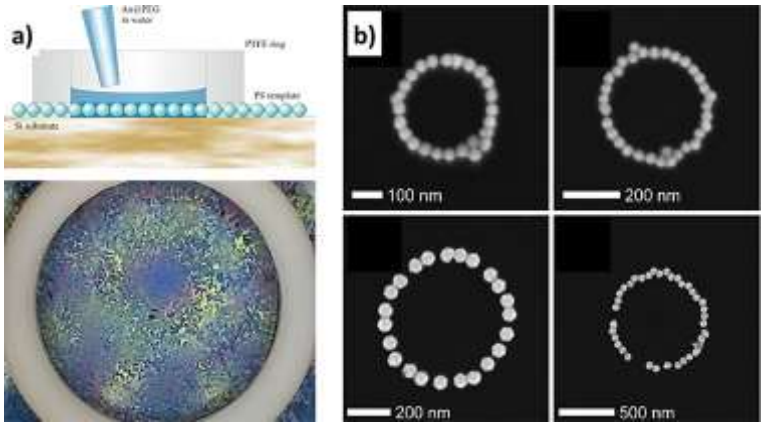

Figure 2 *(a): Nanoparticle 'necklace' structures preparation by the controlled dewetting of a nanoparticle solution over at a template monolayer. (b): Depending on the template diameter, rings with different diameters could be obtained.*

2. Nanoparticle assemblies based on interaction-potential engineering

Assembling nanoparticles into certain structures often results in enhanced or new emerging properties. Assemblies prepared from noble metal nanoparticles can find applications in sensorics, while their hybrid assemblies with luminescent particles (e.g., perovskites) can allow improved light management in absorbing and emitting devices (solar cells, LEDs). Assemblies of magnetic nanoparticles can allow achieving higher contrast in MRI imaging. For the successful preparation of

nanoparticle assemblies, extensive knowledge about the (colloidal) particle-particle interaction. This is necessary to identify the factors that allow control over the assembly process. These factors on the other hand, depend on the specific material system (type of nanoparticle, surface coating, desired structure, etc.) and hence require proper engineering of the process from the very beginning. With two recent examples we have shown how implementation of such a holistic approach enables the preparation of compact nanoparticle clusters consisting of hundreds of nanoparticles (Fig. 3), and site-selective directed assembly of single nanoparticles (Fig. 4).

Polyethylene glycol grafted on the nanoparticle surface renders the particles extremely stable against aggregation due to steric repulsion. At increased ionic strength of the medium, however, the polymer chains collapse, that – together with the attractive contribution from the van der Waals interaction – allows to achieve a soft-sphere type interaction with moderate well-depth (Fig. 3a). According to theory, these latter two characteristics are required for the preparation of compact nanoparticle clusters. Dynamic light scattering experiments (Fig. 3b) and electron microscopy images (inset in top panel) confirm the successful preparation of the nanoparticle clusters.

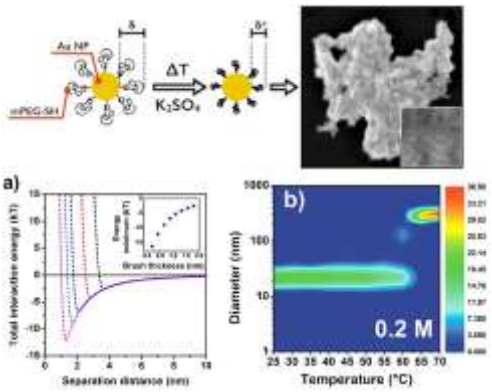

Figure 3 *Thermally activated clustering of gold nanoparticles (see main text for details.*

When region-selective surface modification of nanoscale object is achieved, it can allow high-precision localization of other small particles, as we have shown recently. By selectively rendering the tips of gold nanorods positively charged while coating the sides of the nanorods with a high molecular weight polymer, tip selective localization of 20 nm gold particles could be achieved (Fig 4a). As the size ratio between a nanorod and the assembled particle is changed, however, the structure changes into a single nanoparticle assembled at the side of nanorods (Fig. 4b). This intriguing finding can be explained by carefully analyzing colloidal interactions involved in the process, and would allow a more rational design of patchy colloids for nanoparticle networks and complex nanoparticle assemblies.

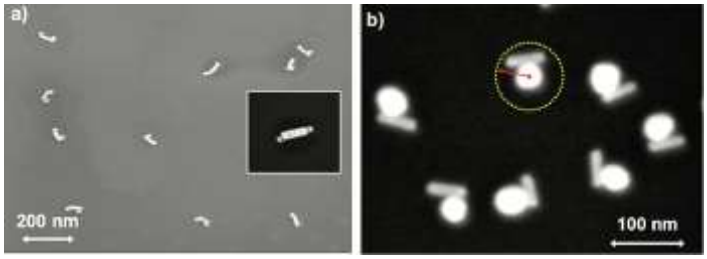

Figure 4 *(a): Patchy nanorod (tip: cysteamine; side: polyethylene glycol) assembled with negatively charged 20 nm god spheres. (b): As the relative size of the sphere increases, side selective assembly prevails.*

NOTABLE EVENTS

Acknowledging his decade-long research and scientific results in the field of micro/nanotechnology as well as his excellent direction of the Institute of Technical Physics and Materials Science of the HAS, the director of the institute obtained on March 15, 2015 from the president of state in the Parliament the ***Széchenyi Prize****.*

The biannual meeting and workshop of the World Materials Research Institute Forum was held in May 2015 at the Lawrence Livermoore Laboratory, US, where MFA, as partner institution was represented by János Volk.

The „International Year of Light" was celebrated in August 2015 by a special session, organised by MFA's ***Dr. Miklós Serényi*** *with participation of the Hungarian scientific coordinator of the events,* ***Prof. Norbert Kroó****. The main speaker was* ***Dr. Kaenders*** *from the world leading optical firm, TOPTICA in Germany.*

*A scientific highlight of the year was the visit of **Prof. Hiroshi Amano**, Nagoya University, one of the Nobel-Laureates for the development of the blue-LED. Prof. Amano, a real modest and polite scientist delivered a nice talk on the progress of III-V nanodevices for a very interested audience, and had a chat with top scientists of our institute on November 5 2015.*

In October a successful „International Workshopon on 2D materials" was organized by the participants of the Korea-Hungary Joint Nanolaboratory, headed by ***Dr. Levente Tapasztó*** *and* ***Prof. László P. Biró*** *of MFA, and* ***Dr. Chanyong Hwang*** *(RISS, Korea).*

In September 2015 in Freiburg, Germany, the EUROSENSORS trophy was passed by the chair ofthe EUROSENSORS 2015 conference, ***Prof. Gerald Urban*** *to the designated general chair of the next conference.* ***Prof. István Bársony*** *is to organise the 30th anniversary event in Budapest from September 4-7, 2016 under the auspices of the Engineering Chapter of the Hungarian Academy of Sciences.*

PUBLIC OUTREACH


The traditional MFA-Day was held in early June at splendid weather with about 180 guests all participating in cooking on open fire and enjoying sports, children's joy and each-other's company with current and past colleagues and families.





*Raising awareness for the activity of researcher in the natural science field was the event "**Researcher's Night**" in September 2015. The children are instructed by **Dr. Orsolya Tapasztó.***

*The **Summer School** was organised for 23 high school children of age 16-17, selected from the Hungarian schools of the Carpathian basin. Next to research also a program for spending their free time by sports, sight-seeing and different other attractions were compiled by **Csaba S. Daróczi** already the 8th time in 2015 in this traditional event.*

*Farewell party for **Magdolna Erős** (in the centre). Following four decades of excellent laboratory-work in the clean-room of the Microtechnology Department she retired and also obtained the **Distinction of the Secretary General of the HAS**.*

*We could not anticipate, that this will be the last occasion to meet **Éva Vázsonyi** (third from left in the front row), who deceased end of March 2016.*

SCIENTIFIC REPORTS

Nanostructures Laboratory

Head: Prof. László Péter BIRÓ, corresp. member of the HAS

Research Staff

- Zsolt Endre HORVÁTH, Ph.D., Deputy Head of Laboratory
- Prof. József GYULAI, Member of the HAS (Professor Emeritus)
- Antal Adolf KOÓS, Ph.D.
- Géza István MÁRK, Ph.D.
- Zoltán OSVÁTH, Ph.D.
- Krisztián KERTÉSZ, Ph.D.
- Péter NEMES-INCZE, Ph.D. (on leave)
- Enikő HORVÁTH, Ph.D. (on leave)
- Gergely DOBRIK, Ph.D.

Ph.D. students / Diploma workers

- Péter Lajos NEUMANN, Ph.D. student (on leave/left)
- Gábor PISZTER, Ph.D. student
- András PÁLINKÁS, Ph.D. student
- Zsófia JUHÁSZ, diploma worker

2D Nanoelectronics „Lendület" Research Group

Group Leader

- **Levente TAPASZTÓ, Ph.D.** (Head of the Nanostructures Lab since 1st December 2015)

Ph.D. students / Diploma workers

- Péter VANCSÓ, Ph.D. student
- Gábor MAGDA, Ph.D. student
- Péter KUN, Ph.D. student
- János PETŐ, diploma worker

The Nanostructures Laboratory has an almost two decade expertise in the production and characterization of various nanostructures. Recently in the focus of our work were various 2D nanostructures (graphene, h-BN, few-layer graphite and TMDCs), their nanoarchitectures, bioinspired photonic nanoarchitectures and applications of these nano-objects in various fields of nanotechnology, nanoelectronics and sensorics.

- A novel cleaving procedure was developed, which allows production and atomic scale characterization by STM/STS of large area TMDCs flakes.
- Moire type superstuctures were investigated in detail which appear between CVD graphene and HOPG for the full range of misorientation angles from 0° to 30°.
- Hybrids of CVD graphene and Au nanoparticles were produced and revealed was SERS effect of significant magnitude.
- Structural color of two Lycaenid butterfly species were detected and shown were the consequently different prezygotic mating strategies, which exhibit similar scatter around the mean value, but the average intensity of the coloration is related with the mating strategy.

For more details, please feel free to visit the web page of the Nanostructures Laboratory: (http://www.nanotechnology.hu/)

Exfoliation of large-area transition metal chalcogenide single layers

(Lendület2014-14, KHJLN,OTKA-K 10875, OTKA 101599)

G. Z. Magda, J. Pető, G. Dobrik, C. Hwang (KRISS), L. P. Biró, and L. Tapasztó

Layered transition metal chalcogenides (TMCs) display strong intra-layer metal-chalcogenide bonds, and a weak inter-layer bonding between neighboring planes of chalcogenide atoms. The recent interest in studying their two-dimensional (2D) form (consisting of triple to quintuple atomic sheets) is driven by the fact that the properties of atomically thin crystals can drastically differ from their well-characterized bulk counterparts. An eloquent example is the transition in the MoS_2 band structure from indirect to direct band gap as the number of layers is reduced from bulk to a single layer, opening the way towards optoelectronic applications. Furthermore, the family of transition metal chalcogenides is large, covering a broad range of properties from semiconductors (MoS_2, WSe_2) to semimetals (TiS_2, $TiSe_2$), from topological insulators (Bi_2Te_3, Bi_2Se_3) to correlated materials (NbS_2, $NbSe_2$). Such large variety of properties holds a huge potential for both fundamental studies and applications, even graphene cannot compete with in spite of the unique versatility of its properties.

The easy access to large TMC single layers is of key importance for exploring their properties, in a similar manner as the facile isolation of large and high-quality graphene flakes enabled the outstanding pace of the graphene research. As several bulk TMC crystals are layered materials, similar to graphite, individual TMC layers can be isolated by mechanical exfoliation ("scotch-tape" technique). Compared to other methods, mechanical exfoliation provides 2D TMC sheets of high structural quality enabling the fundamental study of their pristine properties, and ultimate device performance, similar to graphene, where most of the fundamental discoveries have been achieved on exfoliated samples, owing to their superior structural and electronic quality. The major limitation of the micromechanical exfoliation of various TMC materials is the small yield of single layers and their relatively small lateral size, typically of a few microns, rendering the subsequent investigations and device fabrication more difficult. This lateral size is about an order of magnitude smaller than that of graphene flakes which can routinely be obtained by the same technique. The reason for this probably originates from the unique mechanical strength and ultra-strong adhesion of graphene to SiO_2 that cannot be matched by the otherwise still excellent mechanical properties of TMCs.

We have developed a novel mechanical exfoliation technique that overcomes the limitations of the scotch-tape technique enabling the exfoliation of TMC single layers with lateral size in the range of hundreds of microns. During the mechanical exfoliation process, isolation of single layers is possible because the adhesion of the bottom layer to the substrate becomes stronger than the adhesion to its own bulk crystal. First, thick multilayer flakes had been peeled off from a bulk MoS_2 crystal using a thermal release tape, and these flakes had been placed on the top of the freshly

cleaved gold substrates. We used a short ultrasonic treatment in acetone to remove the thick MoS_2 flakes from the gold surface. We found that after a few seconds of sonication several thick flakes have been detached; however, underneath them, the last (bottom) MoS_2 layer remained attached to the gold substrate.

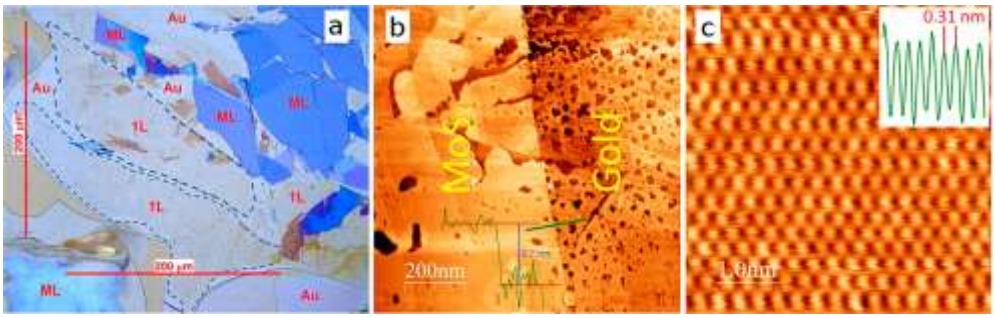

Figure 1 *(a) Optical microscopy image of MoS_2 single layer areas (1L, outlined by dotted lines) with several hundreds of microns lateral size exfoliated on gold (Au 111) substrate. (b) STM image of a MoS_2 single layer exfoliated onto a gold substrate. The line cut displayed was taken along the direction marked by the green line across the edge. (c) Atomic resolution STM image of a MoS_2 single layer revealing a hexagonal lattice corresponding to the crystal lattice of the top sulfur atoms.*

In optical microscopy images the MoS_2 single layers can be identified as the areas of the faintest color contrast as shown in Fig. 1. The optical images revealed several hundreds of micron large areas covered by thin MoS_2 layers. To confirm that these areas of faintest optical contrast are indeed single layers of MoS_2 we have performed confocal Raman spectroscopy measurements. These measurements were indicating that the several hundreds of microns large areas observed by optical microscopy can be identified as MoS_2 single layers. The exfoliated large flakes on top of the conductive Au substrate enabled us to perform Scanning Tunneling Microscopy (STM) measurements on mechanically exfoliated single layer MoS_2 flakes. The height of the investigated layers relative to the Au substrate was found to be about 0.7nm from the STM measurements (Fig. 1b), confirming the single layer thickness of the exfoliated flakes. Atomic resolution images could routinely be achieved even under ambient conditions (Fig. 1c). A hexagonal atomic lattice was revealed with a 3.1Å periodicity, corresponding to the lattice constant of the top layer of sulfur atoms. We have also investigated whether the exfoliation process is specific to MoS_2 or can be applied more generally to various layered materials. We found that our exfoliation method yielding large-area MoS_2 flakes is not specific to molybdenum disulfide or even sulfides, but works equally well for various layered chalcogenides, including selenides and tellurides. Furthermore, in contrast to the standard scotch-tape method, the exfoliation technique reported here is in principle able to achieve high coverage rates of macroscopic substrates with various TMC single layers [78].

Structure and properties of graphene on gold nanoparticles

(EU FP7 Marie Curie CIG No.334377, OTKA-K101599, OTKA-PD-105173)

Z. Osváth, A. Deák, K. Kertész, Gy. Molnár, G. Vértesy, D. Zámbó, C. Hwang (KRISS, Korea), and L. P. Biró

Graphene covered metal nanoparticles constitute a novel type of hybrid materials, which provide a unique platform to study plasmonic effects, surface-enhanced Raman scattering (SERS), and metal-graphene interactions at the nanoscale. Such a hybrid material is fabricated by transferring graphene grown by chemical vapor deposition onto closely spaced gold nanoparticles produced on a silica wafer. The morphology and physical properties of nanoparticle-supported graphene is investigated by atomic force microscopy (AFM), optical reflectance spectroscopy, scanning tunneling microscopy and spectroscopy (STM/STS), and confocal Raman spectroscopy.
Gold nanoparticles were prepared by evaporating a thin gold film of 5 nm onto a 285-nm-SiO2/Si substrate at room temperature. Subsequent annealing was performed at 400 °C in Ar atmosphere for 30 minutes, which resulted in the formation of Au nanoparticles with heights of 15-20 nm and high surface coverage. We transferred graphene grown by chemical vapour deposition (CVD) onto the prepared gold nanoparticles using thermal release tape. Fig. 1a shows a typical AFM image of the transferred graphene which is considerably rippled. Note, that the lower part of the image is not covered with graphene.

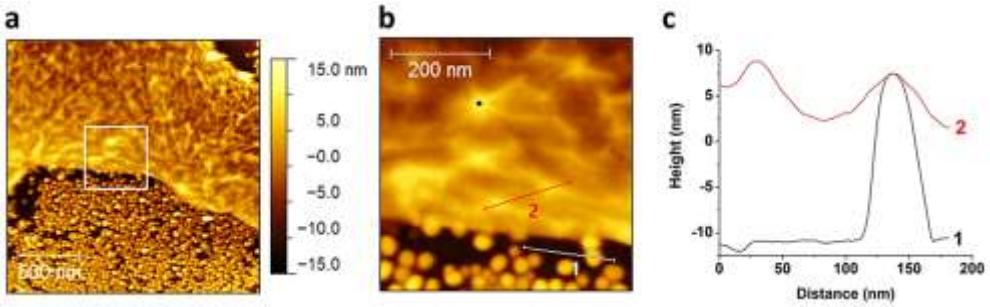

Figure 1 *Tapping mode AFM image of graphene transferred onto Au nanoparticles. The area marked by white square in (a) is presented with higher magnification in (b). The black dot in (b) points out star-shaped rippling centred on the top of the underlying nanoparticle. The height profiles representing the sections 1 and 2 are displayed in (c).*

During the transfer with thermal release tape, the initial large area graphene breaks into smaller sheets with dimensions of several micrometers and not all of them remain attached to the nanoparticles. Fig. 1b is a higher magnification image which corresponds to the white square drawn in Fig. 1a. The height profiles corresponding to the line section *1* and *2* are displayed in Fig. 1c. Line section no. *1* is measured in the area without graphene, showing a typical gold nanoparticle on the SiO_2 surface, with height of 18 nm. On the graphene-covered side, the line section no. *2* displays the wavy shape of the graphene. The peaks in the height profile correspond to

graphene directly supported by nanoparticles, whereas the dip corresponds to graphene bridging two nanoparticles. Comparing the height profiles of line sections *1* and *2*, we find that the graphene part bridging the nanoparticles is located more than 10 nm above the SiO_2 substrate, i.e. it is suspended. In fact, this is a general observation for the transferred graphene: it is suspended between gold nanoparticles.

We investigated the SERS activity of the graphene/gold nanoparticle sample by confocal Raman spectroscopy performed both before and after annealing. Fig. 2a show typical Raman spectra obtained with 488 nm laser on transferred CVD-grown graphene without annealing. Note that there is no significant difference between graphene peak intensities when measured on SiO_2 and on gold nanoparticles, respectively. In contrast, when using the 633 nm laser we observe an almost tenfold enhancement (Fig. 2b) for the graphene G peak (1585 cm^{-1}), as well as 4-fold enhancement for the 2D peak. After annealing at 500 ^oC, these enhancement factors increase to 13 and 22 for the G and the 2D peak, respectively (Fig. 2d). Furthermore, nearly 6-fold peak enhancement is observed with the 488 nm laser also, but only for the 2D peak (Fig. 2c). The higher enhancement at 633 nm laser is due to the fact that this wavelength is closer to the localized surface plasmon resonance of gold nanoparticles (597 nm), where the local electric fields are much more increased compared to the off-resonance at 488 nm [96].

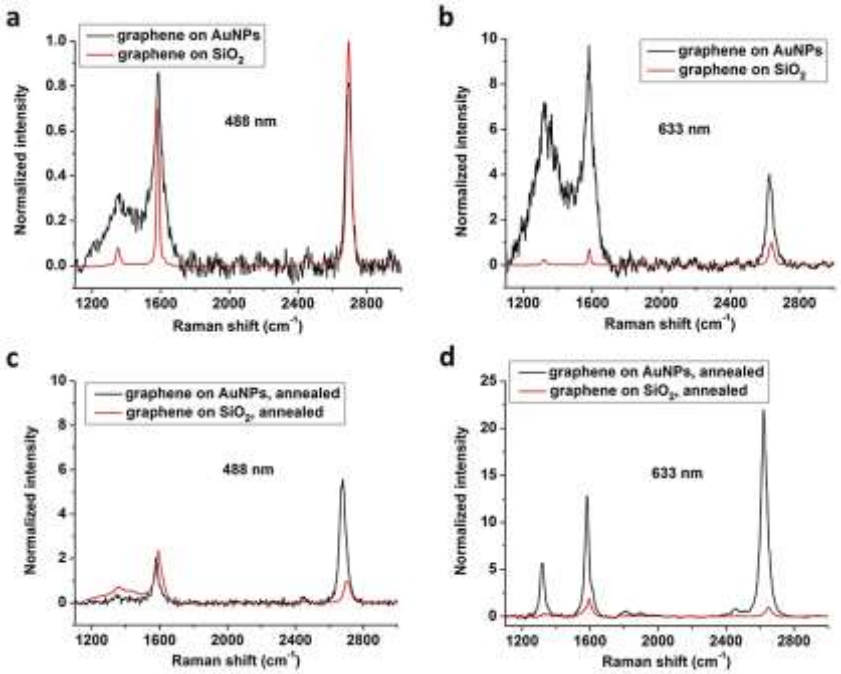

Figure 2 *Raman spectra of graphene transferred onto gold nanoparticles (black line), and of graphene transferred directly onto SiO_2 substrate (red line). All spectra are averaged over areas of 5×5 μm^2 and normalized to the 2D peak height measured on SiO_2.*

Electronic properties of MoS_2 flakes grown on graphite

(János Bolyai Research Scholarship, OTKA K101599, Lendület2014-14, EU REA 334377)

A. A. Koós, P. Vancsó, G. Z. Magda, Z. Osváth, K. Kertész, L. Tapasztó, C. Hwang, and L. P. Biró

Hybrids of 2D materials are expected to become building blocks of next generation high performance nanoelectronic devices, like transistors and sensors. In addition to graphene with zero-gap character, other 2D materials, such as MoS_2 with a direct band gap of 1.9 eV, are really interesting. These materials can complement each other in 2D van der Waals heterostructures, offer a tool to engineer wide range of physical properties and open new possibilities for applications. In order to understand the properties of graphene - MoS2 hybrids, MoS_2 sheets were grown by chemical vapour deposition (CVD) on highly ordered pyrolytic graphite (HOPG). The heterostructures were investigated with Scanning Tunneling Microscopy (STM) and Current Imaging Tunneling Spectroscopy (CITS).

The MoS_2 flakes were triangular (Fig. 1a) and followed the crystallographic orientation of HOPG substrate. The high resolution STM image (Fig. 1b) shows two overlapped periodic structures which form moiré pattern. The smaller 3.16 Å period corresponds to the inter-atomic spacing of S atoms in MoS_2, while the longer 12.5 Å period was caused by the interaction between MoS_2 and HOPG. The 12.5 Å period is nearly 5 times the atomic distance in HOPG, and 4 times in MoS_2, respectively.

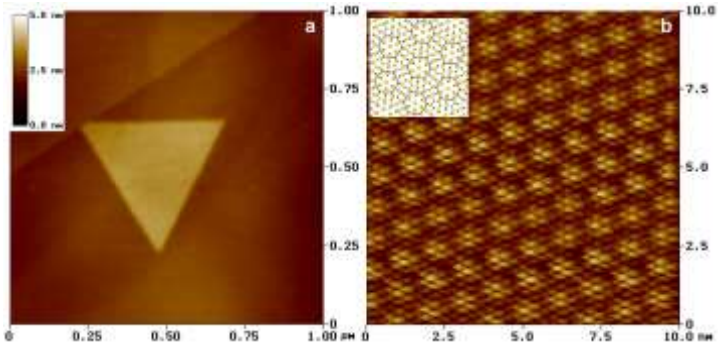

Figure 1 *a) STM image of a single layer MoS_2 flake grown on HOPG (200 pA, 1.5 V). b) Atomic resolution STM image of the flake exhibiting moiré type pattern (1 nA, 100 mV). The inset shows a ball and stick model of sulphur (yellow) and carbon (grey) atoms.*

The electronic properties of MoS_2 flakes grown on HOPG were investigated using CITS (Fig. 2). In CITS operation the scanning is interrupted in each image pixel, a full I-V curve is recorded and the CITS map displays the tunneling current measured at a selected bias voltage. The measured quasiparticle band gap for single-layer (SL) MoS_2 is around 2 eV, which decreases to 1.75 eV for bi-layer (BL) MoS_2, in good agreement with previous calculations and recent STM studies. The tunneling current of MoS_2 edges is different along the entire edge – irrespectively if the edge is located

on HOPG (SL edge) or on MoS_2 (BL edge) - from the current measured on flakes. These changes appear more pronounced at negative voltages. The difference is also clearly visible in the dI/dV spectra (Fig. 2d), where the MoS_2 edges show a metallic behaviour. Our STM measurements have confirmed that the edges of insulating MoS_2 can be viewed as a one-dimensional metallic wire.

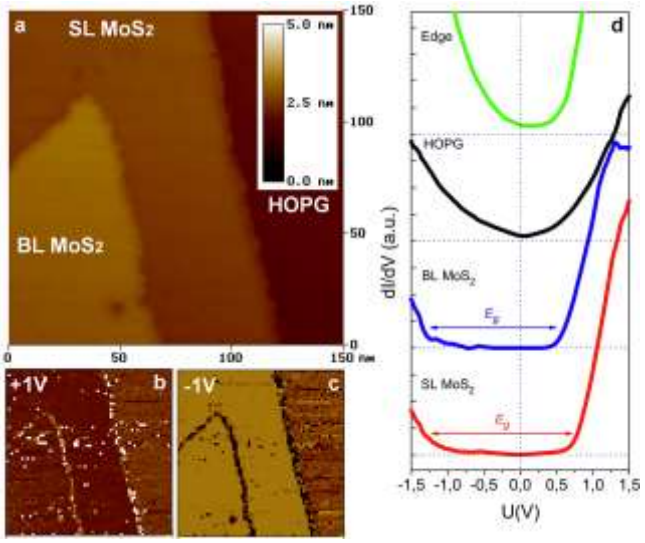

Figure 2 *STM image (a), CITS maps (b, c) and dI/dV spectra (d) recorded on SL and BL MoS_2 flakes grown on HOPG.*

STM nanolithography was used to cut MoS_2 nanoribbons suitable for nanoelectronic devices. The most accurate lines were cut when the cutting was started at the edge of the MoS_2 flake and performed in air with 90% relative humidity. With this method we were able to cut less than 20 nm wide MoS_2 nanoribbons for the first time (Fig. 3).

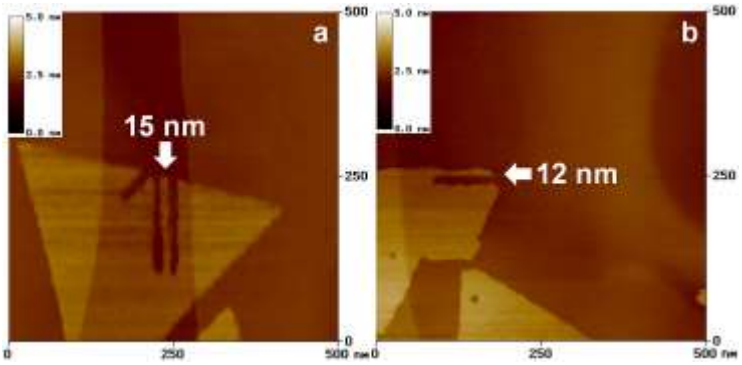

Figure 3 *MoS_2 nanoribbons cut by STM nanolithography on HOPG. a) ~15 nm and b) ~12 nm wide MoS_2 ribbons.*

Atomic and electronic structure of native point defects in MoS_2 single layers revealed by Scanning Tunneling Microscopy

(Lendület2014-14, KHJLN, OTKA 101599, OTKA 108753)

P.Vancsó, G. Zs. Magda, J. Pető, J.Y. Noh (KRISS, Korea), Yong-Sung Kim (KRISS, Korea), C. Hwang (KRISS, Korea), L. P. Biró, and L.Tapasztó

Transition metal dichalcogenide (TMDC) single layers have recently emerged as strong competitors of graphene in electronic and optoelectronic applications due to their intrinsic direct bandgap. However, atomic resolution TEM and electrical transport measurements indicate the presence of a high concentration of intrinsic structural defects. In this work we revealed the structure of native defects at truly atomic scale by STM investigation of large area exfoliated MoS_2 single layers, and we provide information on their electronic properties by ab-initio calculations, too. Fig. 1 shows typical atomic resolution STM images of 20 nm x 20 nm areas of a MoS_2 single-layer. The basic pattern observed is a hexagonal lattice of 0.31 nm periodicity, corresponding to the atomic lattice of the top sulfur layer of the 2D MoS_2 crystal. Line profiles (inset of Fig. 1b) across the dark triangles reveal that they are centered on a lattice site of the top S layer, except that no S atom is present, indicating their origin from a S vacancy. Since during the STM investigation the introduction of novel point defects has never been observed, we can directly estimate their intrinsic concentration in high quality exfoliated MoS_2 single layers which is in the range of 10^{13}-10^{14} cm^{-2}.

Besides the frequently observed triangular defects in STM images (Fig. 2a), defects of circular symmetry (Fig. 2b) have also been observed. To clarify the origin of the point defects we have performed DFT calculations.

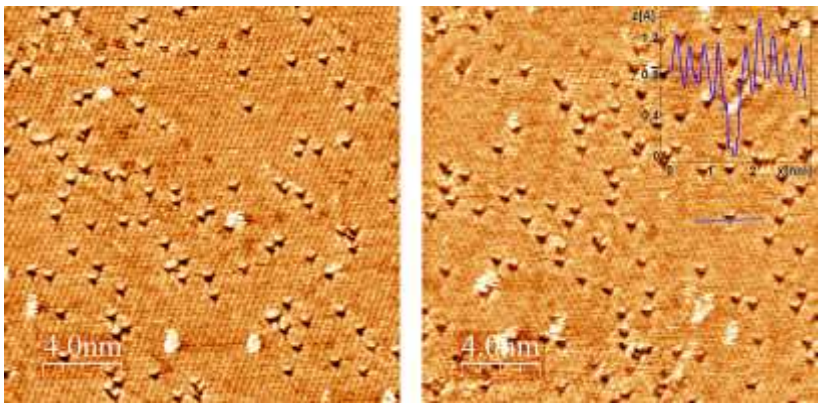

Figure 1 *Atomic resolution STM images of native point defects in MoS_2 single layers. A high concentration (10^{13}-10^{14} cm^{-2}) of native point defects (dark triangles) has been revealed by truly atomic resolution STM investigation of mechanically exfoliated MoS_2 single layers on Au (111). The point defects (dark triangles) are centered on an empty site of the hexagonal S atom lattice (see inset).*

Our calculations revealed two midgap electronic states (Fig. 2e) localized on the S atom vacancy. The simulated STM images from the calculated local density of states of the neutral *a1* and *e* states show triangular and circular form (Fig. 2c,d), pointed out that they are distinct STM images of the same structural defect.
By combining STM measurements with theoretical calculations our results provide insight into the electronic structure of the native defects of MoS_2 single layers, which is of key importance for understanding the operation of realistic electronic devices based on 2D crystals of molybdenum disulfide.

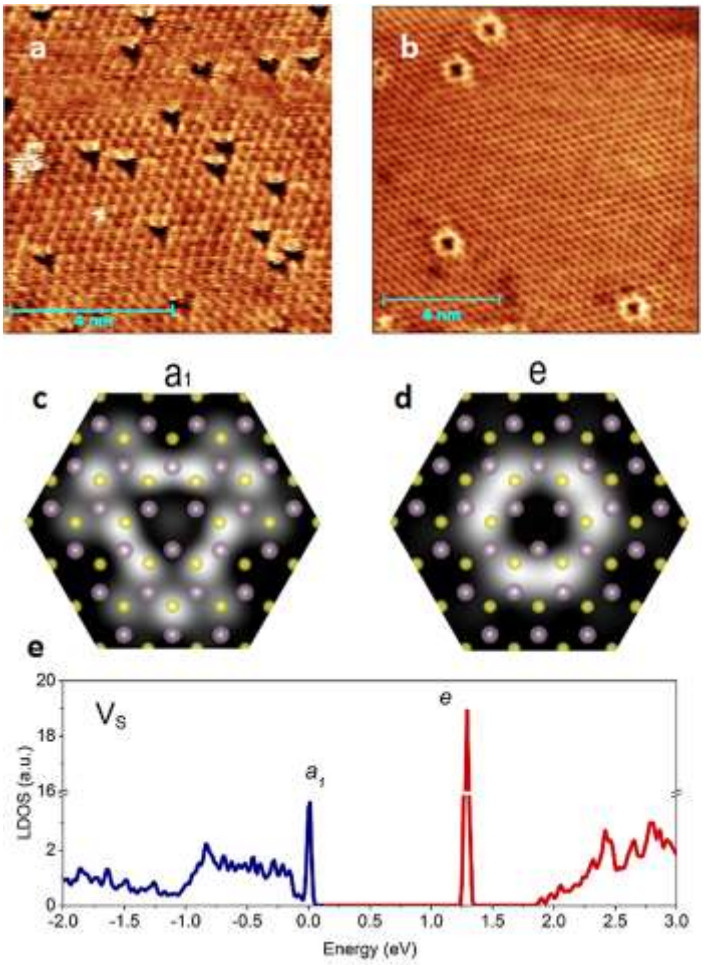

Figure 2 *(a)-(b) Atomic resolution STM images of single-layer MoS2 with triangular and circular shaped point defects at different spatial locations of the same flake. (c)-(d) Simulated STM images of the two electronic mid-gap states of a S atom vacancy based on DFT calculations. The sulfur and molybdenum atoms are shown by yellow and purple circles, respectively. (e) Local density-of-states for a neutral sulfur atom vacancy with midgap states.*

Modulation of physical properties by stacking of 2D materials

(Lendület2014-14, KHJLN, OTKA 101599, OTKA 108753)

G. Dobrik, P. Vancsó, G. I. Márk, L. Tapasztó, Ph. Lambin (UNamur, Belgium), C. Hwang (KRISS, Korea), and L. P. Biró

The extraordinary properties of graphene induced a continuously increasing attention focusing more recently on other 2D materials, too, like for example h-BN and the transition metal dichalcogenides. These 2D layers offer the possibility of building new materials, by stacking in a controlled way atomic/molecular thin layers in a layer by layer sequence, leading to novel properties. The vertically stacked heterostructures of 2D materials open a very wide range of possibilities the exploration of which may offer solution from cheap gene sequencing to high temperature superconductivity. As already demonstrated experimentally, the stacking each over the other of the 2D atomic, or molecular crystals gives birth to a full range of very complex phenomena, like Hofstadter's Butterfly, new optical phenomena, charge density waves etc. These may arise from several sources, for example: the lattice mismatch of the adjacent layers; the chemical composition of the individual layers; the orientation of the crystalline lattices of the adjacent layers. Therefore the investigation of the effects of the above parameters may prove to be of paramount importance in understanding the properties of the new material heterostructures systems.

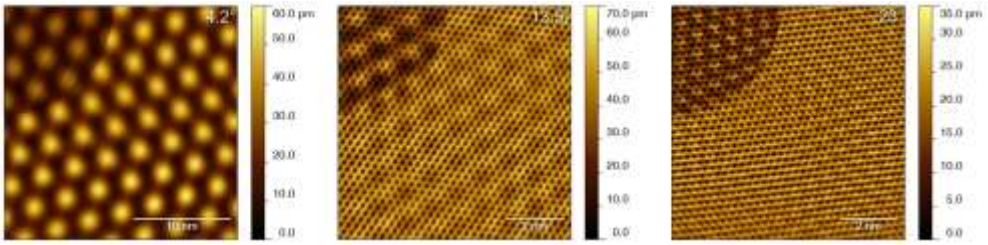

Figure 1 *Moiré structures at different angles of rotation (misorientation angles are given in the upper right corners). The rotation angles accurately determined relative to the HOPG substrate. Top left corner inserts; increased contrast..*

In this work, we propose as a particularly suitable model system for the understanding of vertically stacked 2D materials the CVD graphene on highly oriented pyrolytic graphite (HOPG). A major advantage of this system is that it allows the separation of chemical composition and lattice mismatch effects from lattice rotation effects. The grain misorientation angles ranging from a few degrees to 30 degrees include the entire range of interest. The moiré type superstructures appearing between the CVD graphene layer and bulk HOPG (Fig. 1) was investigated by scanning tunneling microscopy (STM), scanning tunneling spectroscopy (STS) and Raman spectroscopy. We found that the different rotation angles caused various effects. At small rotation angles <2° STS measurements show localized states at the Fermi energy (Fig. 2a). When the rotation angle is increased, (between 2° and 7°) the STS measurements reveal an interesting phenomenon, namely secondary Dirac cones are observed in the

spectra (Fig. 2b). We found that the energy position of the 2nd Dirac cone is tunable by the rotation angle following linear dependence. This peculiar band structure leads to profound changes in the electronic transport measurement by increased resistivity.

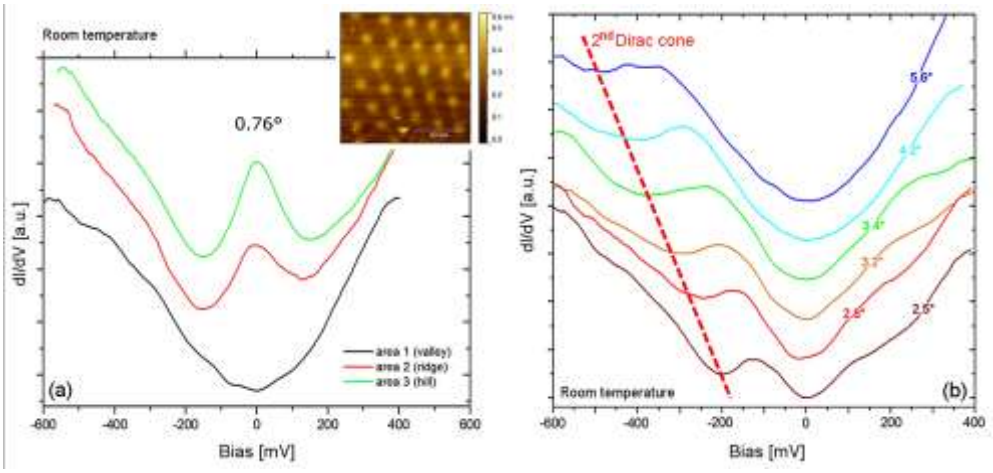

Figure 2 *STS spectra at small rotation angles. (a.) Localized states at the Fermi energy. Inset:STM image with the measured points. (b.) Secondary Dirac cone as a function of the angle of rotation.*

Further increase of the rotation angle (above 15°) the 2D peak of graphene appears near the graphite's 2D peak in the Raman measurements (Fig. 3). This suggests that the graphene layer is vibrationally decoupled from the substrate. The STS spectra also support the decoupling because no significant changes of the electronic properties have been observed compared with the single layer graphene.

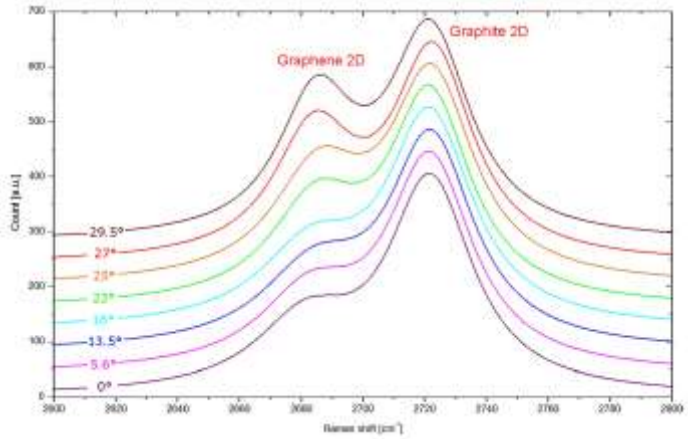

Figure 3 *Raman shift of the rotated CVD graphene layer on HOPG. The graphene layer is vibrationally decoupled from the substrate above 15° rotation angle.*

Variability of structural coloration in blue butterfly wings

(OTKA K 111741)

K. Kertész, G. Piszter, Zs. Bálint (HNHM, Hungary), and L. P. Biró

Variation exists within all populations of living organisms. This is the basis of natural selection where individuals that differ in phenotypes have different survival and reproduction chances: individuals with the appropriate trait may survive and reproduce more successfully than individuals with other, less suitable attributes, thus the population is able to evolve. The reproductive success can be determined by sexual selection, too, where one gender chooses mate based on phenotypic traits. The conspicuous structural colour on the wings of Blue butterfly males constitutes an important sexual communication channel; therefore it is subjected to strong evolutionary pressure as individuals with the "wrong" colour have a lesser chance to transmit their genes to the offspring.

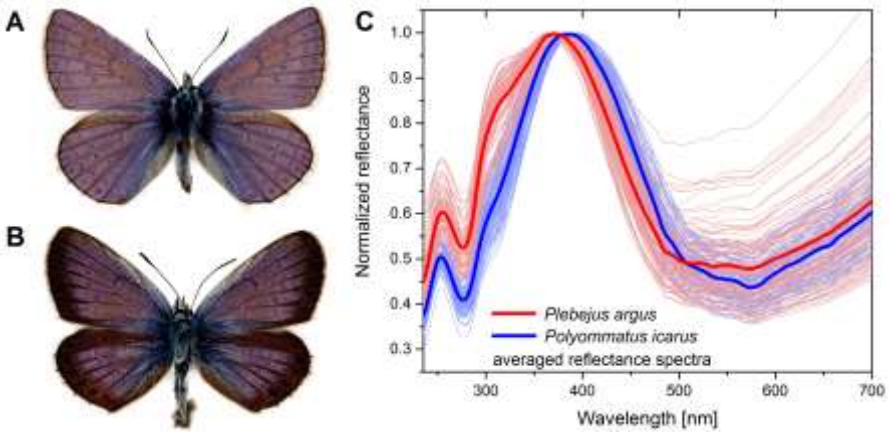

Figure 1 *Photograph images of male Blue butterflies: (a) P. icarus and (b) P. argus specimens are shown. (c) Species-specific reflectance spectra of P. argus and P. icarus. Note the wavelength difference of the main reflectance peak and the shoulder at 320 nm.*

The structural colour of the wings is generated by photonic crystal type nanoarchitecture which is located in the volume of the wing scales. This photonic nanocomposite is constituted of spatially periodic chitin matrix with embedded air holes with the characteristic size range of a few hundred nanometres. This characteristic length of the components' periodicity and the refractive index contrast between them result in wavelength selective reflection in the blue which is the source of the vivid structural coloration.

Structural colours of butterfly wings are more and more in the focus of attention both from the point of view of physics, and biology. However, studies focusing on the biologic variability of the structural coloration are mostly lacking. Therefore, we investigated this variability of structural coloration in the case of two common Lycaenid species living in Hungary. These species use their blue coloration for

conspecific recognition, but display differences in prezygotic strategy as male individuals of Polyommatus icarus (Fig. 1a) are patrolling, whilst Plebejus argus (Fig. 1b) are lacking in their habitats. From both species 25 male individuals were captured and the colour of all four wings was characterized spectrally, thus providing 100 measurements for each species.

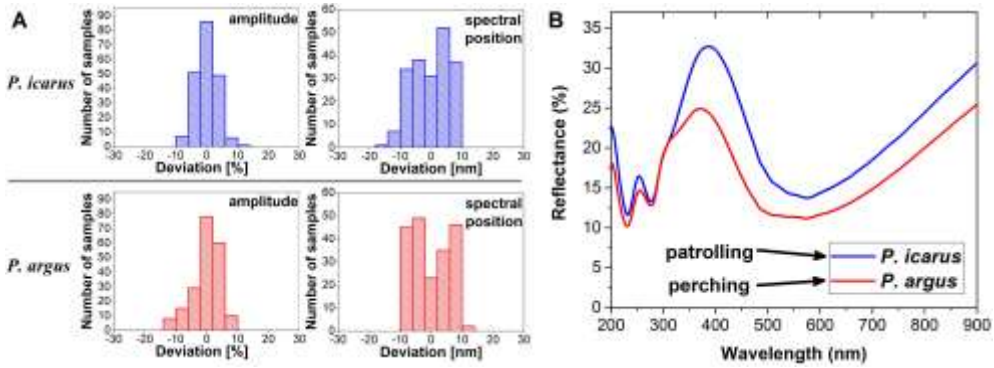

Figure 2 *(a) Histograms of amplitude and spectral position deviations of P. icarus and P. argus males. (b) Averaged reflectance spectra of P. icarus and P. argus males. Significant difference in the measured intensity can be seen.*

The reflectance spectra of the wings were measured using normal incident white light illumination and integrating sphere light collecting. The averaged reflectance spectra of the two species were generated and normalized to the main reflectance peaks in the blue to facilitate comparison. In Fig. 1c the species-specific colour differences of the two species can be observed: there is a small (~15 nm) difference between the wavelength of the maxima in the blue and the averaged spectrum of P. argus males has an additional shoulder at 320 nm compared to P. icarus.

Based on these averaged spectra the averaged parameters (peak position, amplitude) were determined for both species and the deviation of the two quantities were calculated and histograms were generated (Fig. 2a). For the two investigated species the intensity and wavelength deviations were almost identical which show that the natural variability of the structural colour in the case of species living in the same habitat is very similar due to the colour-based conspecific recognition.

To analyse the intensity of the blue structural colour the 100-100 measured reflectance spectra were averaged by species without normalization and were plot (Fig. 2b). The two averaged curves reveal the reflected intensity differences: the P. icarus males show enhanced reflectivity in the visible wavelength range compared to P. argus males resulting in brighter blue colour of the wings. This is in accordance with the naked eye observations and can be a direct consequence of the different prezygotic mating strategies of the two species while it requires different optical properties: the patrolling males of P. icarus have to be more conspicuous for an easy recognition by their females, but the perching mating strategy of P. argus males lacking in their microhabitats requires less intense blue colour as the females have to identify the males from significantly shorter distances.

Photonics Department

Head: Miklós FRIED, D.Sc., Scientific Advisor

Research Staff

- Emil AGÓCS, Ph.D. (on leave)
- Antal GASPARICS, Ph.D.
- András HÁMORI, dr. univ.
- Csaba S. DARÓCZI, dr. univ.
- György JUHÁSZ, dr. univ.
- György KÁDÁR, D.Sc.
- Péter KOZMA, Ph.D. (-)
- Csaba MAJOR, Ph.D. (-)
- János MAKAI, C.Sc. (part time)
- Norbert NAGY, Ph.D.
- Olivér POLGÁR, Ph.D.(-)
- Ferenc RIESZ, C.Sc.
- Tivadar LOHNER, D.Sc.
- Miklós SERÉNYI, D.Sc.
- Gábor VÉRTESY, D.Sc.

Ph.D. students / Diploma workers

- Bálint FODOR, Ph.D. student (on leave)
- Eszter FÜLÖP, Ph.D. (-)
- Judit NÁDOR (1/2), Ph.D. student
- Szilárd POTHORSZKY, Ph.D. student
- Dániel ZÁMBÓ, Ph.D. student

MFA was involved in the UNION (EU FP7) (Ultra-versatile Nanoparticle Integration into Organized Nanoclusters) project with the aim to develop tailored assembly of nanoparticles to be used in the field of theranostics, thermoelectrics and lighting applications. Main parameters investigated are the size of the template particles, wettability of the substrate, and the drying kinetics (temperature). Due to the arrangement of the gold nanoparticles, electromagnetic hot-spots can be created, that can be exploited in different spectroscopy techniques. With proper surface chemistry design, the ring-like structures can be also used to "focus" liquid dissolved molecules to accumulate at the hot-spots upon solvent drying.

Mesoporous silica thin films were patterned at the sub-micron scale utilizing the ion hammering effect in order to combine the advantages of mesoporous character and surface morphology, while preserving the interconnected pore system or creating laterally separated porous volumes surrounded by non-permeable compact zones. Measurements confirmed that the majority of the porous volume can be preserved as interconnected pore system by the application of low ion fluence. By increasing the fluence value, however, separated porous volumes can be created at the expense of the total pore volume.

Magnetic measurements are frequently used for characterization of changes in ferromagnetic materials, because magnetization processes are closely related to their microstructure. The recently developed method (Magnetic Adaptive Testing, MAT) is based on the systematic measurement and evaluation of minor magnetic hysteresis loops. This method was suggested as a highly promising non-destructive alternative

of destructive tests for monitoring structural changes in ferromagnetic objects. MAT introduces a large number of magnetic descriptors to diverse variations in non-magnetic properties of ferromagnetic materials, from which those, optimally adapted to the just investigated property and material, can be picked up. This year, satisfactory correlation between nondestructively measured magnetic descriptors and actual lifetime of the fatigued material were found. The method is able to serve as a powerful tool for indication of changes, which occur in structure of the inspected objects during their industrial service lifetime, as long as they are manufactured from ferromagnetic materials.

We are involved in 2 EU-projects („SEA4KET" and the ENIAC-2012-2 "E450DL") to develop "Imaging Optical Inspection Device With A Pinhole Camera". We developed 30, 45-60 and 60-90 cm wide prototypes.

Finite element simulations were used to calculate optical response of rough surfaces. This way, we can generate any surfaces for the investigation of the usually simplified optical models of ellipsometry or for other characterization methods. In agreement with previous investigations on polysilicon samples, correlation between the thickness of the effective medium layer and the RMS roughness was found. Our method also allows to investigate limits of the effective medium approach more in details.

A special flow cell for plasmon-enhanced, internal reflection, multiple-angle of incidence *in situ* spectroscopic ellipsometry was developed by MFA, which can be used to monitor interface processes with a high sensitivity (~40 pg/mm^2) and speed (less than 1 s for a full spectrum) in a broad wavelength range (350-1690 nm). The device was succesfully applied to study protein adsorption, cell adhesion and polyelectrolyte deposition simultaneously on uncoated and titania nanoparticle-coated gold surfaces.

Nondestructive indication of fatigue damage in ferromagnetic construction materials

(OTKA K 111662)

G. Vértesy, Cs.S. Daróczi, and A. Gasparics

Magnetic measurements are frequently used for characterization of changes in ferromagnetic materials, because magnetization processes are closely related to their microstructure. The recently developed method (Magnetic Adaptive Testing, MAT) is based on the systematic measurement and evaluation of minor magnetic hysteresis loops. This method was suggested as a highly promising non-destructive alternative of destructive tests for monitoring structural changes in ferromagnetic objects. MAT introduces a large number of magnetic descriptors to diverse variations in non-magnetic properties of ferromagnetic materials, from which those, optimally adapted to the just investigated property and material, can be picked up.

Many ferromagnetic components are subjected to alternating load in service, which often causes their structural failure as a result of fatigue. Fatigue evaluation and residual lifetime assessment are challenging issues with a high profile in industry. Nearly 90% of industrial component failures take place due to fatigue that occurs without warning. In order to check up health of ferromagnetic construction materials, it is important to timely monitor their fatigue damage, i.e. to detect initiation and propagation of fatigue cracks, and to predict residual lifetime of the constructions.

Fatigue damage was investigated in cyclically loaded low-carbon steel, by the MAT method. A sample made of cold-rolled S235JR steel was chosen for presentation of a typical MAT-measurement of the fatigue damage process. The specimen is ferromagnetic, it is flat, and it can be magnetized for the MAT-measurement by a short solenoid placed over the critical volume, where the fatigue cracks are initiated in the sample. This critical area is the neck, close to the fixed bottom head of the sample. The MAT-measurement of the samples proceeded in such a way, that always after a chosen number of loading cycles a short solenoid containing both the magnetizing and the pick-up coils was placed over the critical part of the sample, a couple of passive soft magnetic yokes was pressed to the sample so, that they and the sample created a closed magnetic circuit, and one family of the minor permeability loops was recorded. Then the yokes were taken away and a next number of loading cycles were applied. Fig. 1 shows the sample with the yokes and with the yoke-holder during the magnetic measurement.

Fig. 2 presents the result of the magnetic measurements. It is seen here, how the properly chosen MAT descriptor changes due to the cyclic loading. The sample was broken after 230 000 cycles. A very significant and fast increase of magnetic parameters close the end of the sample's lifetime is observed.

As a conclusion, satisfactory correlation between nondestructively measured magnetic descriptors and actual lifetime of the fatigued material were found. The method is able to serve as a powerful tool for indication of changes, which occur in

structure of the inspected objects during their industrial service lifetime, as long as they are manufactured from ferromagnetic materials.

Figure 1 *The critical part of the sample is covered by the magnetizing/sensing solenoid and by a couple of passive soft yokes pressed to the surface of the sample with a plastic spring holder. All are fixed at the bottom in a vice with non-magnetic jaws. The couple of deflection electromagnets can be seen at top of the figure.*

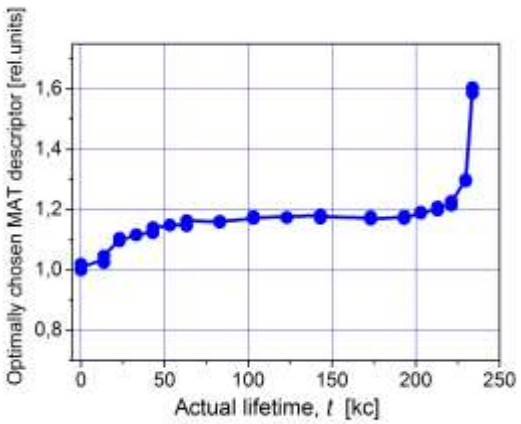

Figure 2 *The optimally chosen MAT descriptor as a function of cyclic loading. The fast upward curvature after 200 000 cycles indicates start of the critical crack spreading through the sample.*

Makyoh topography

F. Riesz, and J.P. Makai

In collaboration with IMEM–CNR, Parma, the surface shape and morphology of hot-wall VPE grown SiC/Si heterostructures have been characterized with Makyoh topography in order to study the effects of the addition of methyl trichloro silane. Low amount of sample bow was obtained in an optimized growth process. Fig. 1 shows a characteristic topogram, showing interference fringes related to thickness inhomogeneity and edge slip lines.

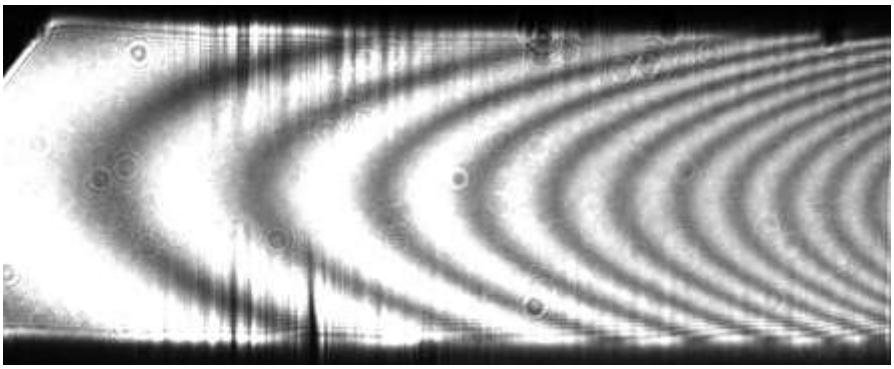

Figure 1 *Makyoh-topography image of a SiC/Si heterostructure.*

Within the project KMR_12-1-2012-0226, in collaboration with Mirrotron, Ltd. and the Wigner Research Centre for Physics, surface flatness of large-area polished Ni(P) coated Al blocks were characterised for neutron guide applications. Fig. 2 shows the purpose-built sample positioning/translation stage.

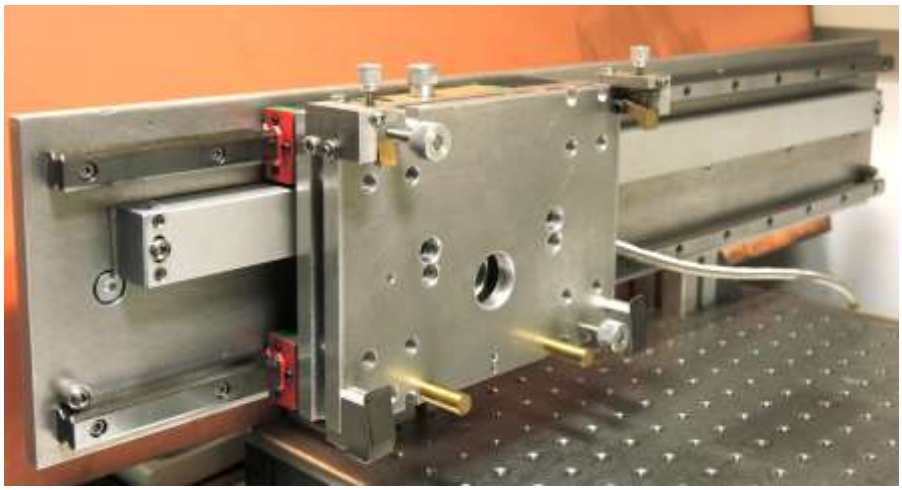

Figure 2 *Sample positioning stage for Makyoh characterisation of large-areas samples.*

Determination of migration of ion-implanted Ar and Zn in silica by backscattering spectrometry

(OTKA K101223)

I. Bányász, E. Szilágyi, E. Kótai, A. Németh, Cs. Major, M. Fried, and G. Battistig

It is well known, that refractive indices of materials important for waveguide fabrication, can be modified by ion implantation. In this work, effect of Ar and Zn ion implantation on silica layers was investigated by Rutherford Backscattering Spectrometry (RBS) and Spectroscopic Ellipsometry (SE). Silica layers produced by chemical vapour deposition technique on single crystal silicon wafers were implanted by Ar and Zn ions. The refractive indices of the implanted silica layers before and after annealing at 300 °C and 600 °C were determined by SE.
The migration of the implanted element was studied by real-time RBS up to 500 °C.
It was found that the implanted Ar escapes from the sample at 300 °C. Although the refractive indices of the Ar implanted silica layers were increased compared to the as-grown samples, but after annealing this increase in the refractive indices has vanished. In case of the Zn implanted silica layer both the distribution of Zn and the change in the refractive indices were found to be stable. Zn implantation seems to be an ideal choice for producing waveguides.

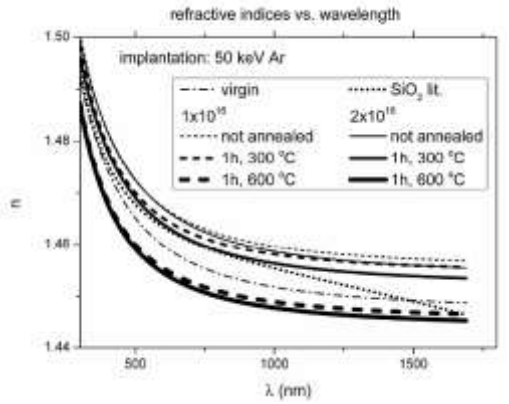

Figure 1 *Refractive indices for Ar implanted samples. For comparison, the refractive indices of virgin sample and the thermal SiO_2 (from literature) are also shown.*

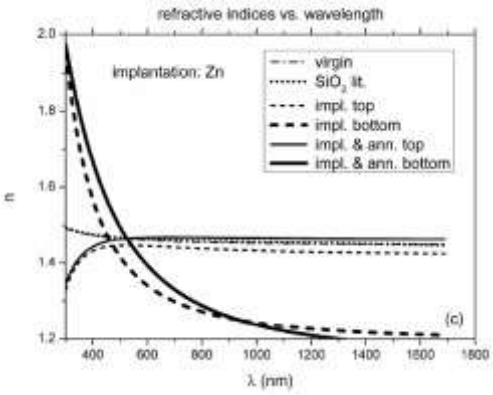

Figure 2 *Refractive indices as a function of wavelength for the two sublayers in the Zn implanted sample. For the sake of comparison the refractive indices of the virgin oxide as well as the thermal oxide are also shown.*

Verification of the effective medium approximation for surface roughness by finite element method

(OTKA K115852, K81842)

B. Fodor, P. Kozma, S. Burger, M. Fried, and P. Petrik

Finite element simulations were used to calculate optical response of rough surfaces. This way we can generate any surface for the investigation of the simplified optical models of ellipsometry or other characterization method. In agreement with previous investigations on polysilicon samples, we found a correlation between the thickness of the effective medium layer and the RMS roughness. Our method also allows to investigate limits of the effective medium approach in more detail (see Fig. 1 and Ref. B. Fodor, P. Kozma, S. Burger, M. Fried, P. Petrik, "Effective medium approximation of ellipsometric response from random surface roughness simulated by finite element method", accepted for publication in Thin Solid Films in 2016).

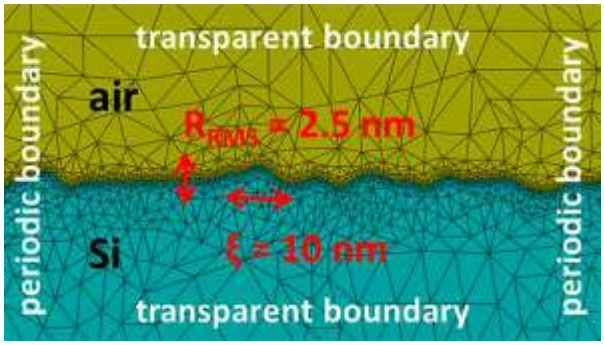

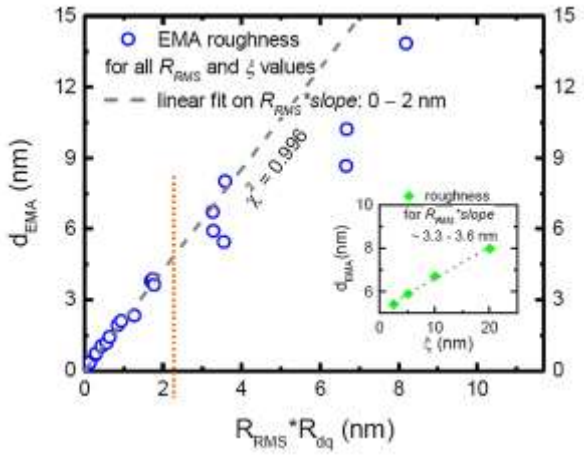

Figure 1 *(top) Random surface generated by the JCMWave finite element method. (bottom) Correlation between the product of RMS roughness and RMS slope (R_{RMS}*R_{dq}) and the thickness of the effective medium roughness (d_{EMA}) with linear fit for abscissa values smaller than 2 nm. The inset shows the secondary effect of correlation length (ξ) on d_{EMA} for points which have an R_{RMS}*R_{dq} value of ~3.4 nm.*

Plasmon-enhanced two-channel Kretschmann ellipsometry

(OTKA K115852, M-ERA.NET "WaterSafe")

J. Nádor, B. Kalas, E. Agócs, A. Saftics, P. Kozma, L. Kőrösi, I. Székács, M. Fried, R. Horváth, and P. Petrik

We have developed a flow cell in semi-cylindrical Kretschmann configuration for plasmon-enhanced, internal reflection, multiple-angle of incidence in situ spectroscopic ellipsometry, which can be used to monitor interface processes with a high sensitivity (~40 pg/mm^2) and speed (less than 1 s for a full spectrum) in a broad wavelength range (350-1690 nm) (see Fig. 1, [109]; and [J. Nádor, B. Kalas, A. Saftics, E. Agócs, P. Kozma, L. Kőrösi, I. Székács, M. Fried, R. Horváth, and P. Petrik, "Plasmon-enhanced two-channel in situ Kretschmann ellipsometry of protein adsorption, cellular adhesion and polyelectrolyte deposition on titania nanostructures", submitted for publication]. The cell has a small volume (10 μl), and it can readily be used with conventional table-top ellipsometers. Configuration with the semi-cylinder allows multi-channel measurements when moving the cell parallel to the axis of the cylinder using a conventional mapping stage.

The device was successfully applied to study protein adsorption, cell adhesion and polyelectrolyte deposition simultaneously on uncoated and titanium nanoparticle-coated gold surfaces.

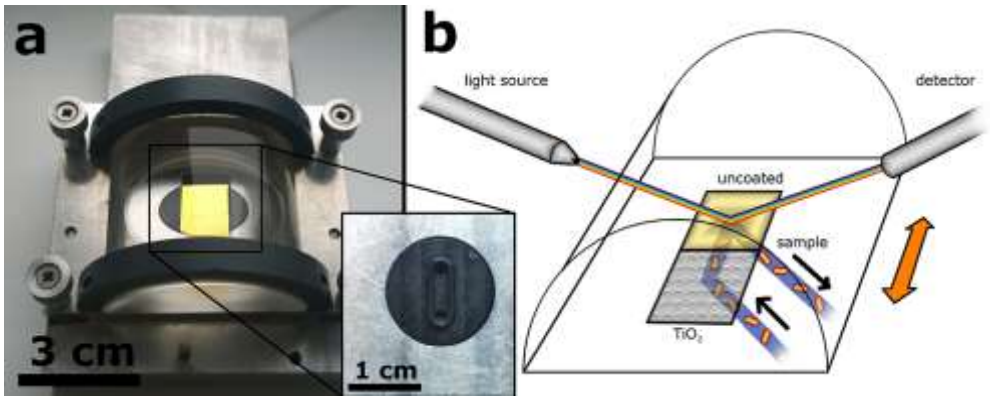

Figure 1 (a): *Flow cell with a semi-cylindrical lens in the Kretschmann configuration with a gold-covered glass substrate.* ***inset:*** *The 10 μl flow–cell surrounded by an O-ring.* ***(b):*** *A schematic graph of the measurement geometry.*

Protein adsorption, cell adhesion and polyelectrolyte deposition on titania nanoparticle coatings studied by two-channel Kretschmann ellipsometry

("Lendület" grant LP2012-26/2012 of HAS, OTKA K115852, M-ERA.NET "WaterSafe")

J. Nádor, B. Kalas, E. Agócs, A. Saftics, P. Kozma, L. Kőrösi, I. Székács, M. Fried, R. Horváth, and P. Petrik

A flow cell in a semi-cylindrical Kretschmann configuration for performing in situ two-channel measurements with a high sensitivity (~40 pg/mm^2) was developed. A setup was applied allowing to carry out simultaneous measurements on titania nanoparticle (TNP) coated and uncoated gold surfaces, in order to reveal the effects of the coating on protein adsorption, cell adhesion and polyelectrolyte layer deposition [J. Nádor, B. Kalas, A. Saftics, E. Agócs, P. Kozma, L. Kőrösi, I. Székács, M. Fried, R. Horváth, and P. Petrik, "Plasmon-enhanced two-channel in situ Kretschmann ellipsometry of protein adsorption, cellular adhesion and polyelectrolyte deposition on titania nanostructures", submitted for publication]. One of the main advantages of this approach is that the measurements on the two different surfaces are performed in the same process, under same conditions (temperature, pH, concentration etc.). Therefore, comparison of the two kind of measurement is more reliable than before, because most of the systematic errors can be ruled out, and concerns about repeatability are minimized.

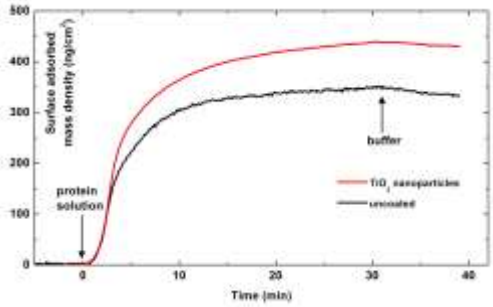

Figure 1 *The typical curves of a representative in situ ellipsometric measurement of Fgn adsorption on TNP-coated and uncoated surfaces.*

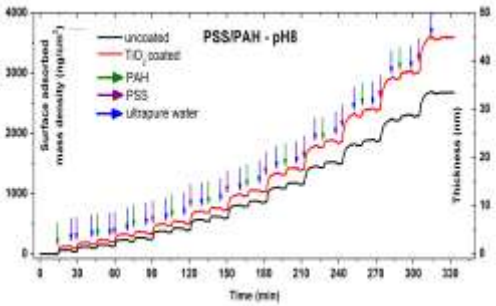

Figure 2 *The adsorbed mass density and the thickness of the deposited 10 pairs of PSS/PAH layers at pH 8 on TNP-coated and uncoated gold surfaces*

In the protein adsorption experiments a stable and widely used protein, fibrinogen (Fgn) was investigated. Kinetic curves showed that adsorption of proteins was enhanced on TiO_2-coated surface (Fig. 1), which can be explained by the increased specific surface area due to the TiO_2 nanoparticles.

In the case of preosteoblast cell adhesion no proper ellipsometric model was found in the evaluation, so the ellipsometric measurement proves only that the coating

modifies the adhesion of the cells. After the measurement, images were taken with phase-contrast microscope of the residual cells on the surfaces. On the TNP-coated surface significantly more cells were observed, which reveals that the cells adhered stronger to the coated surface.

For the process of polyelectrolyte layer-by-layer adsorption, poly(allylamine hydrochloride) (PAH) and poly(styrene sulfonate) (PSS) was applied as positively and negatively charged polyelectrolyte, respectively. Ten pairs of layers were built and measured in real-time, at pH 8, where both the titania and the gold thin film has negative charges on its surface. The thicknesses of the layers were demonstrated to be increased by the TNP-coating (Fig. 2).

The measurement was also carried out at pH 4, where the surfaces are positively charged. The thickness of the deposited layers was significantly larger at the basic pH than at the acidic pH (Fig. 3). The difference between the thicknesses of the bilayers at the acidic and basic pH can be explained by the strong pH-dependence of the polyelectrolyte layer deposition.

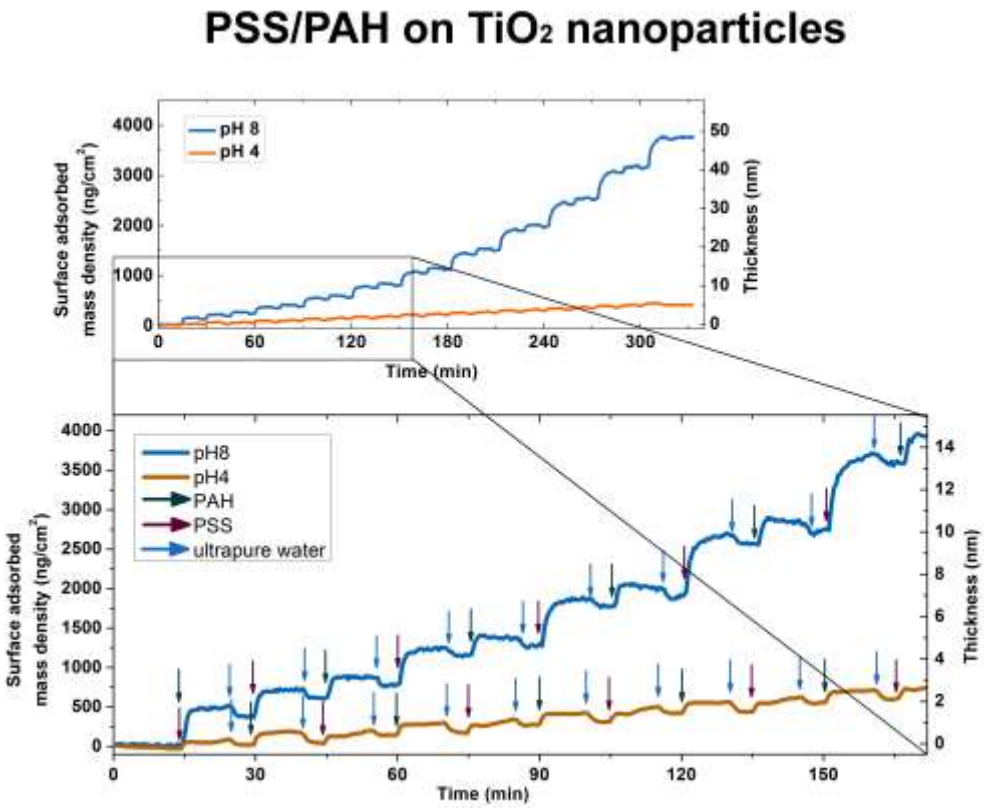

Figure 3 *The adsorbed mass density and the thickness of the deposited 10 pairs of PSS/PAH layers on TNP coated surface at pH 8 and pH 4.*

Development of optical metrology tool for in-line qualification of thin films on large area

(EU FP7 SEA4KET, ENIAC E450EDL)

Cs. Major, Gy. Juhász, P. Petrik, and M. Fried

We are involved in 2 EU-projects („SEA4KET" and the ENIAC-2012-2 "E450DL") to develop "Imaging Optical Inspection Device With A Pinhole Camera". We developed 30, 45-60 and 60-90 cm wide prototypes (Figs 1, and 2).

Figure 1 *We successfully installed our mapping device in the clean-room of IISB (Erlangen, Germany). A 300 mm diameter wafer can be seen on the robotic arm (left side).*

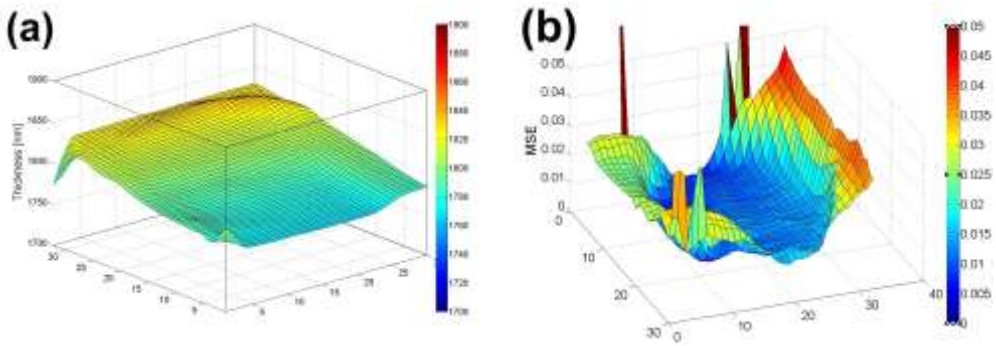

Figure 2 *Thickness-map of a nominally 2000 nm thick oxide layer on a 300 mm diameter Si-wafer (a) and the Meaned Squared Error-map showing the edges of the 30 cm diameter wafer (b).*

Preparation of compact nanoparticle clusters from polyethylene glycol-coated gold nanoparticles by fine-tuning colloidal interactions

(OTKA K112114, PD105173 and FP7 No.310250 UNION)

D. Zámbó, Gy. Z. Radnóczi, and A. Deák

Control over colloidal interactions might allow the creation of nanoparticle assemblies from individual, nanometric building blocks, giving rise to special optical or optoelectronic properties. These assemblies are excellent candidates for some advanced applications in the field of sensorics, energy harvesting, catalysis, biomedical contrast agents, or even theranostics. Gold nanoparticles are exceptional building blocks for nanoparticle assemblies as they support localized surface plasmon resonances, which is very sensitive to the interparticle distance caused biplasmon coupling. Polyethylene glycol homopolymers are commonly used as a stabilizer agent of gold nanoparticles in various media.

Low-molecular weight polyethylene glycol (PEG) has a lower critical solution temperature well outside the boiling point of water at ambient pressure, but it can be reduced at high ionic strengths. We extend this concept to trigger the clustering of gold nanoparticles through the control of colloidal interactions. At high ionic strengths, low-molecular weight (<2000 Da) mPEG-SH-modified gold nanoparticles show clustering with an increase in the solution temperature. The clustering temperature decreases with an increasing ionic strength. The clustering is attributed to the delicate interplay between the high ionic strength and elevated temperature and is interpreted in terms of chain collapse of the surface-grafted PEG molecules.

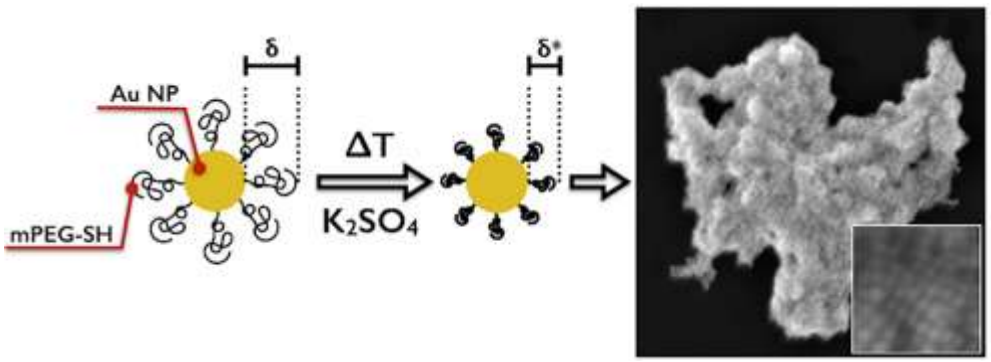

Figure 1 *Schematic representation of self-assembly of PEG-covered gold nanoparticles into compact nanoparticle cluster.*

The chain collapse results in a change in the steric interaction term, whereas the high ionic strength eliminates the double-layer repulsion between the particles. The observations are backed by nanoparticle interaction model calculations. We found that the intermediate attractive potential on the order of a few kT allows the

experimental fabrication of compact nanoparticle clusters in agreement with theoretical predictions.

A new approach for the predesigned, externally triggered clustering of gold nanoparticles was also presented. On the basis of the calculations on the colloidal interaction between the particles and the measurement data, it can be inferred that the experimentally observed clustering of the nanoparticles at high ionic strength and elevated temperature is a result of the chain collapse of the surface-grafted PEG molecules. Threshold temperature of the clustering can be influenced by the ionic strength of the medium. We found that the presence of the PEG shell significantly influences the kinetics of the clustering. The deceleration of particle association can be interpreted in terms of a moderate attractive potential after the chain collapse.

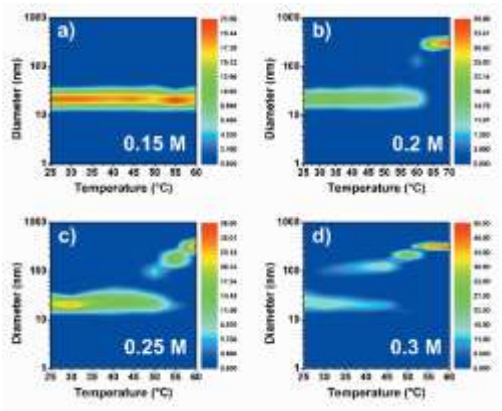

Figure 2 *DLS size distribution of gold nanoparticles as a function of temperature for different salt concentration.*

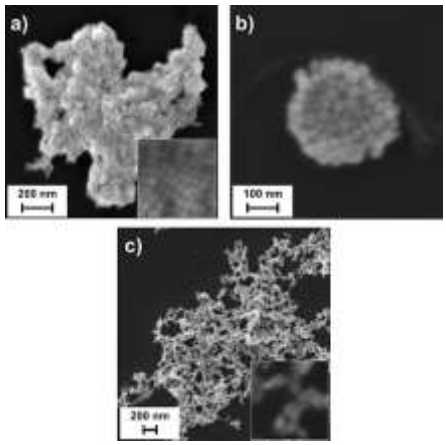

Figure 3 *SEM images of compact nanoparticle clusters from PEGylated particels and fractal-like aggrates of citrate stabilized nanoparticles.*

The structure of the clusters agrees well with theoretical predictions for such a model system. When the attractive potential between the building blocks is large, the position of two attaching particles gets kinetically trapped and not allowed to reconfigure during the assembly process, resulting in a fractal-like structure. This can be observed for our control sample (Fig. 3c), where the elimination of the double-layer forces leads to a rapid aggregation and fractal-like structure. For the PEG-grafted nanoparticles, at moderate interparticle attraction, reconfiguration of the building blocks is allowed; hence, the structure of the cluster becomes more compact. The presented approach allows preparation of complex nanoparticle clusters, where different type of nanoparticles can be incorporated into a single cluster [160].

Introducing nanoscaled surface morphology and percolation barrier network into mesoporous silica coatings

(OTKA K112114, PD105173 and FP7 No.310250)

E. Albert, P. Basa, A. Deák, A. Németh, Z. Osváth, G. Sáfrán, Z. Zolnai, Z. Hórvölgyi, and N. Nagy

Mesoporous silica thin films were patterned at sub-micron scale utilizing the ion hammering effect in order to combine advantages of mesoporous character and surface morphology, while preserving the interconnected pore system or creating laterally separated porous volumes surrounded by non-permeable compact zones.

Thin coatings of mesoporous silica on Si substrate were prepared by sol-gel method with ordered and disordered pore system using Pluronic PE 10300 and CTAB as molecular templates. Hexagonally ordered Langmuir-Blodgett films of spherical silica particles were transferred on the top of the porous silica coatings and applied as mask against Xe^+ ion irradiation (Fig. 1). The ion energy was chosen according to Monte-Carlo simulations to achieve structures with high lateral contrast between irradiated and unirradiated, *i.e.*, masked areas.

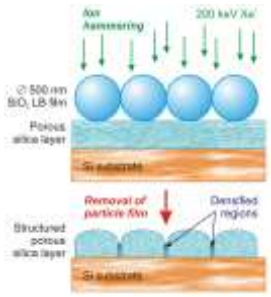

Figure 1 *Schematics of the key step of sample preparation: ion irradiation with 200 keV Xe^+ through an ordered monolayer of silica spheres then removal of the particles.*

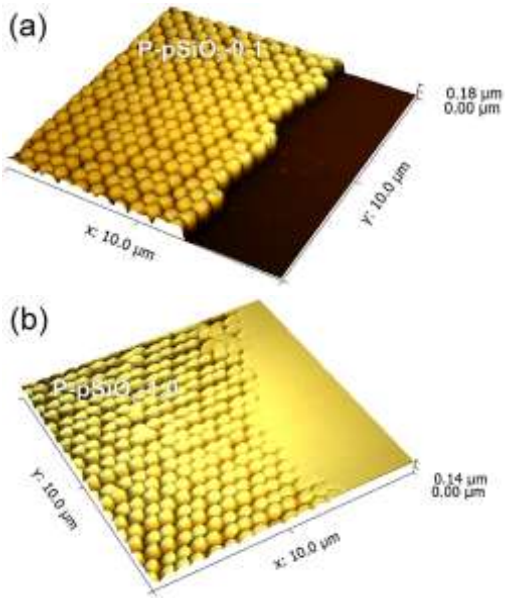

Figure 2 *AFM images of Pluronic-type silica coatings after ion irradiation with fluences of (a) 0.1×10^{16} cm^{-2}, and (b) 1×10^{16} cm^{-2}, respectively. The measurements were carried out (a) where the edge of the particulate LB mask was located and (b) at the border of irradiated and unirradiated regions of the LB film.*

The aspect ratio of resulted morphology was proved to be high; the created surface structures were very similar irrespectively of the type of template molecules and ion fluences applied (Fig. 2). The densification of both types of porous silica coatings almost reached its maximum already at the lowest fluence. For CTAB-templated coatings the degree of densification was significantly higher than in the Pluronic-templated ones.

The HRTEM analysis revealed that the pore structure remained intact where the silica spheres were non-transparent for the bombarding ions. For Pluronic-templated silica samples with disordered pore system the pore structure remained interconnected near the Si substrate surface at the lowest fluence. Contrarily, at the highest fluence, the regions surrounding the intact porous columns were fully densified thus forming non-porous border zones (Fig. 3). Therefore, the interconnected or the separated character of the pore system can be tailored by the applied ion fluence, while the created surface morphology is essentially the same in both cases. In case of CTAB-templated coatings with ordered pore structure the results were similar. The densified regions are thicker, while the intact porous volumes are smaller than in the Pluronic-templated case irradiated with the same fluence. Comparing the two different molecular templates the disordered Pluronic-templated pore system proved to be more resistant against Xe-bombardment.

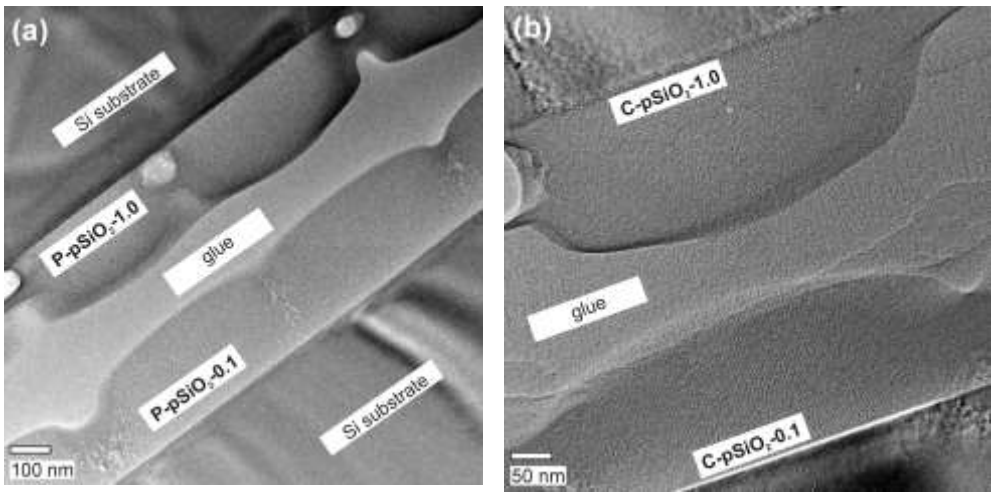

Figure 3 *HRTEM images of* ***(a)*** *Pluronic-type and* ***(b)*** *CTAB-type coatings irradiated with fluences of 0.1 × 10^{16} cm^{-2}, and 1.0 × 10^{16} cm^{-2}.*

Confocal fluorescent images and ellipsometric porosimetry measurements confirmed that the majority of the porous volume can be preserved as interconnected pore system by the application of low ion fluence. By increasing the fluence value, however, separated porous volumes can be created at the expense of the total pore volume [3].

Effect of heat treatments on the properties of hydrogenated amorphous silicon for PV and PVT applications

(MTA 1102, OTKA K-67969, NF 101329, NK 105691, TAMOP 4.2.2.A-11/1/KONV-2012-0036)

M. Serényi, N. Q. Khánh, and C. Frigeri

Photovoltaic (PV) solar cells and photovoltaic thermal (PVT) hybrid devices very often employ hydrogenated a-Si (a-Si:H) because of its cost effectiveness and better performance as light absorber. The properties of a-Si:H can be improved by heat treatments that also help to recover the Staebler-Wronski effect. The effects of heat treatments on the properties of hydrogenated a-Si to be used in PV and PVT devices have been investigated. To better study them the annealing was performed at temperatures (350 °C) higher than those (≈200-275 °C) usually applied to improve the performance of a-Si:H employed in PV and PVT technologies since those effects were expected to be stronger and more easily detectable. It was found that the heat treatment causes changes in the Si-H bonding configuration with the transformation of the SiH monohydrides to the less stable SiH_2 dihydrides and polysilane chains. The latter polyhydrides, in their turn, cause a strong degradation of the a-Si layer morphology with the formation of surface blisters with size of some microns as well as craters depending on the H content and annealing time.

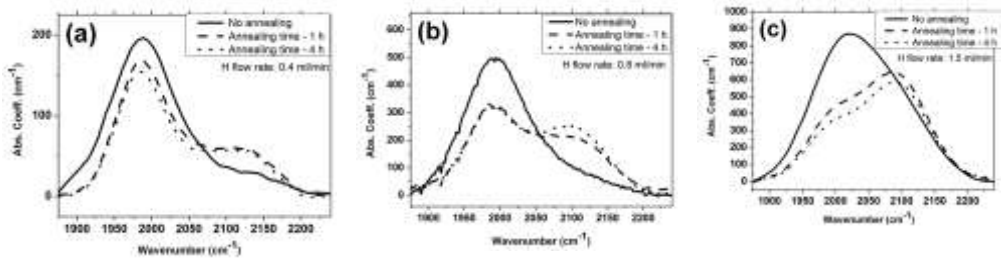

Figure 1 *Typical IR absorption spectra in the stretching mode range of the wavenumber for the H content of a) 10.8, b) 14.7, c) 17.6 at%. For each plot the spectra for the unannealed (solid curve), annealed for 1 h (dash curve) and for 4 h (dot curve) are reported.*

Microtechnology Department

Head: Gábor BATTISTIG, Ph.D., senior research fellow

Research Staff

- Zsófia BAJI, Ph.D.
- István BÁRSONY, Member of HAS
- Gábor BATTISTIG, Ph.D.
- László DÓZSA, Ph.D.
- Csaba DÜCSŐ, Ph.D.
- Zoltán FEKETE, Ph.D. (on leave)
- Péter FÖLDESY, Ph.D.
- Péter FÜRJES, Ph.D.
- Zoltán HAJNAL, Ph.D.
- Nguyen Quoc KHÁNH, Ph.D.
- Zoltán LÁBADI, Ph.D.
- István LUKÁCS, Ph.D.
- György MOLNÁR, Ph.D.
- Andrea Edit PAP, Ph.D. (part time)
- Anita PONGRÁCZ, Ph.D.
- Vilmos RAKOVICS, Ph.D.
- István RÉTI, Ph.D.
- Attila Lajos TÓTH, Ph.D. (retired)
- János VOLK, Ph.D.
- Zsolt ZOLNAI, Ph.D.

Ph.D. students

- Zsófia BÉRCES
- Zoltán SZABÓ
- Ferenc BÍRÓ
- Máté TAKÁCS
- Róbert ERDÉLYI
- Gergely MÁRTON
- Tamás KÁRPÁTI
- Eszter HOLCZER
- Eszter TÓTH

Technical Staff

- János FERENCZ (engineer)
- Levente ILLÉS (engineer)
- Csaba LÁZÁR (engineer)
- Róbert HODOVÁN (engineer)
- András LŐRINCZ (engineer)
- Erika TUNYOGI (engineer, on leave)
- Katalin VERESNÉ VÖRÖS (engineer)
- György ALTMANN (technician)
- Gabriella BÍRÓ (technician)
- Sándor CSARNAI (technician)
- Tibor CSARNAI (technician)
- Magda ERŐS (retired)
- Károlyné PAJER (technician)
- Csilla ARIAS-SOTONÉ FARAGÓ (technician)
- Attila NAGY (technician)
- Magda VARGA (technician)

The task of the Microtechnology Department is

Fundamental research on:

- sensing principles;
- novel materials and nanostructures;
- novel 3D fabrication techniques.

Research and development of physical, chemical/biochemical sensors and integrated systems:

- **MEMS** – R&D on micropellistor-type gas sensors, 3D force sensors, thermal sensors, CMOS compatible and related techniques.
- **BioMEMS** – Development of novel microfluidic systems, their application in new fields of biochemistry.
- **NeuroMEMS** – Development of Si- and polymer based sensors for biomedical applications with special focus on brain science.
- **NEMS** – Synthesis and characterization of quasi-one-dimensional semiconducting nanostrucrures, semiconductor nanodevices, their integration into functional sensors, optoelectronic and photovoltaic devices.

Modelling, structural and device characterization methods available:

- Electrical characterization;
- Thermo-mechanical characterization;
- Scanning Microprobes;
- Ion beam analysis methods;
- SEM, TEM, EDX;
- Spectroscopic Ellipsometry.

The Department runs two (300 m^2 + 160 m^2) clean labs (Class 100-10000) comprising a complete Si-CMOS processing line and a mask shop, unique facility in Hungary. The technology allows to manufacture layers, patterned structures and devices with line resolution of 1 μm by optical and down to ≈10 nm by e-beam lithography on 3" and 4" Si and glass wafers.

Competences (available also for our industrial and academic partners and customers):

- High temperature annealing, diffusion and oxidation;
- Ion implantation;
- Rapid Thermal Treatment;
- Low Pressure Chemical Vapor Deposition of poly-Si, SiO_2 and Si_3N_4 layers;
- Low Temperature Chemical Vapor Deposition;
- Atomic Layer Deposition;
- Physical Vapor Deposition – Electron beam evaporation, DC and RF Sputtering;
- Reactive Ion Etching, Deep Reactive Ion Etching;

- Photolithography with back-side alignment and Nanoimprinting;
- E-beam lithography;
- Nanopatterning, deposition and etching by Focused Ion-Beam;
- Wafer-bonding;
- Wet chemical treatments;
- Electro-chemical porous Si formation;
- Molecular Beam Epitaxy of III-V compound semiconductors;
- Mask design, laser pattern generator;
- Polymer (PDMS, SU8, Polyimide) structuring by photolithography and micro-molding techniques;
- Chip dicing, packaging especially for sensor applications;
- Materials and structural analysis & characterization: SEM, FIB, EDX, Atomic Force Microscopy, Electrochemical Impedance Spectroscopy, Stylus Profiler;
- Electrical and functional modeling and characterization.

For detailed information please visit our web-site: **www.mems.hu**
or contact us bye-mail: **dragon@mfa.kfki.hu**

MEMS

Activity leader: Cs. Dücső

Group members: Z. Baji, I. Bársony, G. Battistig, L. Dózsa, P. Földesy, P. Fürjes, Z. Hajnal, Z. Lábadi, G. Molnár, A.E. Pap, V. Rakovics, I. Réti, A.L. Tóth, Z. Zolnai, F. Biró, T. Kárpáti, M. Takács

Projects:

- ENIAC CALL 2013-1 – "Intelligent Catheters in Advanced Systems for Interventions – INCITE"
- OTKA K109674 – "Graphen based terahertz modulators"
- OTKA PD116579 – "ZnO és Ga_2O_3 nanostruktúrák készítése atomi réteglevalasztással"
- OTKA K112114 – "Kombinált mikro-nanotechnológiai eljárások és ellenőrzésük lokális analitikai technikákkal: a mintázatképzéstől az alkalmazások felé"
- KMR-12-1-2012-0107 – "Műszerfejlesztés talajvíz és egyéb vizek szénhidrogén szennyezettségének folyamatos megfigyelésére"
- KMR-12-1-2012-0226 – "Új generációs neutronos vizsgálóberendezések komponenseinek fejlesztése (2012-2015)"
- KMR_12-1-2012-0031 – "Beágyazott informatikai rendszer fejlesztése energiapozitív közvilágítás optimálására"

Fine-tuning of gas sensitivity by modification of nano-crystalline WO_3 layer morphology

Hexagonal WO_3 layers of different morphologies were deposited on micro-hotplate gas sensors and gas sensitivity for NH_3 was tested. The layers were synthesized by hydrothermal acidic precipitation method using different catalytic chemicals. Thin film sputtered layers were also deposited as reference material. WO_3 suspensions of quasi-equivalent quantity were dropped on the micro-hotplate for all the materials investigated. Additional ultrasonic agitation was introduced to destroy conglomerates of nano-crystals. If Na_2SO_4 or K_2SO_4 catalyst were added to the acidic solution of Na_2WO_4, ultrasonic treatment proved to be very effective and resulted in uniform sized individual WO_3 nano-rods of 80nm diameter. Addition of $ZnSO_4$ catalyst leads to disordered nano-fiber net with typical diameter of 70 nm. Ultrasonic agitation had no effect in case of NaCl catalyst and Zocher methods; thereby the formed WO_3 layers are composed of micrometer size conglomerates of 80-150 nm nano-rods. SO42- ions facilitate the formation of long crystallites.

Layers composed of individual nano-rods exhibit 2-5 times higher sensitivity up to 60ppm NH_3, while layers of larger conglomerates show linear response in the 10-100ppm range. The size effect is explained by the comparable sizes of nano-wire

width and space charge layer at the solid-gas interface. This effect was also demonstrated by the sputtered thin films of different thicknesses.
Na_xWO_3 contamination deteriorates gas sensitivity. No relationship between specific surface and gas sensitivity could be detected.

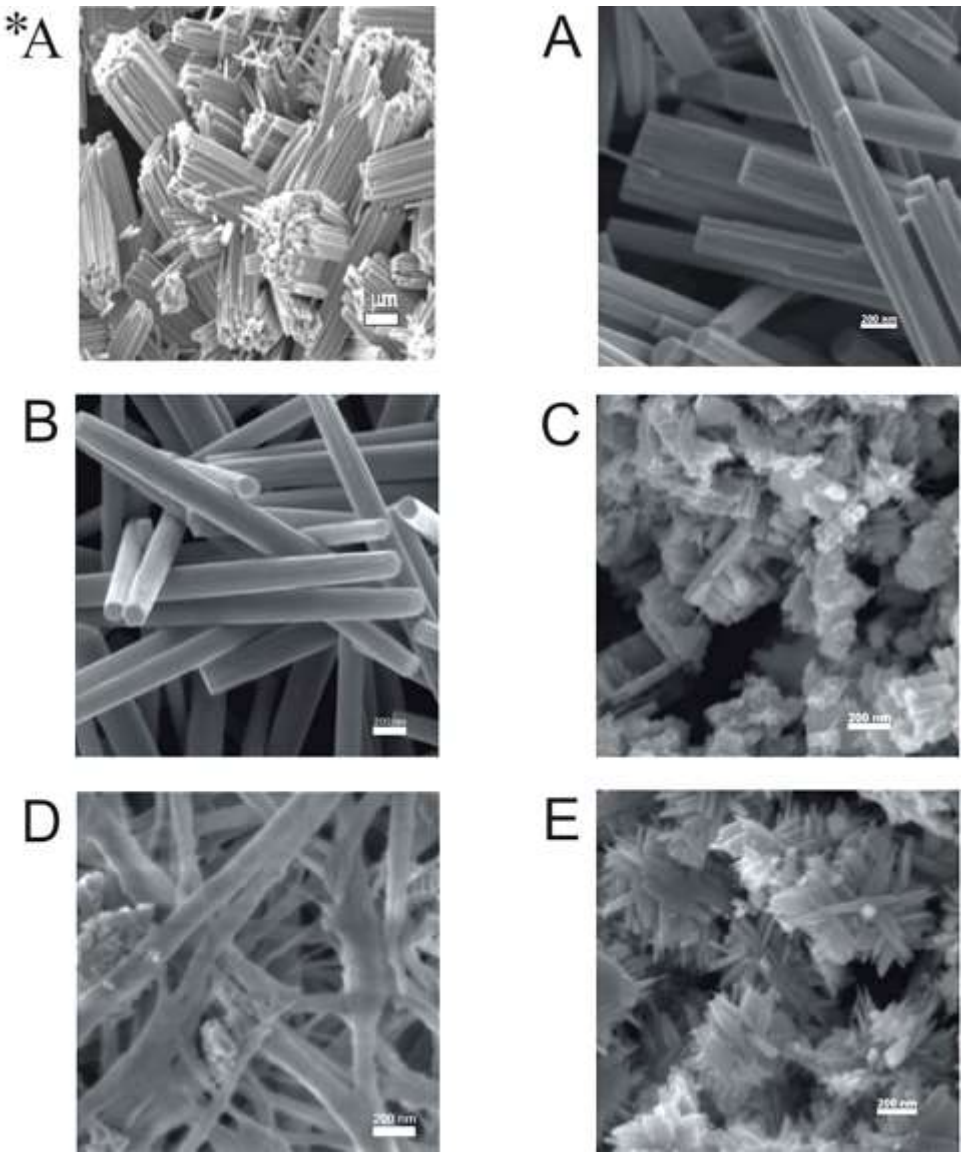

Figure 1 *SEM views of hydrothermally synthesised WO_3 layers with different catalysts: (A*): Na_2SO_4 without ultrasonic treatment, (A): Na_2SO_4 with ultrasonic treatment, (B): K_2SO_4 with ultrasonic treatment, (C): NaCl with ultrasonic treatment, (D): $ZnSO_4$ with ultrasonic treatment, (E): Zocher-method.*

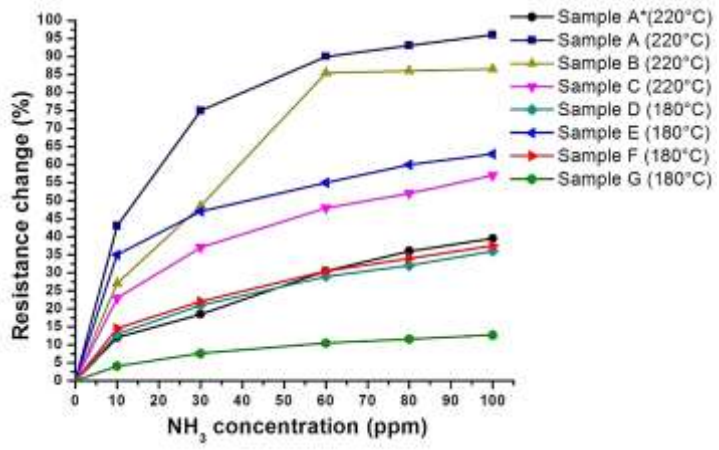

Figure 2 *Summary of sensor responses for 0-100ppm NH_3 in synthetic air.*

The different characteristics of the alternatively processed WO_3 enables fine tuning of sensitivity. Combination of two layers also offers the possibility to expand measuring range.

Wavelength conversion in GaInAsP/InP near infrared surface emitting diodes[2]

Quality control in food industry and clinical diagnostics requires powerful, versatile and relatively cheap spectrometers. Semiconductor light sources are characterized by small dimensions and low power consumption; therefore they can be suitable components in low price miniature devices. The only disadvantage of their application is that they are temperature sensitive and have a narrow spectrum. Infrared emitting diodes have 50 – 75 meV spectral bandwidths depending on the growth conditions. Thereby a series of spectrally tailored GaInAsP/InP surface emitting LED chips is required by micro-spectroscopy to cover the NIR (1000 – 1700 nm) wavelength range completely. Although these chips were developed in our lab and are efficiently applied by our partners, the need for spatially homogeneous, broad-spectrum and bright light sources drove us to develop a monolithic integrated NIR light source.

Present description demonstrates the results of a novel structure and its related technology to form single-chip broad or multi-peak spectrum LEDs. The output spectrum of the LED chip is substantially modified by introducing wavelength converter layers outside of the p-n junction of a normal LED structure. Light emitted from the active region is partly absorbed by the smaller band gap quaternary layers and re-emitted with smaller photon energy (Fig. 1). The emission spectrum and the

[2] Patent pending

light intensity can be tailored by the compositions, the thicknesses and number of the absorber layers. As an example, this absorption and re-emission process of the modified LED chips results in substantially broader two-peak emission spectrum (Fig. 2). A special advantage of the novel chip is that the spectral bandwidth of the device does not change with the driving current in the range of 10 mA to 100 mA. Moreover, the temperature dependence is also similar along the whole spectrum. More than 1 mW optical power can be obtained at 100 mA driving current and the corresponding operating voltage is 1.2 V.

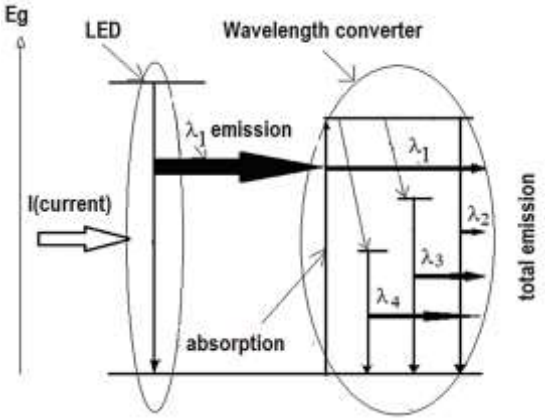

Figure 1 *Operation principle of the wide spectrum NIR light source.*

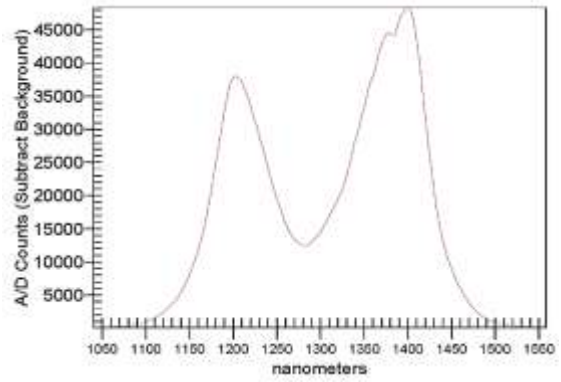

Figure 2 *Demonstration of the broad emission spectrum by a two-wavelength single-chip NIR light source. Peak at 1200 nm is from the LED, peak at 1400 nm is from the integrated single absorber layer light converter.*

We have obtained even broader spectrum by inserting more additional different composition quaternary GaInAsP layers into the structure. These layers have lower band gap than the active and the first absorption layer. Sandwiching the absorber layer in additional narrow band gap GaInAsP layers the formed potential well enhance the direct recombination of the optically excited charge carriers. The device works similarly to phosphor conversion white LED structure, but it is more compact and stable, because all layers are lattice matched to the substrate. Its optimization is relatively easy if the light emitting layers are substantially thinner than the confining absorption layers. The novel one-chip LED structure provides point-like light source with broader spectra and facilitate the construction of low power miniaturized NIR

spectrometers. The multilayer structure enables to form stable light sources of emission spectrum tailored to any dedicated task.

3D force sensors for minimal invasive surgery applications

Minimally invasive surgery offers several advantages for the patient and also for the society. The quicker recovery and the smaller trauma are obviously essential for the patient, whereas the reduced hospitalization and recovery time helps the society to spend the medical costs more effectively.
INCITE project is intended to reveal and describe the advantages of the integration and application of various sensing capabilities in Minimal Invasive Surgery (catheter or surgery robot) systems. These subsystems are applicable to extend the functionality of the proposed medical systems to be applied by improving feedback for the operators and surgeons during the intervention. The future aim is to improve the functional characteristics, safety and standards of medical devices (catheters, robotic tools) applicable to minimal invasive cardiac intervention and surgery.

Figure 1 *Surgery robots (FRK) and the head where the force sensors will be integrated.*

In order to improve the safety of the laparoscopic intervention the surgeon must get on-line information about the physical and chemical parameters during operation. The principal parameter required is the force as measured at different locations of the laparoscope head. Built inside the gripper the sensor can measure the strength of which the laparoscope holds the surgical tool. Placed on the tip the sensor can provide information about the hardness and surface roughness of the tissue the laparoscope touches (Fig. 1).

Design and fabrication of the 3D MEMS force sensors

3D force sensors were developed for the further integration in laparoscopic heads of surgery robots. The Si sensors operate with piezoresistive transduction principle by measuring the stress induced signals of the symmetrically arranged four piezoresistors in the deforming membrane. As the chip size has to be reduced to a few mm2, the conventional anisotropic alkaline etching technique was replaced by deep reactive ion etching (DRIE) for membrane formation. Besides, DRIE has no practical limitation in membrane geometry and offers the formation of monolith force transfer rod

protruding over the chip surface. SOI (silicon on insulator) wafers of appropriate device layer thickness provide the uniformity of membranes and reproducibility of the process.

According to the medical and functional requirements the MEMS sensors will be covered by biocompatible elastic polymer coating. Nevertheless, the elastomer drastically effect on the performance of the device. Therefore, the proposed sensor structures were modeled by coupled finite element simulation to determine the appropriate geometric parameters to meet the functional requirements. Sensors were covered with spherically shaped PDMS (polydimethylsiloxane) polymer and the effect of the elastic coating was also studied in terms of sensitivity and response time.

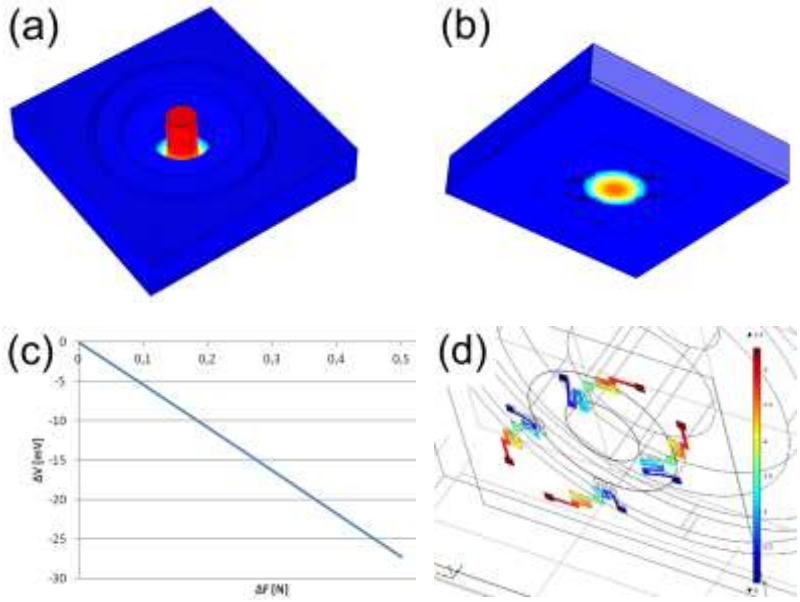

Figure 2 *Demonstration of the multiphysical coupled FEM simulation of the piezoresistive 3D force sensors: (a): membrane deformation, (b): stress distribution along the integrated piezoresistors, and (c,d): the (perpendicular) force dependent sensor signal.*

Four half Wheatstone-bridges were formed on full Si membranes, each composed of two identical resistors and arranged such as to represent maximum out-of-balance voltages over mechanical deformation. The geometric design was aided by FEM calculations for any force range to be measured (Fig. 2).

The processed wafer was anodic bonded to boron glass to provide enhanced mechanical stability, cavity underneath the membrane and wire contacts for assembly. Processed chips (Fig. 3a) were mounted on TO8 headers or PCB header (Fig. 3b) for preliminary tests. In order to investigate the effect of the elastic coating, identical chips were covered by PDMS layer (Fig. 3c) and characterized as well.

The standard test includes the measurements of the four out-of-balance voltages over the applied force range in perpendicular directions of loads. (Fig. 4). The sensitivity is

heavily affected by the geometry and elasticity of the elastic coverage and this may result in up to 50-90% sensitivity loss.

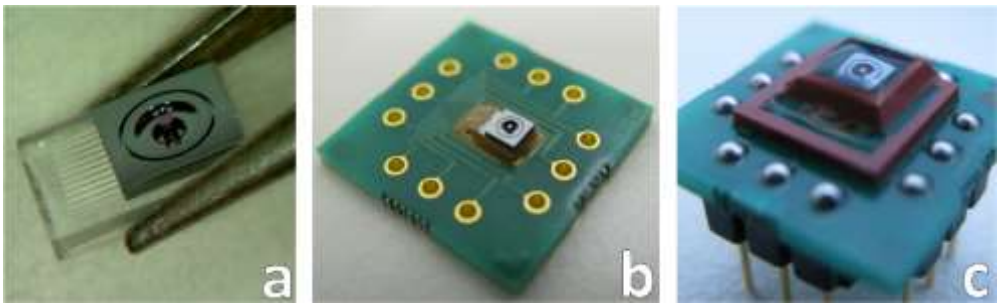

Figure 3 *2×3 mm² full membrane force sensor chip (a), bare reference (b), and PDMS coated membrane type chips mounted on a specific PCB header for functional tests (c).*

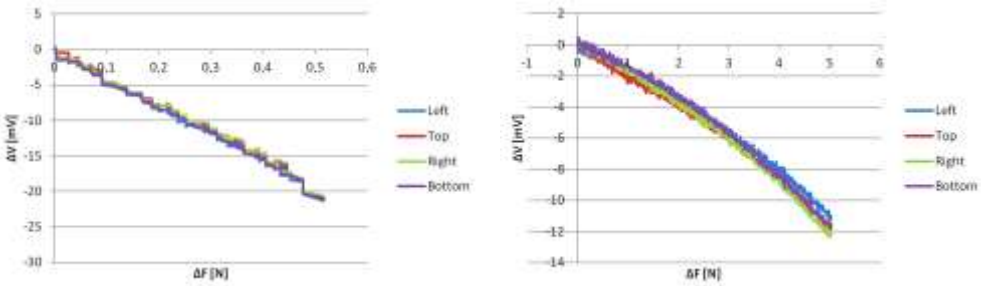

Figure 4 *Out-of-balance voltages of the four half Wheatstone-bridges for perpendicular loads. Bare chip (left), PDMS coated (right).*

Modeling and Simulation @ MEMS Lab

Finite Element Modeling (FEM) and multiphysics simulation, as implemented in COMSOL® have been the principal "workhorse" of semiconductor process work-flow of the MEMS laboratory since many years. Several undergraduate and graduate thesis activities, related to deep brain electrodes, 3D (tactile) force sensors, numerous microfluidics devices were designed and optimized relying on insights gained from parametric simulation and models created in MATLAB® and COMSOL.

This year concluded the development of the thermoelectric measurement device for the FP7 UNION project. The device is capable to carry out the complex task of capturing a micron-size composite cluster of nanoparticles from a solution and measuring electric potential drop across it while exposing it to a temperature gradient.

Also, as part of OTKA PD-105173 (A. Deák: Nanochemistry for controlled self-organization), the finite element framework has been used to study the elementary physical components of the interaction of surface functionalized (core-shell) nanoparticles in electrolyte with each other and a potential wall. We attained the

complete thermodynamical description, changes in the Gibbs free energy depending on characteristic geometrical parameters of the 2D or 3D model systems. An example of the electric potential distribution between two nanoparticles is shown in Fig. 2.

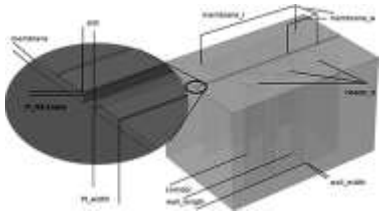

Figure 1 *Schematic view of the parameters of the UNION micro-thermoelectric measure-ment device.*

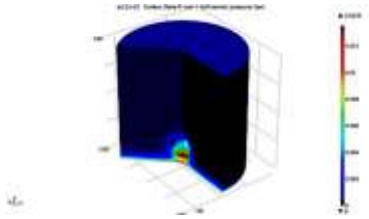

Figure 2 *Van't Hoff osmotic pressure arising from electrostatic interactions in the electrolite near a nanoparticle and potential wall.*

3D interpolated potential for MD

We began development of a novel computational approach, based on multivariate interpolation for a complete and accurate description of three-body interactions in atomic and molecular ensembles. A natural 3-dimensional counterpart of the London dispersion is the so-called Axilrod-Teller-Muto (ATM) potential. For intermediate and large distances, ATM describes the three-body contribution to the energy of interacting particles. When particles (e.g. noble gas atoms) get in the vicinity of each other, quantum-mechanical correlation effects come into domination. Even their approximate (post Hartree-Fock) calculation requires considerable computational resources and time. To make these contributions more available for large ensemble, longer molecular dynamics (MD) simulations, a proper twice differentiable interpolation scheme was developed and implemented, smoothly fitting also the ATM potential at larger distances.

First test calculations on many-body systems (4, 5, 6 atom random clusters of He atoms) show, that the total interaction (or cohesive) energy of these can be very closely approximated by the sums of 2 and 3-body contributions. Fig. 3 shows the example of He-4 clusters.

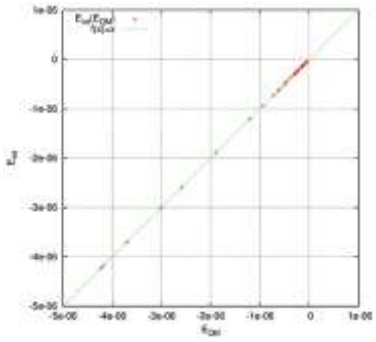

Figure 3 *Comparison of the interpolated and "exact" (QM) cohesive energies of random He-4 clusters. The diagonal (green) line means perfect correspondence, which the red points fall indistinguishably close to.*

Nanosize effect on the evolution of magnetism on curved surfaces

Similarly to the well-known Moore's law for the number of transistors in an integrated circuit, an analogous tendency was recognized by Mark Kryder for magnetic disk storage density. His prediction shows that the capacity of a 2.5" disk will reach 40 TBit/ in^2 by 2020. Several developments are now on the way in order to reach, or even to exceed this density.

There are two dilemmas about storage capacity increase. Once, when the magnetic grains are very small, the further reduction leads to the super-paramagnetic effect, where the spontaneous magnetization fluctuation results in data loss. On the other hand, the magnetostatic and exchange interaction between the adjacent grains sets a limit on how "strong" the magnetization should be in a grain without being perturbed by the neighbors.

A possible solution could rely on bit patterned media where the information unit is bound to a nanostructure. In this case the strong exchange coupling within the particle, the shape anisotropy and the isolation of the particles may increase the energy barrier for thermal switching. Such structures are predicted to be eligible to store up to 20-300 Tbit/in^2. As material properties may differ from bulk when entering the nanoscale regime and this is particularly true for magnetic materials, scientists from all over the world are working to reveal the nanosize effects on magnetism. Our institute EK MFA is also participating in this challenge in cooperation with the ESRF group at the Nuclear Resonance Beamline ID18, the KU Leuven, and the Wigner Research Centre in Budapest.

In this work, an ultrathin iron film was deposited by molecular beam epitaxy (MBE) on a flat silicon substrate as well as on 20 nm and 400 nm diameter silica spheres (Fig. 1), and the effect of morphology such as curvature and interparticle distance, on the evolution of magnetism was studied. The thickness of the iron film was varied in the range where iron shows a nonmagnetic/magnetic transition. To describe the 3D structure, the composition and the magnetic properties of the samples a wide range of analytical tools has been applied such as in situ nuclear forward scattering (NFS), X-ray reflectivity (XRR), grazing-incidence small-angle X-ray scattering (GISAXS) and

ex situ atomic force microscopy (AFM), magnetic force microscopy (MFM), field electron scanning electron microscopy (FESEM), and Rutherford Backscattering Spectrometry with 3D structure evaluation tool (3D-RBS). Based on the detailed characterization, micromagnetic simulations were carried out to model the magnetic moment configurations in the iron cap (Fig. 1).

We concluded that for the two particle diameters largely different evolution of magnetism occurred with increasing the iron thickness. For the 400 nm diameter spheres, the system could be considered as a sum of individual magnetic particles. Here the formed magnetic structure was determined by the topology of the spheres. With increasing the iron thickness, first the upper part of the sphere became magnetic, showing a spiral like (vortex) magnetic pattern on top and out of plane magnetization at the side. For thicker iron layers the out of plane component was gradually eliminated and replaced by a magnetic vortex (Fig. 1b).

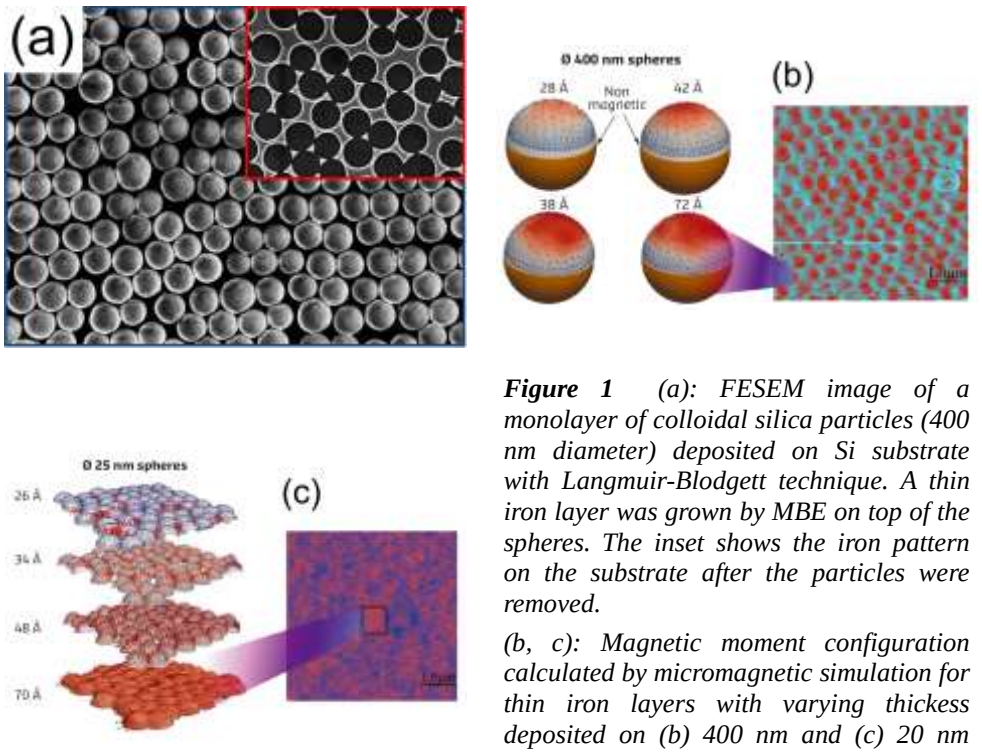

Figure 1 *(a): FESEM image of a monolayer of colloidal silica particles (400 nm diameter) deposited on Si substrate with Langmuir-Blodgett technique. A thin iron layer was grown by MBE on top of the spheres. The inset shows the iron pattern on the substrate after the particles were removed.*

(b, c): Magnetic moment configuration calculated by micromagnetic simulation for thin iron layers with varying thickess deposited on (b) 400 nm and (c) 20 nm diameter silica spheres. The magnetic force microscopy (MFM) images of the thickest iron layer are also shown.

In contrast, for 25 nm diameter particles, iron became magnetic first in the contact region of the spheres and a uniformly distributed, well isolated magnetic structure appeared. With further deposition, the whole layer became magnetic and a topology

independent magnetic structure incorporating several particles with in plane magnetization could be observed (Fig. 1c).

BioMEMS

Activity leader: P. Fürjes

Group members: Zs. Baji, I. Bársony, P. Földesy, Z. Hajnal, A. L. Tóth, V. Rakovics, I. Réti, E. Holczer, and E. Tóth

Projects:

- ENIAC CALL 2013-1 – "Intelligent Catheters in Advanced Systems for Interventions – INCITE"
- OTKA CK 83821 – "Mikrocsatornák készítése protonnyalábos mikromegmunkálással és alkalmazásuk Lab-on-a-chip eszközökben"
- KTIA VKSZ_14 – "Multiparaméteres Point of Care in vitro diagnosztikai rendszerek fejlesztése"
- EURIPIDES / EUREKA 13-1610 – "Particle Matter sensors for indoor air quality – PAMIAQ"

Microfluidic system for separation of circulating tumor cells (CTC)

Cell sorting could have particular importance in medical diagnostics and therapy – see Clinical Cancer Advances – since it can be applicable to select specific cell types or to remove the background cells from such important and limited volume biological samples as taken from blood or liquid biopsy. Microfluidic Cell Capture Devices (MCCDs) are promising tools for detection, capture and enrichment of the targeted cells since the geometrical dimensions of the cells and the applied channels are in the similar order of magnitude. Due to their small dimensions (with the benefit of high surface to volume ratio), they can offer unusual physical behaviour that is in the macroscopic world.

The specific aim of this project is to design and fabricate microfluidic cell capture devices with special 3D geometry utilizing the advances of combining conventional lithography based rapid prototyping with Proton Beam Lithography (PBW) to improve cell manipulation efficiency. Tilted micropillars were fabricated and applied in order to increase the active surface area, the effective cross-section of the capturing microstructures and to modify the local hydrodynamic behaviour in the sample transport system, in cooperation of the research groups of Prof. A. Guttmann (Univ. of Pannonia) and I. Rajta (ATOMKI).

Computational Fluid Dynamics (CFD) simulations revealed that tilting the pillars not only increases their surface area on which the fluid can interact with the bonded affinity layer but also improves the fluid characteristics of the system. Based on the results of the preliminary FEM calculations special 3D structures were designed and fabricated by multiple tilted proton beam writing method in SU-8 epoxy based

negative photoresist and poly-dimethylsiloxane (PDMS) to enhance the cell capturing capability of the proposed microfluidic system. The developed 3D microstructure of the microfabricated cell separation system was imaged by scanning electron microscopy as demonstrated in Fig. 1.

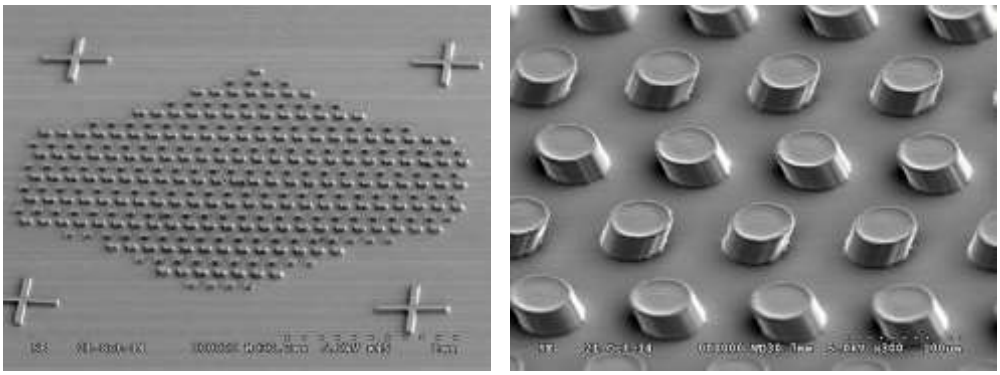

Figure 1 *SEM images of doubly tilted micropillars fabricated from liquid PDMS by polymerization with focused proton beam on the top of a cross-linked PDMS layer.*

The presented methodology and the applied structural materials are compatible with MEMS/NEMS (micro/nano-electromechanical systems) technology considering the integration requirements for subsystem development. The PBW patterned micropillar array was integrated into the transport microfluidic system manufactured by soft lithography and its performance was characterized by cell injection. The sealed device is presented in Fig. 2.

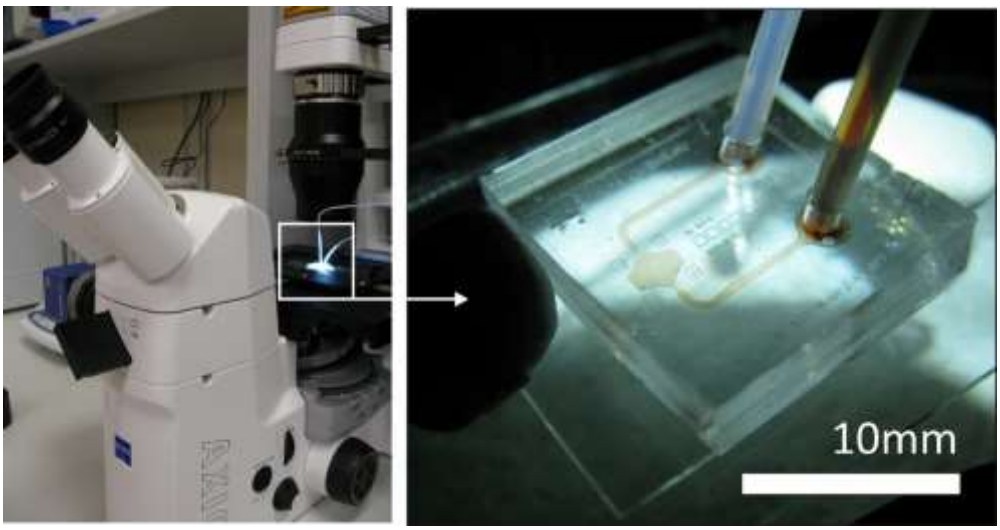

Figure 2 *The fabricated cell capturing device sealed by O_2 plasma enhanced bonding of the microfluidic and sorting subsystems was filled by biological test solution containing yeast cell culture.*

To validate the FEM modeling of the hydrodynamic processes evolving in the cell capturing chamber, the particle movements were monitored in the fabricated microfluidic system by using fungi cells in typically similar size of red blood cells. The cell trajectories were monitored and followed by microscopic imaging. The experienced deterministic lateral displacement is governed by the asymmetric local hydrodynamic characteristics evolving around the tilted pillars. The particle behaviour corresponds to the FEM modeling results clearly demonstrating the asymmetric pressure and shear force distribution near by the tilted micropillars. These satisfied the expectations that the device is capable for size dependent sorting of injected objects and the microfluidic system is offering advanced cell capturing capability at the functionalized surfaces.

Finite Element Modeling (FEM) and characterization of cell and molecular advection in continuous microfluidic systems

The aim of the research is the characterization of the fluid-particle interaction in biological samples (blood, environmental samples, etc.) considering cellular and molecular advection and implementation of targeted preparative functions on microscale. Considering the main sample preparation tasks the behaviour of particle- and cell suspensions in the microfluidic systems was analyzed focusing on the separation of the formed elements and particles by size.
Several medical diagnostic tests are based on human blood as sample solution due to its complex and representative marker molecule composition considering pathological issues. Most of these tests require separation of plasma or serum from the whole blood. Recent development of microfabricated Lab-on-a-Chip systems provides outstanding solutions for analytical problems although integration of high performance continuous separation function is challenging. Passive microfluidic inertial plasma separation structures could be promising candidates due to their relatively simple structure and fabrication technology. Zweifach-Fung bifurcation type microscale separation systems utilize viscous lift and shear forces evolving in the low Reynolds regime and developing a cell-depleted layer near the channel walls. This structure could provide excellent plasma purity in single branch, however, in case of cascade separation systems purity is deteriorated subsequently from branch to branch due to the thinning of the cell-depleted layer. In our work the possible recovery of the cell-free layer was studied considering inertial forces evolving in special geometrical singularities.

Characterization of cascade plasma separation structures

Series of different geometric singularities (six types of different expansions) were integrated with bifurcations branching from main stream channel in order to reveal their inertial effects on particle movement and characterized regarding their enhancement of blood plasma separation performance of cascade Zweifach-Fung bifurcations. The evolving flow behavior and particle trajectories were modeled by

Computational Fluid Dynamics (CFD) simulation and particle tracing modules of COMSOL Multiphysics and the results were verified experimentally by recording particle trajectories. Microfluidic test structures were fabricated by soft lithography in poly-dimethylsiloxane (PDMS) and fungi cells were injected in to reveal particle movement applying dark field microscopy. The modeled flow fields were compared to the recorded particle trajectories in case of different flow rates (Fig. 1).

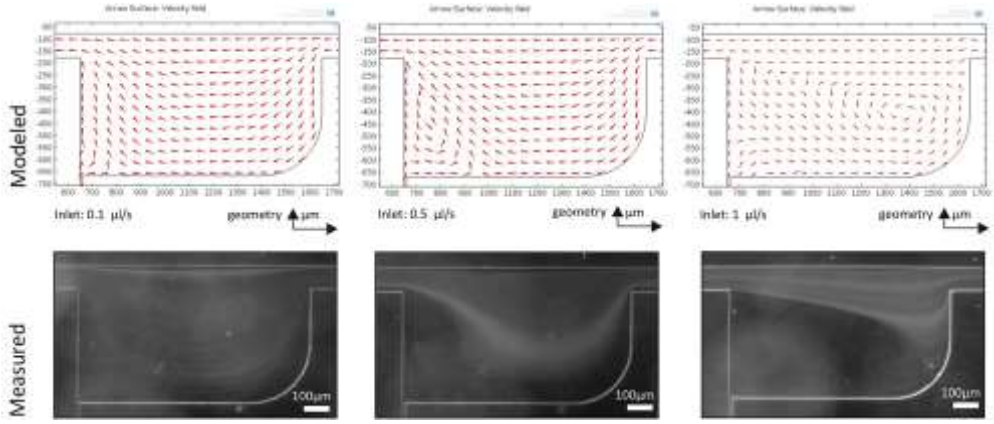

Figure 1 *Modeled flow velocity fields in a representative singularity in case of different injected flow rates compared to the experimentally recorded particle trajectories.*

Both simulation and experiment proved the development of the cell-depleted layer due to the applied series of singularities as demonstrated by the modeled particle distribution and the recorded backscattered intensities in Fig. 2.

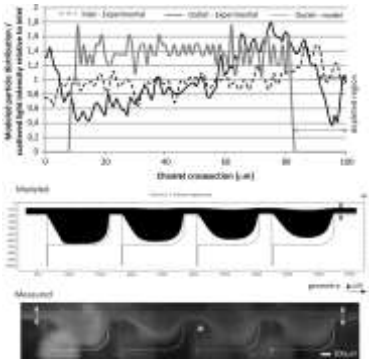

Figure 2 *Modeled and experimentally recorded particle trajectories representing the development of depleted layer. The particle distribution and the measured scattered light intensities demonstrate the effect of lateral migration.*

The development and recovery of a cell-depleted layer near the channel walls due to lift and shear forces were analyzed considering the applied flow rates and number of singularities. To avoid deterioration of plasma purity due to cell recirculation in evolving vortices but maximize separation efficiency optimal flow rate regime was defined for further experiments. The recovery of the cell-free layer in geometrical singularities was validated and their applicability in enhanced cascade type plasma separation systems was proposed. The effect of the developing cell-depleted layer thickness on the plasma purity was studied to prove the improvement of the separation technique due to the integrated inertial subsystems.

Autonomous microfluidic sample transport systems

Autonomous capillary micropumps could be substantial brick stones of cheap, simple and self-powered microfluidic systems being capable to manage the sample transport in Lab-on-a-Chip applications. Accordingly the precise control or improvement of the fluid conducting characteristics of these integrable micropumps is in forefront considering their capacity and efficiency. Moreover the management of the achievable flow rate and the transported sample amount could be critical regarding various applications considering the requirements of controlled microreactors or high sensitive diagnostic devices, and the transported amount has to be adjusted by the geometric and surface parameters of the developed passive pump.

Development of self-driven microfluidic systems

To achieve controlled and autonomous sample transport in Polydimethylsiloxane (PDMS) based microfluidic system the surface behaviour of the material was modified, and the efficient transport of patient serum was proved. Since the functionality of the proposed biosensing/Lab-on-a-Chip device is highly affected by the flow conditions during the sample injection, incubation and washing steps, microfluidic chamber system was developed to ensure controlled transport of the sample suspension over the biosensing surface by capillary forces. The microfluidic structure was fabricated by soft lithography technique in PDMS using SU-8 epoxy based photoresist as molding replica. The PDMS was modified to improve its sample transport performance by embedding special PDMS-b-PEO amphiphilic molecules in the matrix.

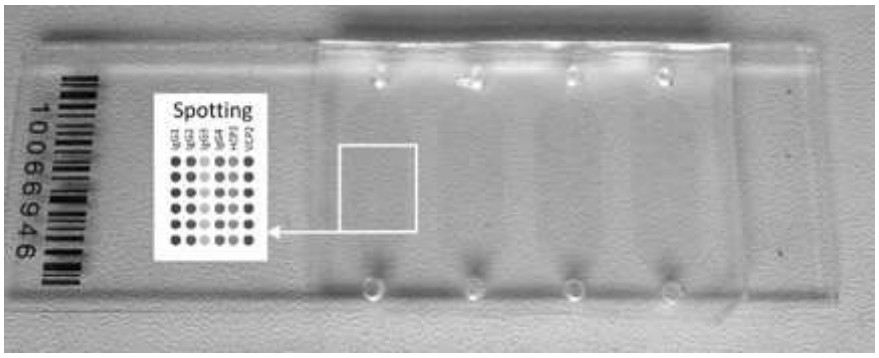

Figure 1 *The fabricated PDMS based microfluidic chamber.*

Biosensing applications

In cooperation with the ELTE/MTA Immunology Research Group the developed self-driven polymer based microfluidic system was applied for a biosensor to be able to monitor immune cell adhesion and activation on protein microarrays consisting of antigens, antibodies and complexes indicating specific autoimmune diseases. Cells as biosensors were applied for monitoring immune complex composition. When the capillary system was mounted above the slide, first serum samples derived from

patients then purified human neutrophil granulocytes were transferred through the capillary system by capillary force. Applying the adequate peptide targets of specific autoantibodies, the adhesion of neutrophil granulocytes on the functionalised surface regions clearly indicated the diseased patient sample. The readout of the assay can be the quantitation of bound fluorescently labeled cells by a microarray scanner as schematically represented in Fig. 2.

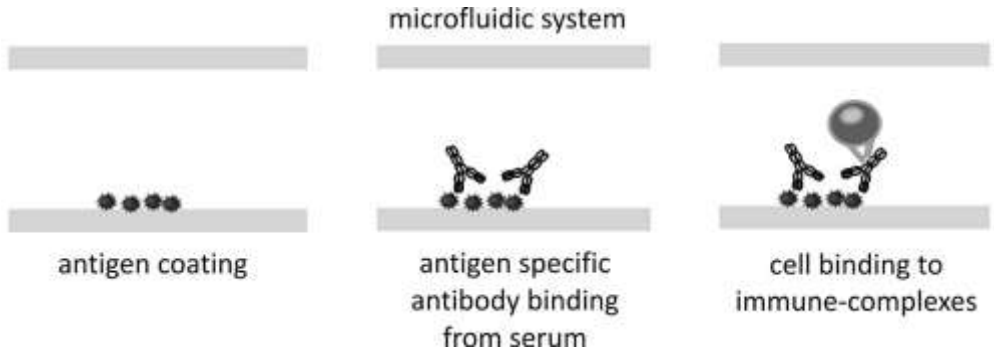

Figure 2 *Schematic working principle of the cell-binding biosensor assay for detection antigen specific antibody in the patient serum.*

We proved that the capillary driven microfluidic transport system applied for filling the sample chambers of microarrays can significantly improve the effective cell binding and the ease of handling and reproducibility of these assays in diagnostics of disease positive patients.

Complex bioinspired microcapillary systems

The functional behaviour of the capillary structures and the non-specific protein binding on the channel surfaces were also studied to prove the auspicious effect of the surface modification. The geometry and the 3D design of the channels were inspired by the most complex natural microfluidic system, the water-conducting tissue (xylem) of trees and different geometric shapes were developed at the bottom of the channels as stripe and serpent type grooves. The combined effects of different 3D geometries and surface modifications were systematically characterized by flow rate measurements applying ultra fast imaging system for recording fluid movement. The surface modification methods were compared and the advantages of bioinspired capillary systems were also demonstrated.
Bioinspired microfluidic structures as fluidic diodes were also designed and characterized to systematically control the sample flow rate and direction in the microcapillary systems. 3D geometry of the skin of Texas Horned Lizard was adopted and proved for flow direction control in autonomous sample transport systems. Based on the preliminary result autonomous sample transport microfluidic systems were designed and fabricated to be integrated in Point-of-Care Lab-on-a-Chip based diagnostic cartridges in the cooperation with 77 Elektronika Ltd.

Cell and particle sorting in microfluidic systems

The aim of the PAMIAQ project in cooperation with Technoorg Linda is the development of a complex analytical system for particle counting and identification by size distribution with integrated sample transport, manipulation and optical detection. Microfluidic systems capable of particle separation by their size utilizing the Dean drive and inertial effects were designed and analyzed. Fluidic chips were fabricated in PDMS by soft lithography and bonded to glass plates. These devices will perform passive separation of the pollutants by their size and the hydrodynamic focusing. The microfluidic devices were characterized with respect to their ability of spatial separation of specific pollutants into sub-channels and focusing of the particles in the field of view of the optical measuring setup maintaining the perme-ability/capacity of the channels. The size ranges of the targeted pollutants were defined as cells – with diameter under 5 μm, particulates with diameter between 1 and 10 μm and pollen with diameter between 10 and 100 μm.

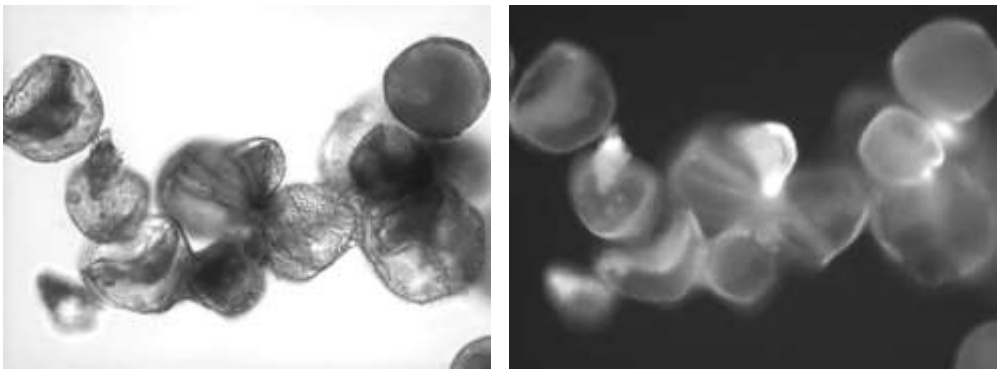

Figure 1 *Tulip pollens visualised by bright field (left) and fluorescent (right) microscopy.*

The channel layout design is based on four physical phenomena. Pinched flow fractionation utilizes the inertia of the particles deflecting their paths in varying degrees based on their size. Inertial and Dean forces divert the smaller particles closer to the channel centre and the larger particles towards the channel walls in curved channels. With hydrodynamic filtering the smaller particles can be separated using a comb-like design and a secondary flow.

The mask layout of the combination of fundamental elements was designed, a manufacturing process and measuring method was defined allowing the optical evaluation of the samples. Fluorescent polystyrene beads (10 and 15μm diameter) were injected into the flow in order to assist optical evaluation. The trajectories of these beads are well defined using fluorescent microscopy.

The combination of Pinched flow fractionation, Dean and Inertial forces was found to be efficient for size dependent particle separation. The hydrodynamic filtering, however were not feasible on the given size scale and technical conditions.

Hydrodynamic 3D focusing was also studied using finite element modeling. The design for the pinched flow fractionation is considered sufficient for the 3D focusing combining the Dean effect with classical 2D hydrodynamic focusing.

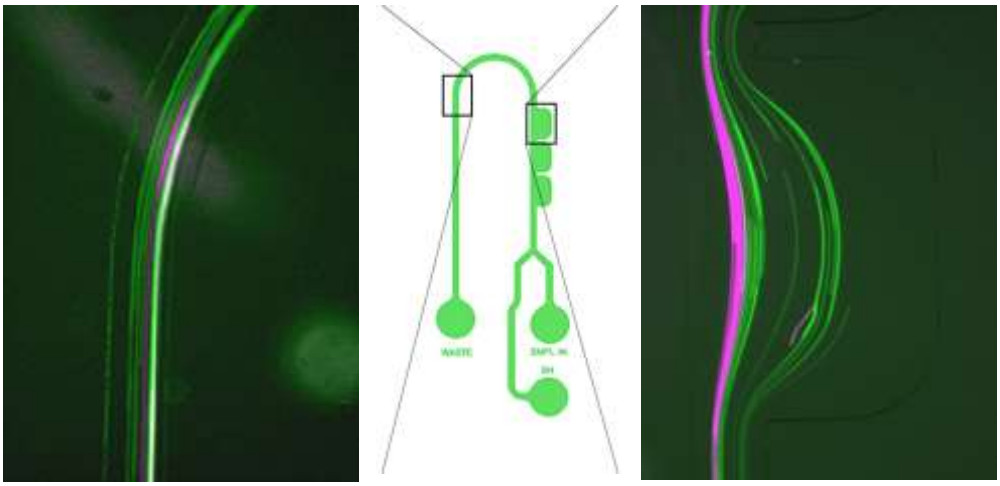

Figure 2 *The size dependent separation of the fluorescently labelled particles were proved by recording their trajectories in the different regions of the microfluidic systems (**10µm: green**, **15µm: violet**).*

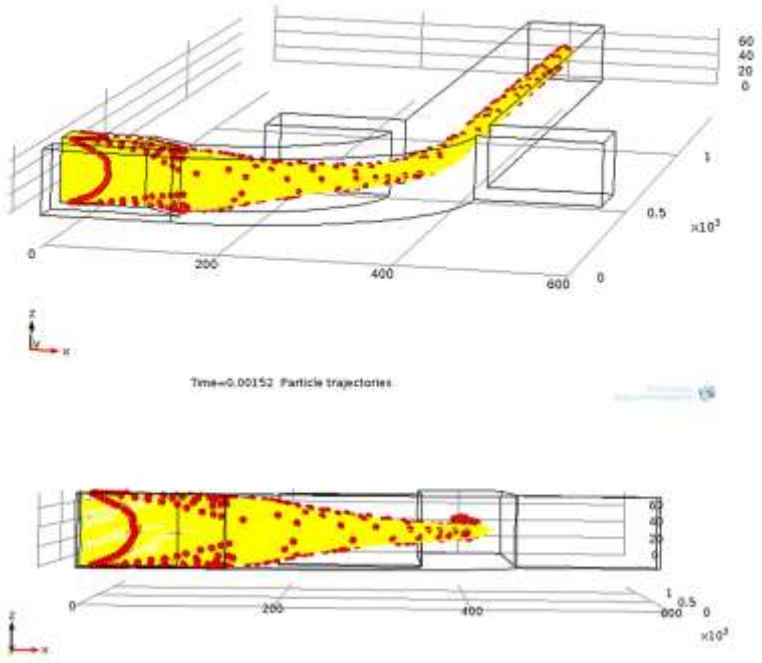

Figure 3 *Finite element modelling of the particle trajectories affected by combined lateral focusing and Dean effects.*

NeuroMEMS

Activity leader: Z. Fekete

Group members: A. Pongrácz, P. Fürjes, I. Lukács, Z. Hajnal, Gy. Molnár, A. L. Tóth, Z. Bérces, and G. Márton

Projects:

- Richter Témapályázat – "Memória és az autizmus kutatásában felhasználható, ipari igényeket kielégítő, lokális gyógyszeradagoló csatornával ellátott sokpólusú szilícium alapú in vivo elektrofiziológiai mérőrendszer fejlesztése szabadon mozgó állatokban történő gyógyszer hatóanyag tesztelésére a pre-klinikai fázisban"
- KTIA 13 NAP A IV/6 National Brain Research Program – "NAP A - MEMS érzékelők és beavatkozók vizsgálata agykutatási célokra"
- KTIA NAP 13-2-2015-0004 – "Hippokampális és mélyagyi struktúrák optikai stimulációjának újszerű megközelítései mikro- és nanotechnológiai megoldásokkal"
- TÉT_14_FR-1-2015-0030 – "Agyi jelek szerveződési szinteken átnyúló integrált módszertani vizsgálata újszerű elektródával"
- OTKA NN 116550 – "Nanostruktúrálás hatásának vizsgálata az idegsejt - szilárdtest kölcsönhatásra agy-gép interfészek fejlesztéséhez"

Silicon probes designed for infrared neural stimulation

Infrared neural stimulation (INS) was discovered in 2005, when action potentials were successfully evoked using infrared light. Histology was performed after revealing that there is a radiant exposure range, where action potentials are elicited without damage. In our work, a Michigan-type silicon microprobe for infrared neural stimulation was designed and investigated in terms of technology induced surface roughness and optical transmission. The fabrication of such optrode was realized by deep reactive ion etching and subsequent wet chemical polishing.

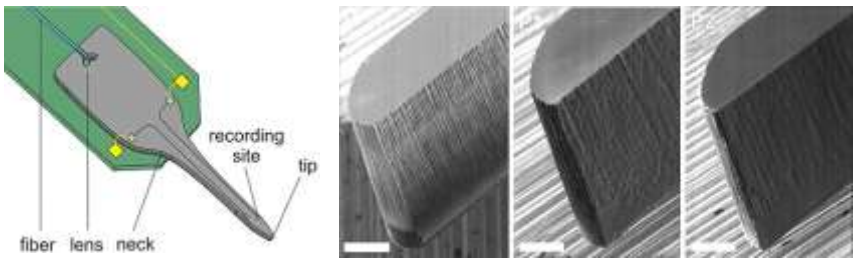

Figure 1 *Concept of a silicon microelectrode that provides infrared stimulation and records the electrical activity of neurons simultaneously (a). Perspective and side view of the microprobe tips. R: reference sample before polishing. P1, P2: polished samples after one and two minutes, respectively. Scale bar is 100 µm.*

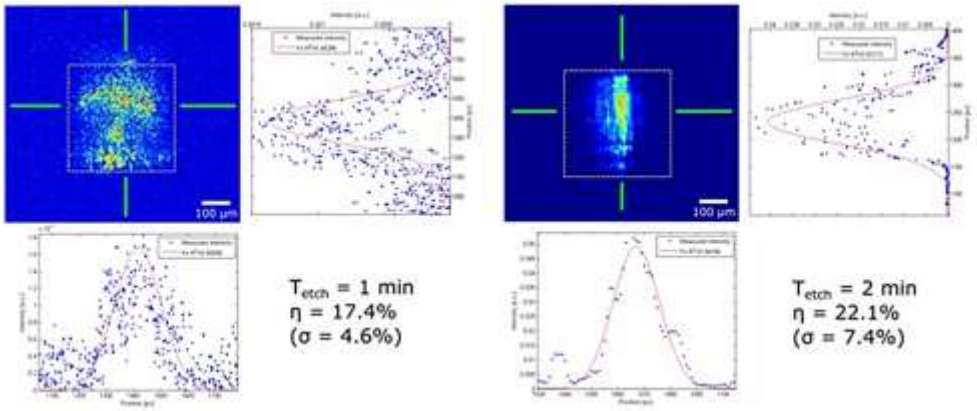

Figure 2 *Beam profile of P1 (a-c) and P2 (d-f). Dashed yellow lines represent the contour of the probe shaft, while green lines indicate the X and Y cross-section of represented data on optical power.*

The overall efficiency was further boosted by integrated couplers and focusing microlenses etched into the silicon substrate. Due to the proposed fabrication approach, 22.1% in system efficiency was achieved at a wavelength of 1310 nm. We observed that system efficiency does not increase significantly by increasing the time of sidewall polishing; however, the beam shaping effect of the coupling lens is more remarkable, if the tip roughness is reduced down to 8.7 nm RMS value. The spatial distribution of the delivered light can be also controlled through integrated micromirrors at the probe tip, which facilitates lateral out-coupling with a Gaussian beam profile.

Iontophoretic injection microsystem delivering pathway tracer molecules in the living tissue

Exploring the structure and function of the brain's connectome is in one of the major scope of recent neuroscience research. Complementing neuronal recording with pathway tracing is still an indispensable tool to achieve such goals specifically at the microcircuit (single neurons) and mesoscale (neuronal populations) levels of the neural network. However, electrophysiology and neuronal tract tracing are usually applied separately even if combined in the same experiment. In our work, we present the results of *in vivo* local release of a neuronal tracer, biotinylated dextran amine (BDA) in the rat somatosensory cortex using monolithically integrated microfluidic channel of a silicon neural microelectrode. The tracer injection is controlled by iontophoresis using Pt electrodes in the vicinity of the outlet of the microfluidic channel. Using 3-5 µA, 5-7 s on/off cycle and 15-20 min total injection time the localized injection resulted in clear anterograde and retrograde BDA labeling both within the cortex and in subcortical structures. Anterograde and retrograde labeling revealed the fine details of neuronal processes including dendritic spines and axon

terminal-like endings. Injection sites appeared clear lacking any strong diffuse background labelling. Electrophysiological recording performed with the same microdevice immediately after the iontophoresis indicated normal cortical functioning. The results prove that the combination of in vivo multichannel neural recording and controlled tracer injection using a single implanted microdevice is feasible, and therefore it can be a powerful tool for studying the connectome of the brain.

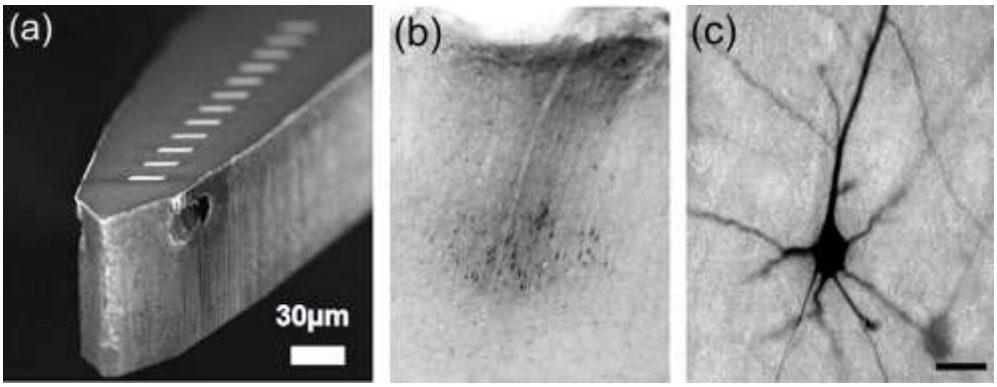

Figure 1 *(a): SEM image of a silicon neural electrode with 12 Pt contact sites on the top surface and two buried microfluidic channels. The outlets of the channels are on the sidewalls. Contact closest to the outlet serves as counter electrode during iontophoresis, while the reference electrode is placed in the microfluidic interface connected to the probe. The remaining contacts are applied for electrophysiology. (b): BDA labeled neuronal cell bodies (black dots) are present all along the electrode track and accumulate in the deep layers. Note the lack of a dense tracer deposit and that the labeled neurons are clearly distinguishable. (c): Close view of a both anterogradey and retrogradely labelled neuron.*

Polymer microECoGs optimized for in vivo pharmacological investigations

The connectivity between the cortical representations of the visual system through temporary oscillations plays an important role in the pathomechanism of the so-called connectome diseases like schizophrenia or autism. The complexity of the visual cortex makes it difficult to find a reliable electrophysiology technique, which is able to measure the electrical activity of the whole cortical connectome simultaneously. Our goal was to elaborate a chronically implantable polymer based microelectrode grid that is able to monitor large cortical areas in rodents. The feasibility of the subdural electrode system was tested in visual steady-state response experiments, in ketamine induced schizophrenia models and in 4-aminopiridin induced epilepsy models using mature Wistar rats. Our results prove the potential of our microelectrode grid system in future pharmacological research.

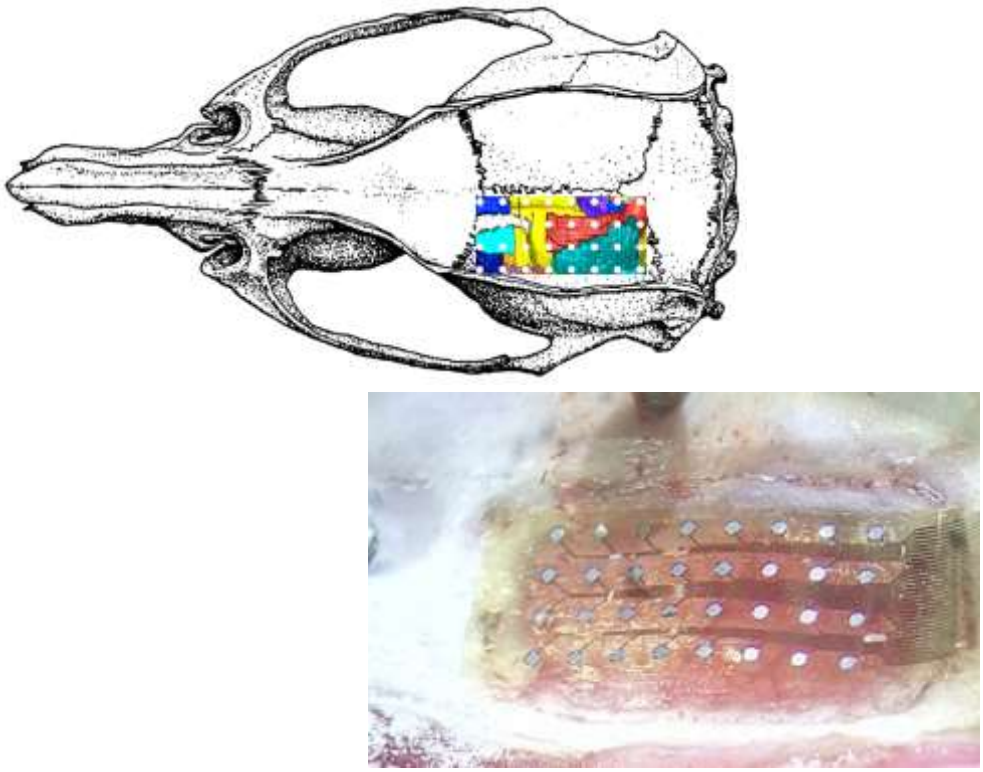

Figure 1 *Schematic of rat skull with the implantation sites of the microgrid (left). Our polymer microgrid during surgery (right).*

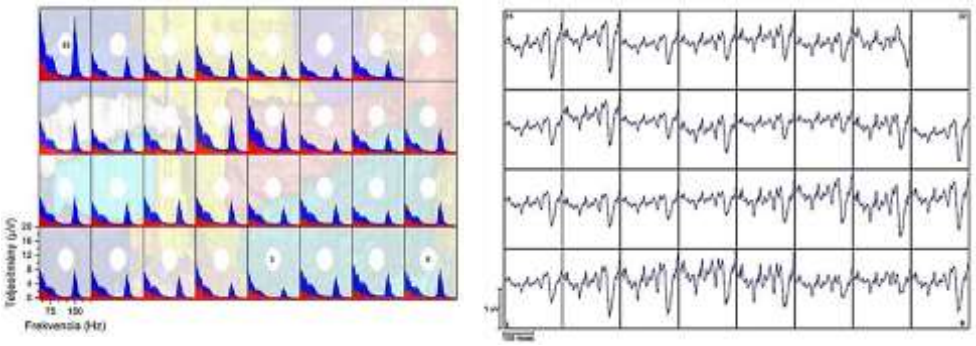

Figure 2 *Ketamine induced dissociation state in schizophrenia animal model. Red and blue area represent spectral power density in a control period (10s) and after ketamine injection (10s). Measurements were using a 32-channel microelectrode grid directly placed on the visual cortex. Fig. 4: EEG recorded by our microgrid during an epileptic seizure after 4-AP injection.*

In vitro studies revealing the immune response of the living tissue to nanostructured implant surfaces

Our goal is to design and fabricate nanostructured surfaces to reduce the extent of glial cell encapsulation of Central Nervous System implants and to promote neural attachment and regeneration, which improve the biocompatibility and functionality of the interfaces. Recent findings showed that specific glial cells prefer flat surfaces over nanostructured ones with certain geometries, while neural cells proliferate both on nanostructured and flat surfaces.

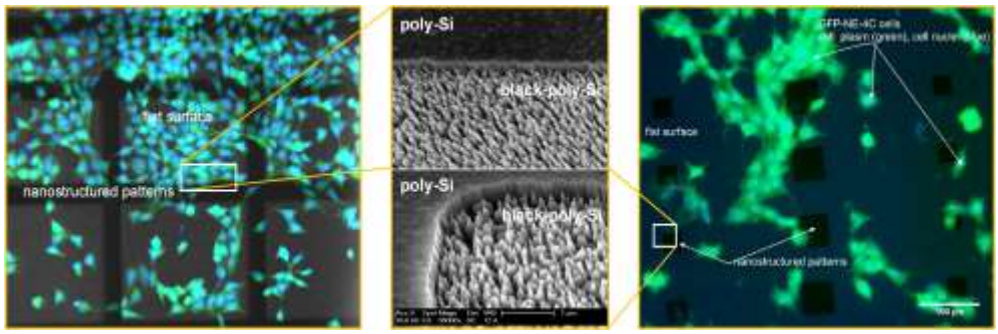

Figure 1 *Two channel fluorescent images of GFP-NE-4C cells on nanostroctured chips after 24h adhesion (blue channel: DAPI staining - cell nuclei; green channel: green light is emitted by the GFP expressed in the cytoplasma). Black regions are the nanostructured patterns on the samples. Inset images show the transition region, where flat poly-Si regions meet the nanostructured Si grass. Nanostructured surfaces are less preferred by the NE-4C cells compared to flat regions.*

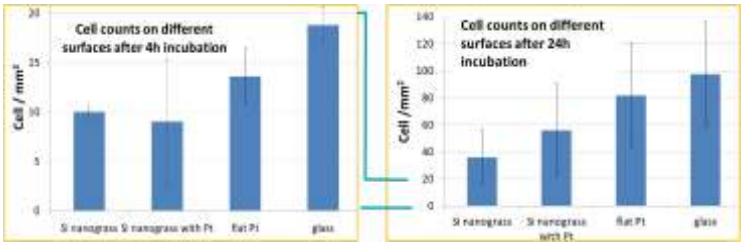

Figure 2 *Comparison of cell counts after 4 hr and 24 hr long incubation of NE-4C neural progenitor cells on different surface types (nanostructured Si, nanostructured Pt, flat Pt and glass). Nanostructured regions hinders the adhesion of the stem cells compared to their flat references.*

Neural progenitor cells were cultured on flat and nanostructured Si and Pt surfaces. Based on the MTT tests, the nanostructured surfaces are non-toxic compared to the glass surfaces. Cell adhesion was hindered by the nanostructured surfaces compared to the flat ones. Analysis of fluorescent microscopy images suggests that the cell number increases on every investigated surface type (Si nanograss, Pt, nano-structured Pt, glass), however, the proliferation is slower on nanostructured regions.

NEMS

Activity leader: J. Volk

Group members: Zs. Baji, G. Battistig, Cs. Dücső, P. Földesy, N. Q. Khánh, I. Lukács, Gy. Molnár, A. L. Tóth, Zs. Zolnai, R. Erdélyi, Z. Szabó, and I. Bársony

Projects:

- OTKA K108869 – "Széles tiltott sávú félvezető anyagok, nanoszerkezetek és korszerű eszközök"
- OTKA K112114 – "Kombinált mikro-nanotechnológiai eljárások és ellenőrzésük lokális analitikai technikákkal: a mintázatképzéstől az alkalmazások felé"
- FP7-ICT-2013-10- 611019 – "High-resolution fingerprint sensing with vertical piezoelectric nanowire matrices (PiezoMAT)"

Homogeneous transparent conductive ZnO:Ga by ALD for large LED wafers

Transparent conductive oxides are widely used in photovoltaics, thin film transistors and light emitting devices. The most common TCO material is indium doped tin oxide (ITO), but in the past decades the price of indium has been rapidly increasing. One of the most promising replacements due to its excellent transparency in the visible wavelength range and similar electrical conductivity is highly n-doped zinc oxide. Ga doped ZnO (GZO) has an excellent transparency and low resistivity combined with an electrical stability at elevated temperatures and excellent crystalline properties. Atomic layer deposition (ALD) is a promising candidate to produce high quality GZO layers at relatively low temperatures (300 °C) and at large wafer sizes as well.

We used atomic layer deposition to acquire a series of GZO thin films with varying nominal Ga concentrations. Homogeneity tests were carried out on GZO thin films deposited on a 4" glass wafer. The effect of the annealing and the fabricated devices were investigated on GZO layers deposited on a commercial InGaN/GaN LED-wafer, whereas for electric and electroluminescence measurements fully processed GZO coated LED-chips were used. We also tried a number of different thermal annealing processes to gain a film with properties optimized for LED applications.

To find the optimal concentration, GZO/c-sapphire films with Ga concentrations of 1, 2, 3, 4, 5, and 10 at% were used. According to the Hall measurements, the increasing doping level reduces the specific resistivity of the layers down to 3.3×10^{-4} Ωcm at 3 at% then it increases monotonously with the growing doping concentration. This behavior is governed mainly by the change in free carrier concentration: The doping increases the free carrier concentration up to 1.38×10^{21} cm^{-3}, until reaching an optimal Ga content of 3 at%. In this regime the volume concentration of Ga is close to

the free carrier concentration, which indicates a nearly perfect, uncompensated substitutional doping at Zn cation sites (GaZn). In contrast, the electron mobility decreases from 17 to 11 $cm^2V^{-1}s^{-1}$ as the Ga concentration increases from 1 to 10 at%. This can be attributed to the ionized impurity scattering.
The homogeneity of the GZO layers with respect to thickness and conductivity was tested on a 4" diameter glass wafer. As it can be seen in Fig. 1, the wafer scale uniformity of the films was excellent. The relative standard deviation of the average thickness was 2.1 %. As revealed by Eddy current mapping the ALD GZO layer has an average sheet resistance value of 137.1±2.7 Ohm/sq and a relative uniformity of 2.0 % over the wafer (Fig. 1b). By calculating the specific resistivity map as a production of t and R_{sh} we obtain an excellent uniformity of 0.8 % (Fig. 1c).

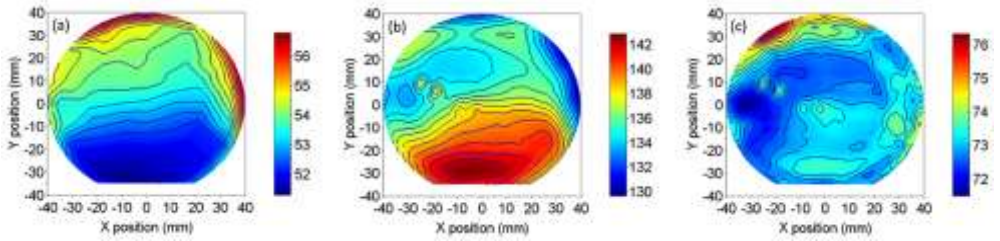

Figure 1 *Thickness (a), sheet resistance (b), and the calculated resistivity map (c), recorded on a limited wafer area in a diameter of 80mm.*

For LED operation it is also essential to have a high electrical quality TCO/p-GaN interface with ohmic conduction. In order to address this issue, a proper thermal annealing sequence had to be adopted. We carried out a series of post deposition thermal annealing experiments in the range of 400-800 °C, i.e. above the deposition temperature of 300 °C. Tests by the transmission line method on ALD GZO deposited on commercial InGaN/GaN blue LED wafers were performed. With increasing annealing temperature we found that the I-V curve is gradually improving and becoming fully linear at 700 °C. On the other hand the annealing at such a high temperature deteriorated the bulk conductivity of the GZO films. Therefore we introduced an 'interrupted growth by ALD' method i.e. the annealing was performed on a thin ALD grown buffer-layer (of ca. 15 nm). The deposition of the missing thickness followed after that by a second ALD step. This two-step deposition scheme resulted in a slightly improved threshold voltage compared to the as deposited one (2.8 vs 2.9 V, at I=20 mA), which is even more prominent at higher currents (20-100 mA) (blue vs. black solid line in Fig. 2.). More importantly, the two-step annealing treatment led to a ca. 40-times enhancement in electroluminescence intensity at a driving current of 20 mA (blue vs. black dashed line in Fig. 2).
As a conclusion, ALD proved to be a promising candidate for the deposition of Ga doped ZnO films for LED applications. The 3% doped GZO films have excellent electrical properties, and an annealing treatment can also optimize the quality of the GZO/p-GaN interface.

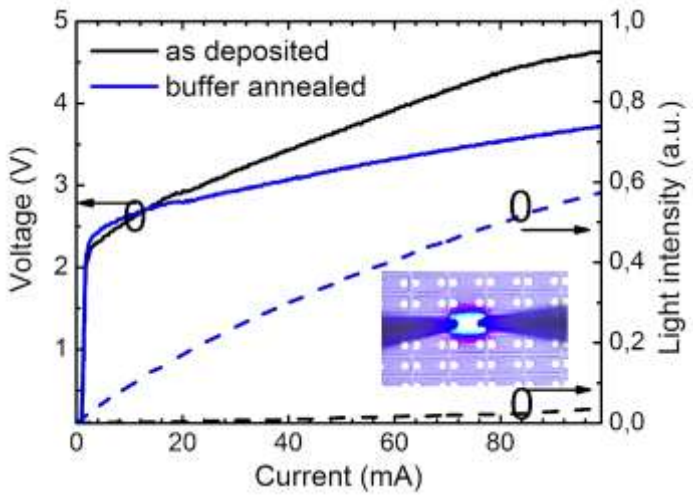

Figure 2 *Voltage (left vertical axis) and output electroluminescence intensity (right vertical axis) as a function of driving current recorded on the LEDs for the thin (ca. 45 nm) non-annealed (black) and 2-step deposited annealed GZO TCO (blue), respectively.*

Double Markers for Direct Contact Formation on Ultra-Low Dimension Objects

For contact formation on very small objects, like TiO_2 nanowires (NWs) with ultra-low dimensions (few nm wide and few tens nm long), determination of the coordinates of the objects in a pre-deposited marker array is a challenge. Thin NWs are hard to see by Scanning Electron Microscopy (SEM), because of weak contrast. Also, the sample becomes contaminated fast at such high SEM magnification.

So far, we carried out very thin metal contact pairs formation with very narrow gap (few tens of nm) to avoid the problem mentioned above. Then Atomic Force Microscope (AFM) has been used to find the adequate NWs, which were accidently contacted at both ends. Later on, the second metal is to be deposited to make a connection between the leads and the contact pairs. This approach therefore, is very time-consuming due to large number of AFM measurement. Also, the NW's location to the contact is not well controlled. With the new facility (RAITH 150), we have developed a novel technique, where we use a double marker array to enable the contact formation directly on a selected NW.

In our new approach, the thick markers are used to give sufficient contrast of SEM image for alignment at e-beam lithography, while the thinner ones ensure fast determination of the wire coordinates by AFM. The main steps of the procedure are followings:

- Thick marker formation by e-beam lithography and metal deposition. Markers are exposed during alignment procedure, so the thick markers ought not to be located close to the object to be processed
- Thin marker formation with alignment on thick markers
- AFM measurement at thin makers
- Object selection and contact design based on the AFM images
- Contact formation using thick markers

Despite of uncertainties (errors at thick marker alignments, drift in AFM measurements), the results of all NWs of the batch (8 NWs) are acceptable as seen on Fig. 1.

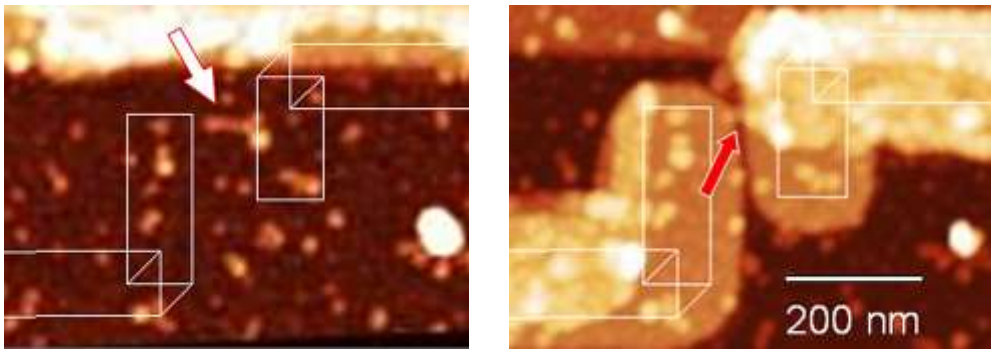

Figure 1 *AFM image of the NW to be contacted indicated by the arrow, the contact design is also shown. Part of the thin marker can be seen on the top of the image (left). Contacted NW with ca. 24 nm gap (right).*

Thin Film Physics Department

Head: Dr. Béla PÉCZ, D.Sc., Scientific Advisor

Research Staff

- Katalin BALÁZSI, Ph.D., Deputy Head of Department
- Ildikó CORA, Ph.D.
- Zsolt CZIGÁNY, D.Sc.
- László DOBOS, Ph.D.
- András KOVÁCS, Ph.D., (on leave: Ernst-Ruska Centrum, Jülich)
- Viktória KOVÁCSNÉ-KIS, Ph.D.
- Miklós MENYHÁRD, D.Sc. (Prof. Emeritus)
- Fanni MISJÁK, Ph.D.
- György RADNÓCZI, D.Sc.
- György Zoltán RADNÓCZI, Ph.D.
- György SÁFRÁN, C.Sc.
- Attila SULYOK, Ph.D.
- Péter SÜLE, Ph.D.
- Lajos TÓTH, C.Sc.
- Orsolya TAPASZTÓ, Ph.D.
- Árpád BARNA, D.Sc., emeritus inst.
- Péter B. BARNA, D.Sc., emeritus inst.
- György GERGELY, D.Sc., emeritus inst.

Ph.D. students

- Zsolt FOGARASSY
- Ákos Koppány KISS
- János SZÍVÓS
- Nikolett OLÁH
- Márton SZENDRŐ
- Erzsébet DÓDONY

Technical Staff

- Noémi SZÁSZ
- Sándor GURBÁN
- Andor KOVÁCS
- István KOVÁCS
- Katalin PUSKÁS (50%)
- Viktor VARGA
- Fenyvesiné Andrea JAKAB
- Valéria OSVÁTH (50%)

Thin Film Physics Department was dealing with numerous subjects in 2015; four main research areas were in focus. The first one was the study of the structure evolution in polycrystalline layers, development of thin coatings, and layers for hard coatings, for magnetic layers and for composites. Development of biocompatible surgical implants was also an important part of this area. The first results on high entropy alloys were achieved. Second main subject was the research of semiconductor layers, heterostructures. The morphology of graphene which influences the electronic properties was determined. After a project was successfully finished on heat management in high power gallium nitride devices, papers with high recognition were published on the heat conductivity of diamond. A lot of new information was collected how nickel can induce crystallization of amorphous silicon. The third main field of study was the development of methodology in electron diffraction and on ion-solid interactions. The most recent results presented tools for

the description of grain boundaries based on electron precession on grain boundary characterization based on electron diffraction. The last subject studied was the development of ceramic/graphene nanocomposites by powder technology for tribological applications in aqueous environments.
In 2015, 28 papers were published in refereed journals with cumulative impact factor of 91, and additional 15 papers in conference publications with no impact factor. The members of the group presented 8 invited lectures, 15 oral talks and 23 posters at international conferences. The group received 1400 independent citations in the examined interval of the last two years.
Summarizing other activities, members of the group lectured three theoretical courses at universities and four members held laboratory practices, all courses were for full semesters (ELTE, BME). Additionally, 12 weeks of summer practice and special labs were also conducted. In addition to the 5 Ph.D. students, 3 diploma workers were also supervised.
Social activity of the group is landmarked by 15 memberships in different committees of the Hungarian Academy of Sciences (HAS) and of boards of societies, giving two elected representatives to the General Assembly of the Academy of Sciences.
Our colleauge, Prof. Peter B. Barna received for his lifetime achievements the prestigious R. F. Bunshah Award (http://www.mfa.kfki.hu/hu/node/827/).

New approaches in the development of Hypoallergenic implant material in Orthopedics: steps to personalised medicine

(OTKA 105355, EU FP7 HypOrth)

K. Balázsi, O. Tapasztó, N. Oláh, Zs. Fogarassy, V. Varga, D. Delfonse (Mathys, Switzerland), C. Lohman (Magdeburg Un., Germany), J. Lorenzen (Teknologisk Institute, Denmark), M. Ignatiev (INOP, Poland), and Cs. Balázsi

The European collaborative project HypOrth (http://www.hyporth.eu/) aims to develop hypoallergenic material for endoprostheses, pursuing two major goals: HypOrth intends to improve the understanding and diagnosis of complications associated with an implant, primarily focussing on adverse immune reaction and infection. Based on these insights the project is developing innovative approaches for renewals in orthopaedic arthroplasty with improved biocompatibility.
The project central database allows the compilation of all relevant data and brings together clinical and scientific results. These data are also available to material researchers and developers. For patients with the risk of getting an adverse immune reaction to conventional material composition we developed a new material combination with hypoallergenic and antibacterial properties and a new hypoallergenic endoprosthesis prototype.
The materials used for artificial prosthesis by default are Titanium ($TiAl_6V_4$, $TiAl_6Nb_7$ – forged alloy), CoCrMo (forged alloy), ceramics and UHMWPE (Ultra High Molecular Weight PolyEthylene).

The role of Thin Film Physics Department is the development of novel ceramic coatings for existing Mathys implants. The main part of research is confidential.

Characterization of biocompatible ceramic TiC / amorphous C thin films prepared by DC magnetron sputtering

(EU FP7 „HypOrth 602398: New approaches in the development of Hypoallergenic implant material in Orthopaedics: steps to personalised medicine)

N. Oláh, Zs. Fogarassy, A. Sulyok, J.Szívós, M. Veres (Wigner Research Centre for Physics), G. Kaptay (Bay Zoltán Nonprofit Ltd for Applied Research), T. Csanádi (IMR SAS, Slovakia), and K. Balázsi

Over the last few years, TiC/a:C nanocomposite protective surface coatings, consisting of hard TiC nanoparticles embedded in a soft amorphous matrix, have attracted a special attention because of their passivation effect on different implant materials. Therefore, our development is focused on the biological application of these thin films [http://www.hyporth.eu/].

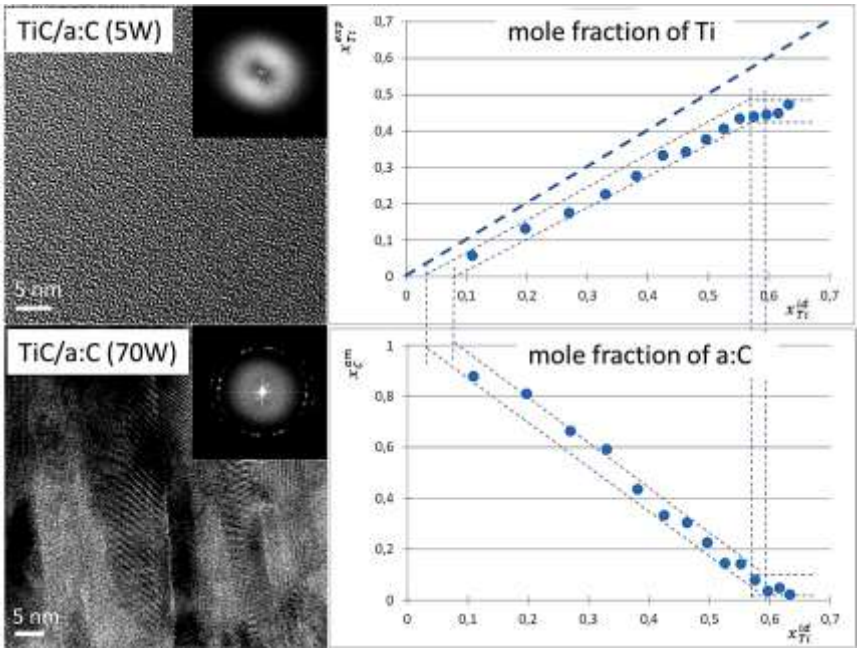

Figure 1 *Structure of TiC/a:C films by HRTEM deposited at 5 and 70 W of Ti target power (left) and the measured mole fraction of Ti in the deposited layer (over) and the measured mole fraction of amorphous carbon in the deposited layer (under).*

The main goal of our research work is the understanding of deposited TiC/a:C growth mechanism and the determination of TiC crystal formation at different Ti:C ratios. A secondary aim was to investigate the relationship between the exact elemental composition and mechanical and tribological properties of the different films.
TiC/a:C thin films were prepared by DC magnetron sputtering. The detailed preparation steps of the coatings were described in our previous works [N. Oláh, M. Veres, A. Sulyok, et al., J Eur Ceram Soc. 34(14) (2014) 3421-3425], [N. Oláh, Zs. Fogarassy, et al., Ceram. Inter. 41(4) (2014) 5863-5871]. Magnetron sputtering of carbon and titanium were performed simultaneously. The film´s composition and morphology were studied in details by High Resolution Transmission Electron Microscopy (HRTEM), X-ray photoelectron spectroscopy (XPS) and Raman spectroscopy. The mechanical characteristics of the TiC/a:C thin films were investigated by nanoindentation technique while the tribological behavior of the films was examined by a ball-on-disk tester (CSM tribometer) moving on circular trajectory at room temperature.
Very good agreement was observed between theoretical calculations and experimental measurements. The thickness of amorphous carbon matrix decreased simultaneously with the increasing Ti content. The amorphous carbon has not gone through to a graphitization process. The highest hardness (H) of ~ 26 GPa and modulus of elasticity (E) of ~ 140 GPa with friction coefficient of 0.268 was observed in case of the film prepared at ~ 40 at% Ti content (by XPS) which consisted of 4-10 nm width TiC columns separated by 2-3 nm thin a:C layers. The H^3/E^2 ratio was 0.9 GPa that predicts high resistance to plastic deformation of the C-Ti nanocomposites beside moderate wear-resistant properties (H/E=0.19).

Graphene-ceramic composites for tribological application in aqueous environments

(OTKA M-ERANET "Grace")

O. Tapasztó, Zs. Fogarassy, V. Varga, C. Balázsi (Bay Zoltán Ltd, Hungary),
J. Dusza (IMR SAS, Slovakia), A. Kailer (IMW Franhoufer, Germany), and K. Balázsi

Advanced ceramic materials have proved their superior wear resistance as well as mechanical and chemical properties in a wide range of industrial applications. Today there are standard materials for components and tools that are exposed to severe tribological, thermal or corrosive conditions. The main aim of the project is to develop novel, highly efficient tribological systems on the basis of functionalized graphene and ceramic-graphene-nanocomposites and to prove their superior quality and suitability for technical applications e.g., for slide bearings and face seals in aqueous media.
Current research in the field of ceramic nanocomposites shows that is possible to make ceramic materials with improved mechanical and tribological properties by incorporating graphene into the ceramic microstructure. The electric conductivity of

these materials, which is reached already at low graphene contents, offers the possibility to reduce efforts in manufacture and to create new functions that may be utilized in technical applications.

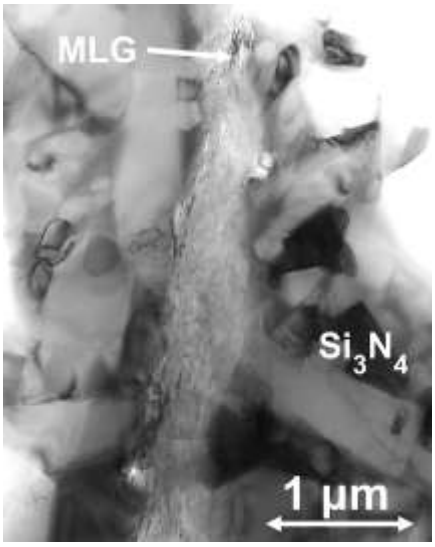

Figure 1a *Milled and hot pressed Si_3N_4 composite with 10 wt% MLG.*

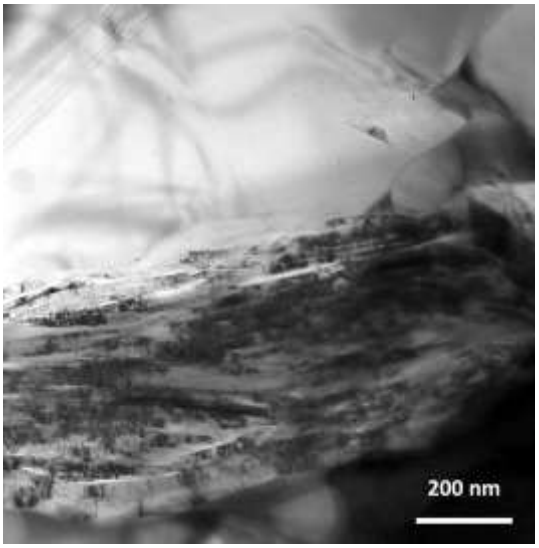

Figure 1b *Milled and hot pressed Si_3N_4 composite with 10 wt% MLG.*

Multilayered graphene (MLG) was prepared by attritor milling technique. 10 hours intensive milling of 1 and 5 micrometer sized graphite powders yielded MLG with 20-30 layers. The large quantity, very cheap and quick preparation process is a main strength of our MLG. Si_3N_4 / graphene nanocomposites prepared by attritor milling and sintered by spark plasma sintering (SPS, partner IMR SAS, Fig. 1a) and hot pressing (HP, partner IMR SAS, Fig. 1b). The Si_3N_4 with 1wt%, 3wt%, 5wt% and 10wt% MLG were produced and their structure was fully examined by our department.

This new approach is very promising, since ceramic microstructures can be designed, that are electrically conductive, possess high toughness and provide improved wear resistance at low friction. Furthermore, electrical conductivity can be utilized for monitoring and electrochemical protection devices.

Low cycle thermomechanical fatigue of a reactor steel: microstructural investigations

(TAMOP 4.2.2.A-11/1 /KONV-2012-0027, Dunaújvárosi Egyetem)

B. Fekete[1,2], F. Misják[3], P. Trampus[1], and G. Radnóczi[3]

[1]College of Dunaújváros, Táncsics u. 1A, Dunaújváros, H-2400 Hungary
[2] Deptment of Applied Mechanics, Budapest University of Technology and Economics,Műegyetem rakpart 5, Budapest, H-1111 Hungary
[3]MTA EK MFA, 1121 Budapest, Konkoly-Thege M. u. 29-33

One of the possible damage mechanisms in pressurized water reactors is the low cycle thermomechanical fatigue caused by simultaneous thermal and mechanical loading, during transient operating processes (e.g., at start up and shut down) and accident conditions. The reactor pressure vessel has a key role in the safety of the nuclear power plant operation and possible lifetime extension. It is necessary to ensure the integrity of the reactor pressure vessel during normal and off-normal operating conditions, so the knowledge on low cycle fatigue degradation phenomena is important. In this work we investigated the thermomechanical low cycle fatigue behaviour of the VVER-440 reactor pressure vessel structural materials. Low cycle continuous and interrupted thermomechanical fatigue tests were made on the base metal (15Ch2MFA) of the vessel at parameters corresponding to the exploitation conditions in the reactor. The measurements were carried out at thermo-mechanical fatigue conditions in the range of 150-270 ^{o}C using the GEEBLE 3800 mechanical simulator. All fatigue tests were carried out with a symmetric cyclic strain and a triangular waveform at frequency of 0.083 Hz. The longitudinal total strain amplitude level was 0.3 %. The lifetime of the material was determined to be 2376 cycles. Interrupted fatigue tests were carried out to investigate the kinetics of the fatigue softening of the material at different stages of its lifetime.

Transmission electron microscopy measurements made at different stages of fatigue test show that the dislocation concentration after an initial increase starts decreasing (Fig. 1). At about 50 % of the nominal lifetime the structure of grain and cell boundaries changes from strained to relaxed, i.e. the strain field of captured dislocations (Fig. 2a) dynamically disappears. The recovery of dislocation substructure resulted in decrease of dislocation density accompanied with boundary movements, which are well seen in the TEM images (Fig 2b). The reduction of dislocation density can be a result of two simultaneously operating mechanisms: annihilation during movement and entrapment in cell boundaries. Then the micro-deformation process will be continued in the grain boundaries, where micro cracks initiate.

The investigated low cycle fatigue behaviour can provide reference for remaining life assessment and lifetime extension analysis of Nuclear Power Plant components.

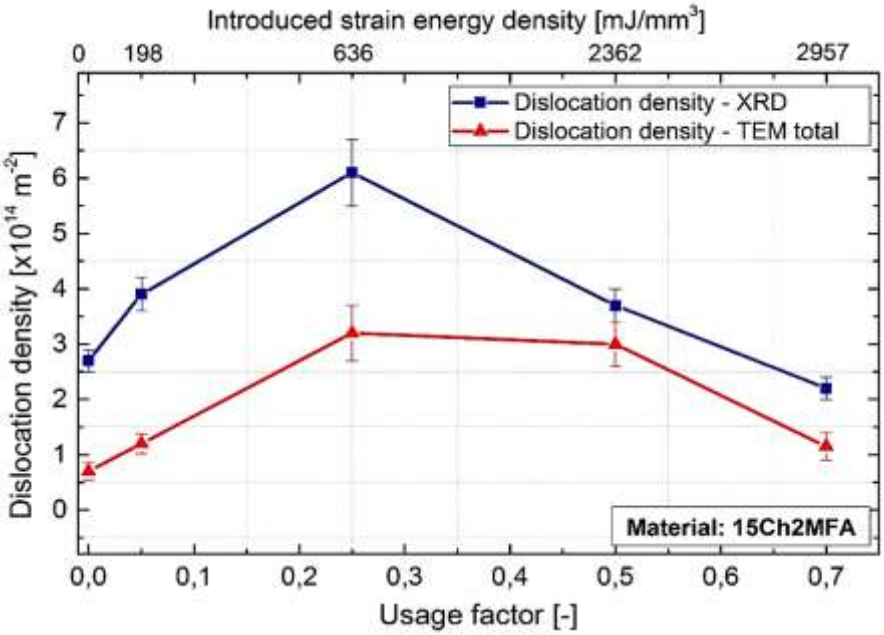

Figure 1 *The variation of dislocation density as the function of the lifetime under thermo-mechanical treatment. (The X-ray measurement was performed at the Eötvös University by Bertalan Jóni.)*

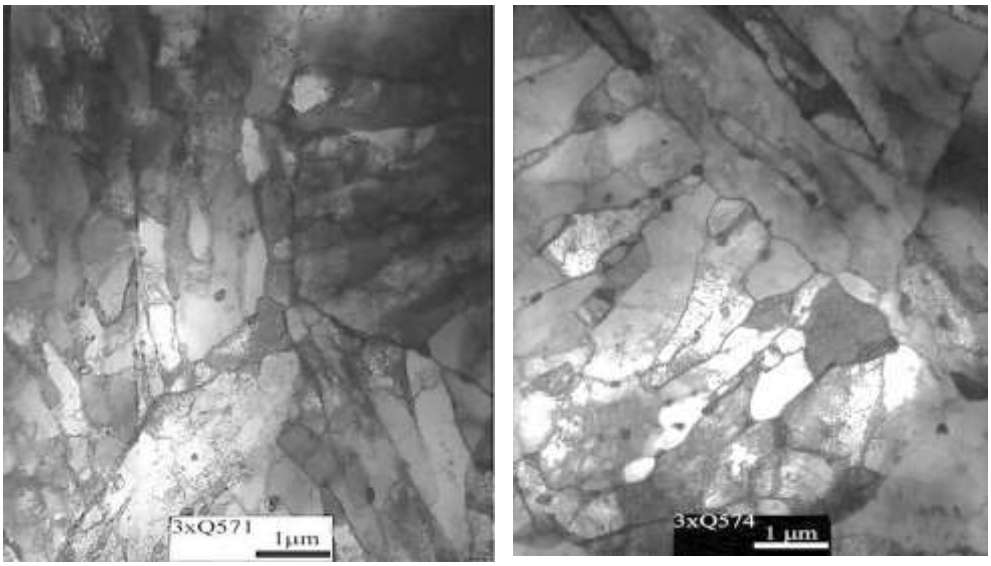

Figure 2 *TEM image of the grain/cell structure of 15Ch2MFA steel after thermo-mechanical fatigue for 5% (right) and 50% (left) of lifetime.*

Characterization of defect structure in electrodeposited nanocrystalline Ni films

T. Kolonits (MFA), P. Jenei (ELTE), B.G. Tóth (Wigner), Zs. Czigány (MFA),
J. Gubicza (ELTE), L. Péter (Wigner), and I. Bakonyi (Wigner)

The effect of organic additives (saccharin and formic acid) on the defect structure in electrodeposited Ni films was investigated by X-ray diffraction (XRD) line profile analysis (eCMWP model) and transmission electron microscopy (TEM) [64]. The main task of the project is to investigate the effect of the additives on the grain structure and defect (dislocation and twin) density which influence the macroscopic properties and application of the layers. The electrodeposited layers were deposited at room temperature at a current density of j= -43.75mA/cm^2. The basic electrolyte contained 0.6 mol/ℓ nickel sulphate ($NiSO_4 \cdot 7\ H_2O$), 0.30 mol/ℓ sodium sulphate ($Na_2SO_4 \cdot 10\ H_2O$), 0.25 mol/ℓ H_3BO_3 és 0.15 mol/ℓ H_3NO_3. The 46 mℓ/ℓ formic acid or 1 g/ℓ saccharine was mixed into this bath.

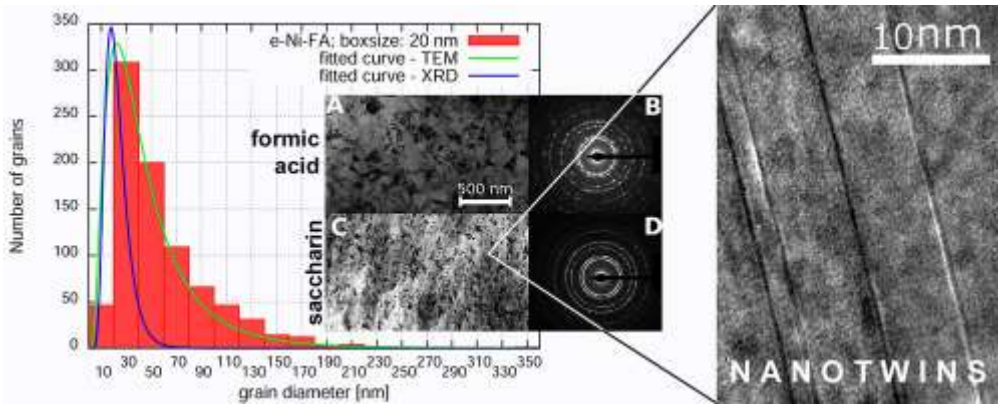

Figure 1 *Grain size distribution of nanocrystalline Ni film deposited with formic acid additives determined by TEM and XRD. The grain size refinement is shown in TEM images and electron diffractions. Nanotwins observed in the film deposited with saccharine are illustrated in the HRTEM image.*

In the film deposited without additives, a columnar structure was observed showing similarities to the T-zone of structure zone models. The typical column width was ~120nm and their length was >3μm. There was no detectable twinning. Both formic acid and saccharin additives resulted in equiaxed grains with reduced size, as well as increased dislocation and twin fault densities in the nanocrystalline films (Fig. 1). Moreover, the structure became homogeneous and free of texture within the total film thickness due to the additives. Saccharin yielded smaller grain size and larger defect density than formic acid. The inhibiting effect of the additives can be attributed to the surface coverage of the hydrophilic functional groups. The incorporation of ~0.3at% sulphur was detected only in the films deposited with saccharine which imply different mechanisms for the two additives. In the layers deposited with formic acid no incorporated contamination was detected by EDS. A detailed analysis of the grain

size and twin boundary spacing distributions was also carried out with the complementary application of TEM and XRD (Fig. 1). It is important to mark the difference between the grain size – determined by TEM and the crystallite size - determined by XRD. The reason of the difference is the high sensitivity of XRD for the small orientation differences due to different kind of crystal defects. Generally the grain size is approximately 2 times larger than the crystallite size. The defect density distributions determined by TEM and XRD showed similar tendencies. Presumptions of the eCMWP model about the grain size distribution (lognormal) were confirmed by TEM. Twin-boundary spacing follows geometric distribution for large spacing values in accordance with the model used in the XRD line profile analysis. However, for twin-boundary spacing smaller than 5 nm, TEM yields a smaller fraction than that predicted by XRD which discrepancy is due to the presence of numerous nanotwins as evidenced by HRTEM (Fig.1).

Characterization of the topography of the graphene moiré superlattice on Au(111) and Cu(111) supports

(OTKA K112811, OTKA K108753, KHJLN)

P. Süle, M. Szendrő, G. Magda, C. Hwang, and L. Tapasztó

In the last two years, we reached remarkable results in the theoretical and experimental study of surface morphology of graphene [124,125], [P Süle, at.al: Carbon 77, 1082-1089 (2014)]. Graphene moiré superlattices formed on various hexagonal supports (e.g. 111 metal surfaces) exhibit convex (protruded) morphology. In rare cases, suspected to be concave (nanomesh with periodic lattice of depressions) topography may exist. However, the experimental verification of the topography convexity is difficult. The curvature of the surface topography can not be clearly specified by STM due to the bias voltage dependence of the measured convexity. Varying the bias voltage contrast inversion occurs which prevents the unambiguous identification of the surface curvature. Using additional first principles DFT theoretical studies were only able to prove the existence of convex morphology e.g. on Ru(0001). Why is it important to know the precise topographic curvature of the graphene surface? According to our present knowledge and assumptions convex and concave superlattices may exhibit different electronic structure properties such as LDOS or band structure. Moreover, the surface activity, such as the adsorption energy of various molecules and/or the local magnetic property of surface Carbon atoms may depend on the morphology of the superlattice.

The most important results:

- The detailed description of the topography of moiré superlattices using a combined theoretical and STM approach [124,125].

- The coexistence of convex and concave superlattices has been explored in the same image which rules out the presence of contrast inversion [124]
- DFT calculations support the possible coexistence of various superlattices with different curvature due to the tiny energy difference between the various morphologies [124]
- The Au(111) surface reconstructs upon graphene adsorption and exhibits an imprinted topography very similar to that of the moiré superlattice [124]

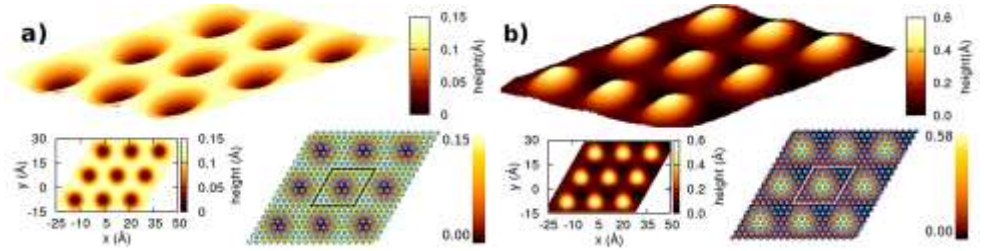

Figure 1 *Concave (a) and convex (b) graphene moiré superlattices as computed by molecular dynamics simulations.*

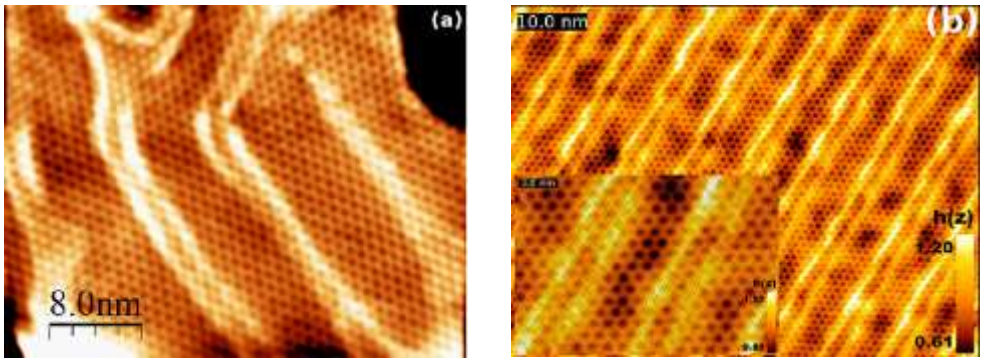

Figure 2 *Concave graphene superlattice (nanomesh) on a herringbone reconstructed Au(111) surface. Topographic images as obtained by STM (a) and by molecular dynamics simulations (b).*

Microscopy of high quality cubic SiC grown on Si

(OTKA K 108869 and bilateral agreement between CNR and MTA)

M. Bosi[1], G. Attolini[1], M. Negri[1], C. Ferrari[1], E. Buffagni[1], C. Frigeri[1], M. Calicchio[1], B. Pécz[2], F. Riesz[2] , I. Cora[2], Z. Osváth[2], L. Jiang[3], and G. Borionetti[4]

[1] IMEM-CNR, Parco Area delle Scienze 37 A, 43124 Parma, Italy
[2] MTA EK MFA, P.O.Box 49, H-1525 Budapest, Hungary
[3] Engineering Sciences, Faculty of Engineering and the Environment, University of Southampton, Highfield, Southampton SO17 1BJ, United Kingdom
[4] MEMC Electronic Materials S.p.A., Viale Gherzi 31, 28100 Novara, Italy

Cubic silicon carbide (β-SiC or 3C-SiC) is a wide-bandgap semiconductor with high hardness, high electron mobility, high thermal conductivity, high resistance to chemical attack and it is biocompatible; for these reasons SiC is interesting for potential technological applications, such as power devices and sensors operating in harsh environments. The growth of this polytype is a challenge.
Several samples were grown by varying the deposition temperature and the MTS (monomethylsilane, CH_3SiH_3) content in order to study how these parameters affect the layer quality and the lattice defects. The use of single source precursor (like MTS) increases the growth rate of SiC.
The grown layers were investigated by several techniques including transmission electron microscopy (TEM), Makyoh analysis and Raman spectroscopy. The TEM specimens were prepare dby Ar ion milling and then investigated by conventional and high resolution microscopy.

Figure 1 *Bright field (left) and dark field (right) images taken on a sample grown with the addition of MTS. Diffraction pattern is inserted to the middle of the above image.*

The TEM images in Fig. 1 show the sample grown at 1400 °C with the addition of MTS. The single crystalline SiC layer contains a lot of stacking faults, which give faint streaks in the diffraction pattern. There is a huge density of defects at the SiC/Si interface, which is however, decreased substantially toward the surface.
When we compare a sample grown at the same temperature, however, without the addition of MTS we can observe that the defect density is higher than the previous sample. Beside the well-known stacking faults there were antiphase boundaries inside SiC. The layer is single crystalline as well, but the defect density is not decreased so

much like in the former case toward the surface. Low magnification images had shown that the surface of the grown SiC layer is not perfectly flat.
Although in all of the grown SiC layers the defect density is high close to the silicon substrate, we observed that in layers grown with the addition of MTS (both at 1300 °C and at 1400 °C) the defect density is substantially lowered towards the surface region. This observation was supported by the Raman analysis based on the shift of the Raman peaks, as well.

Metal (Ni) induced crystallization in amorphous Si thin films

(TÉT-10-1-2011-0570)

Gy. Z. Radnóczi, E. Dódony, G. Battistig, B. Pécz,
I. Stoimenos, N. Frangis, and N. Vouroutzis (AU, Thessaloniki)

The formation of various silicide phases was studied to understand the initial stages of Ni induced crystallization of amorphous silicon (a-Si). During the experiments presented here only silicide formation occurred as the Ni supply was practically unlimited in comparison to the a-Si film.

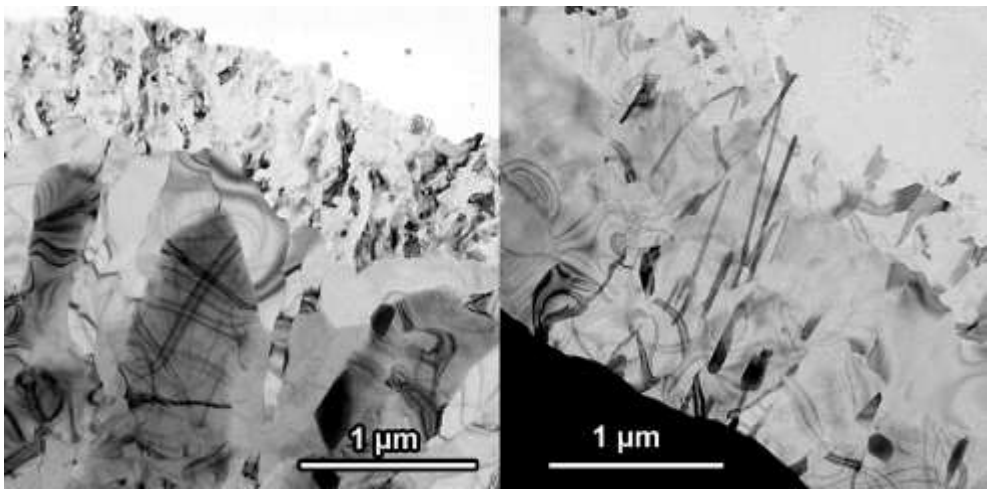

Figure 1 *The result of in-situ heat treatment of a Si film with native oxide layer (left) and a Si film cleaned with HF solution (right).*

The previously developed model system for in situ experiments was used. The amorphous Si foil on Ni microgrid proved to be a stable and reliable system for the investigation of silicide formation at elevated temperatures; however, some concerns were raised about the native oxide on the surface of the Si film. This thin oxide is believed to hinder the Ni diffusion into the Si film and it is also a relevant difference with respect to the usual MILC structures which contain no oxide film between the Ni

and Si. To eliminate this potential diffusion barrier the Si film was transferred to a HF solution before placing it onto the Ni grid. The Ni grids were also cleaned in an etching solution (NH_4OH). In situ experiments were carried out with the new structures. The resulting structure was different from the structures obtained in our earlier experiments. For a comparison see Fig. 1.

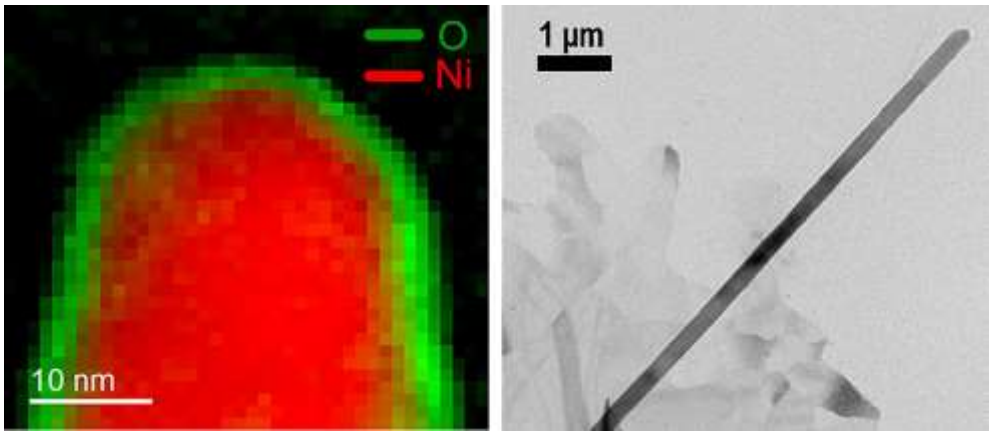

Figure 2 *Ni(red) and O (green) elemental maps (left) of a whisker combined into a single image. The map shows a Ni containing whisker with a (silicon)oxide shell. The bright field micrograph of a whisker is shown on the right).*

In contrast to previous results whiskers were observed in the new structures (Fig. 2). The whiskers were growing out of the plane of the a-Si film as determined by stereo images recorded with 8° tilt difference. The analysis of the whiskers showed that they consist of Ni_2Si phase and they also have an oxide shell as revealed by analytical measurement carried out by Austrian partners within ESTEEM project.
A report on the above experiments and other results obtained in low temperature annealing of MILC structures was published recently [G. Z. Radnóczi, et al: Structural characterization of nanostructures grown by Ni metal induced lateral crystallization of amorphous-Si, Journal of Applied Physics 119, 065303 (2016), DOI:10.1063/1.4941349] and further work is in progress on characterization of Si whiskers obtained at low temperature.

A universal nanopatterning technique using RF plasma etching through templates of Langmuir-Blodgett films

J. Szívós, M. Serényi, Sz. Pothorszky, G. Vértesy, and G. Sáfrán

The nanoscale modification of materials has attracted wide research interest recently. At present, mostly, slow and expensive methods are available for the fabrication of ordered nanostructures. Last year a cheap and fast technique was proposed [J. Szívós, et al: Nanopattern formation in UV laser treated a-AlO_x and nc-Al/AlO_x layers, Vacuum 109, 200 (2014)] to produce ordered nanopatterns directly or to prepare

masks for nanolithography and nanoimprint molds. This technique applies a monolayer of hexagonally self-assembled silica nanospheres (Langmuir-Blodgett (LB) film) as a template and the sample surface is treated by a single UV laser (λ=248 nm) pulse through the LB film. We could produce nano-patterned Al-oxide layers by this technique successfully. Experiments were carried out in 2015, however, it was found that UV laser patterning is hardly effective in case of metal surfaces: the pattern with a pale contrast in the scanning electron microscope image (shown in Fig. 1) was so shallow that it couldn't be visualized by cross-sectional TEM.

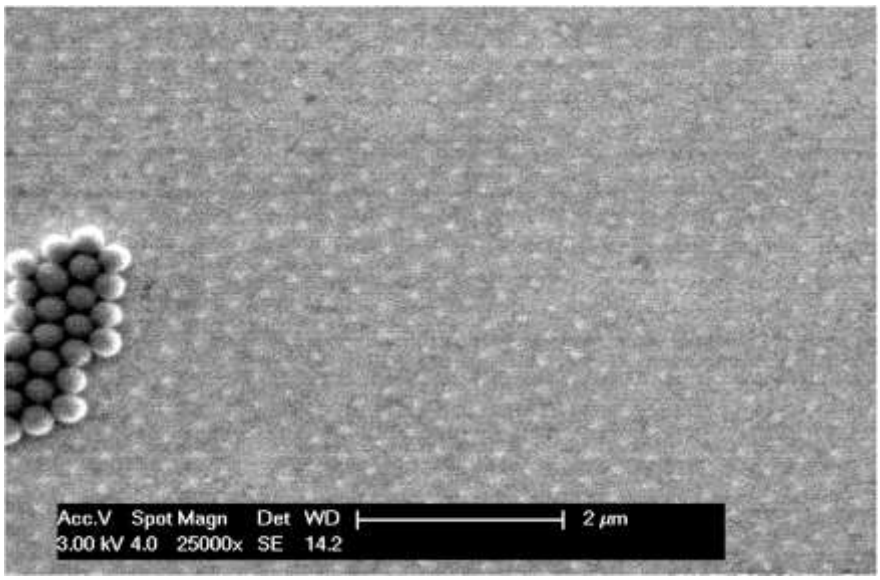

Figure 1 *SEM image of the pattern achieved in Pt by UV laser treatment. Some residual nanoballs of the LB film are seen at the left side.*

The reason of the inefficiency is the absorption mechanism of the UV laser in metals: the (quasi-)free electrons are thermalizing the lattice, thus the whole metal surface absorbs the energy nearly uniformly [M. S. Brown, C. B. Arnold: Fundamentals of Laser-Material Interaction and Application to Multiscale Surface Modification, Springer Series in Materials Science Volume 135, 91-120 (2010)] despite the presence of the LB film. It is likely that femtosecond pulse length would be required to avoid this effect.

The aim of the PhD work is to find simple, cheap and fast solution for nanoscale patterning of metallic, as well magnetic layers. The latter allows increasing the capacity of FePt or CoPt magnetic recording media by the preparation of ordered nanopatterns thus realizing Bit Patterned Media (BPM).

The LB film is suitable to prepare ordered, self-assembled template at large areas. The goal was to transfer the pattern of the template to a wide range of materials. Experiments with 30 kV ion-implantation have shown that in the case of metals the energy (and flux) of the applied ions (Ar^+, possibly Xe^+) is not sufficient. RF plasma

etching, however, proved to be very effective that led to a universal technique capable to nanopattern various materials, e.g. oxides, semiconductors and metals.
The LB film-covered sample is placed at the „target" position of the RF sputtering source 40 mm far from the ground plate and is subjected to 1 kV Ar plasma with pressure 2.5 Pa. The nanospheres of the LB film protect the surface and sputtering takes place between the nanospheres. This way the hexagonal pattern of the LB film can be replicated to almost any material's surface provided that the plasma parameters and etching time are well set. The feature size is determined by the diameter of the nanospheres that, in principle, can be scaled down to about 10 nm.
In order to demonstrate the operability of the technique and the effects of changing the plasma parameters DC magnetron sputtered Pt thin films were nanopatterned. Pt layers are widely utilized e. g. for masking. It is suggested that Pt has a sputtering rate similar to that of FePt and CoPt.
Based on TEM investigations the layer structure of our Pt samples was the following: Si(001) substrate/thermal SiOx (1140±10nm)/TiO_x buffer (11.3±0.3nm)/35±4nm Pt.
A pattern fabricated with optimum parameters is shown in Fig. 2. In (a) the SEM image shows the patterned Pt layer itself. Hexagonally arranged pattern is shown up, but the domains and stacking faults of the LB film are replicated as well.

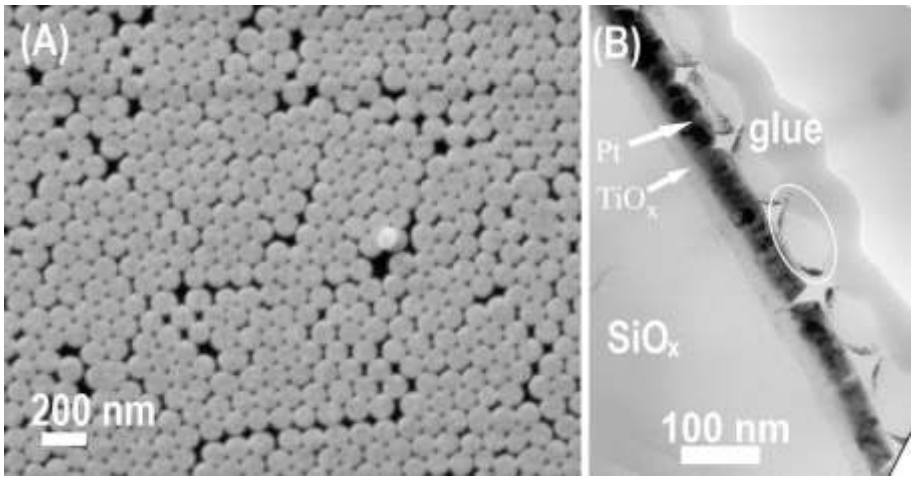

Figure 2 *The pattern prepared by our RF plasma etching technique in the Pt layer. Plan view SEM (a) and cross-section TEM (b) images.*

The cross-sectional TEM image in Fig. 2 (b) represents part of the SiO_x underlayer, the Pt with the plasma etched pits and the residue of the 100 nm diameter nanospheres of the LB film that protected the layer beneath.
Nanopatterning with RF plasma through an LB film is a fast and cheap technique that may be suitable, as well, for mass production. Our plans for 2016 are to study, in collaboration with our Japanese colleagues, the magnetic properties of such nanopatterned $L1_0$ CoPt thin films. That can be an alternative implementation of bit patterned magnetic media.

CoPt/TiN thin films of enhanced perpendicular coercivity by N_2 incorporation during deposition

H. An, J. Wang, J. Szívós, T. Harumoto, T. Sannomiya, S. Muraishi, Gy. Sáfrán, Y. Nakamura, and J. Shi

The structure formation of CoPt thin films was investigated in collaboration with the Technical University of Tokyo (Department of Metallurgy and Ceramics Science, Tokyo Institute of Technology, Tokyo, Japan). CoPt (and FePt) films are the most promising media for future magnetic data storage. These alloys may transform from fcc to tetragonally distorted $L1_0$ phase under heat treatment which turns their magnetic easy axis preferably perpendicular to the surface that is crucial for high density data storage. However, with increasing layer thickness, the deviation of the direction of the magnetic easy axis increases, and at the end it returns to horizontal.
The structure and morphology of CoPt films grown by the Japanese colleagues on crystalline TiN buffer layers with and without N_2 incorporation were investigated by TEM. According to the literature, during deposition the incorporating N_2 expands the lattice constant of the alloy. A subsequent heat treatment releases the N_2 which causes a lattice contraction in the plane of the layer. This facilitates the formation of the in plane magnetic easy axis in case of FePt layers, because, in $L1_0$ phase, the smallest lattice constant is found parallel to the direction of the magnetic easy axis.

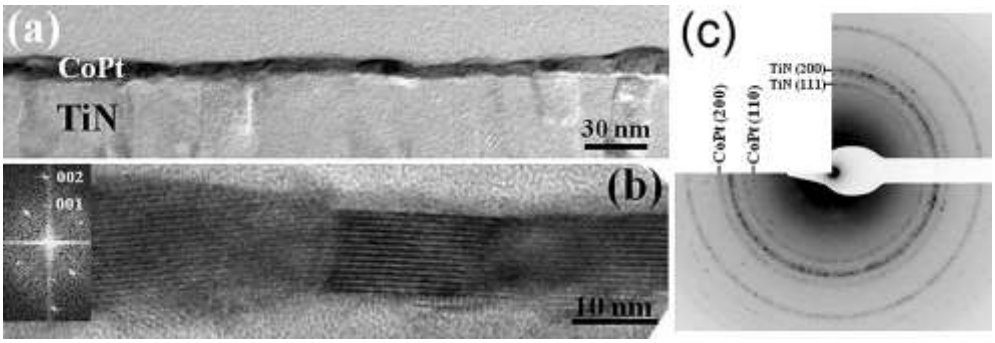

Figure 1 *(a) Cross section TEM image of the heat treated CoPt sample. (b) HRTEM showing the superstructure of CoPt. In the FFT inset the $L1_0$–related reflections are indexed. (c) Plan view SAED pattern of the CoPt/TiN layer.*

The Japanese colleagues have found by XRD that also in the case of CoPt the N_2 is built into the lattice and increases the in plane lattice constant. Under annealing, this lattice constant increases up to ~550 °C due to thermal expansion. At 600 °C, however, the built-in N_2 releases, that results in a contraction of the lattice constant. This phenomenon effectively promotes the transformation of CoPt into the $L1_0$ phase. Magnetic measurements have shown that, in CoPt, the magnetic easy axis is perpendicular to the surface, which is contradictory to the expectations, and to that observed in the case of FePt. The $L1_0$ phase was identified in the annealed samples by TEM in MFA (Fig. 1. (a) and (b)). The layer is polycrystalline with no texture in the layer plane (Fig. 1. (c)).

In one of the several existing CoPt $L1_0$ phases the lattice constant is – exceptionally – the largest in the direction of the magnetic easy axis [U.S. Natl. Bur. Stand. Monogr. 25, 15, 168 (1978) (pdf 29-0498)]. In our samples precisely this $L1_0$ phase was found as revealed by the intensity distribution of the selected area electron diffraction (SAED) patterns (Fig. 2.). There is no similar phase in FePt. It follows that, in our CoPt, the in plane shrinkage of the lattice results in an easy axis formation perpendicular to the surface, that is favourable in magnetic recording media. The results of the collaboration were published in JAP [5].

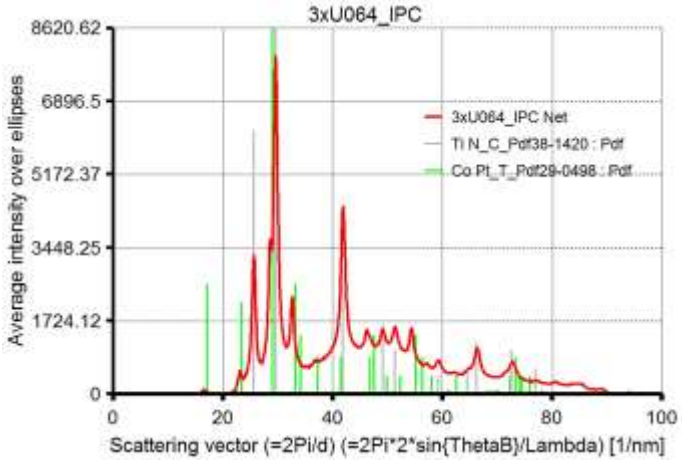

Figure 2 *The intensity distribution of the in plane selected area electron diffraction pattern of the heat treated sample. The layer consists of TiN, and the $L1_0$ CoPt phase.*

A device for micro-combinatorial TEM studies

Gy. Sáfrán

Status of technology: The physical chemical and structural properties of the layer systems of cutting edge technology are strongly determined by their composition. The Binary Alloy Phase Diagrams are well explored, however, phases of thin films are hardly studied and may remarkably differ from that of the bulk. The common procedure to reveal the properties of concentration dependent phases is the preparation and investigation of numerous two-component samples, one for each $C_A/C_{B=1-A}$ composition. This costs enormous time of man and machine.

For a study of high number of samples combinatorial methods are recognized i.e. instead of carrying out numerous individual experiments samples of varying composition are prepared in a single process. P. Schultz et al. [Science (1995) 268 (5218) pp.1738-1740] applied two-fold mechanical mask movement and prepared 200x200 micrometer size individual samples in various compositions at a density of 10000 sample /in^2. K.E. Roskov [J. Comb. Chem. (2008) 10, pp.966–973] prepared for different, fixed composition samples combinatorially, onto individual TEM grids.

The above examples are partly efficient solutions because only the preparation of samples is combinatorial. At the Thin Films Physics Dept. of RITP an experimental arrangement [F. Misják et al: Thin Solid Films 516 (2008) pp.3931–3934] was implemented already as micro-combinatorial, since samples of various compositions were both deposited and investigated in a single TEM grid: A shield with a 1mm diameter aperture was fixed above the substrate. Two sources were facing the substrate through the aperture at inclined angles so that the thin film was deposited at two overlapping areas where two-component film of Ag-Cu was grown. The drawback of that method is that the region of changing concentration is very short (100-150 μm), the phases are accumulated and the sample does not contain the entire (0-100%) composition range.

Objectives: The aim was to construct a micro-combinatorial device that eliminates the incompleteness of the above solutions. The preparation and study have to be carried out in a single TEM grid within the whole 0-100% composition range so that the formed binary phases and variants may be well separated.

Technical design: The recently patented [Hung. Patent No. P 15 00500 (2015)] micro-combinatorial device (Fig. 1.) incorporates a cover plate with a slit that is moved in fine steps above the TEM grid, meanwhile the fluences of the magnetron sources "A" and "B" are regulated adversely. This new solution provides both micro-combinatorial preparation and investigation, so that the length of the concentration transition increases to 1500 microns.

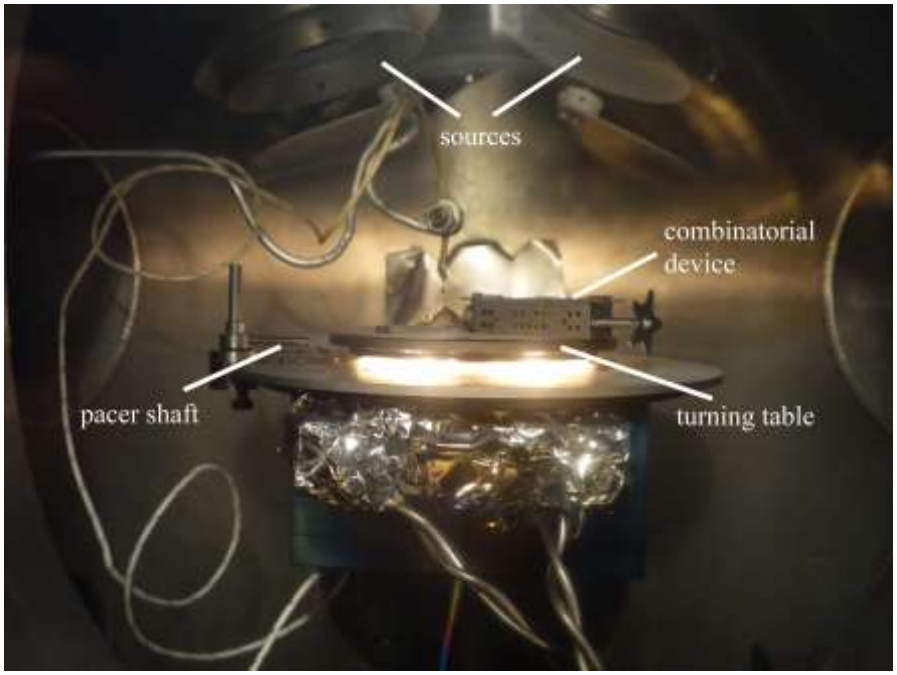

Figure 1 *The micro-combinatorial device in operation.*

A TEM grid with a deposited Mn-Al micro-combinatorial sample is shown in Fig. 2.(a). Fig 2.(b) represents energy dispersive X-ray spectrometer (EDS) data, that aside from the edges, shows linear concentration distribution. The micro-combinatorial sample prepared as above allows detailed and efficient analysis, because it exhibits the entire 0-100% concentration range in a TEM grid spread along a distance of an order of magnitude longer than earlier. The gradient of a limited concentration range can be adjusted to arbitrarily low values for an enhanced areal separation of the formed thin film phases. In addition, the device is suitable for the study of the effects of parameters (residual gas pressure, temperature, etc.) that change with time.

The author thanks J. Szívós for contributing to the measurements!

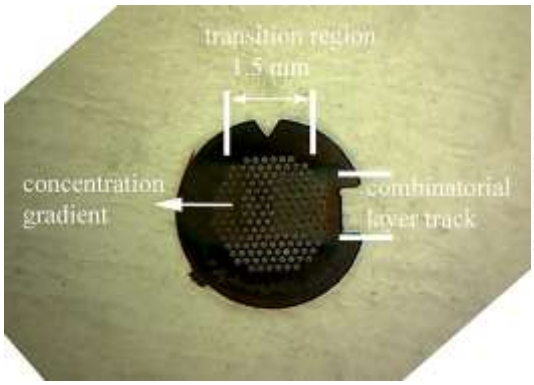

Figure 2(a) *TEM grid with a microcombinatorial MnAl sample (1x1.5mm^2) that was deposited through a moving slit.*

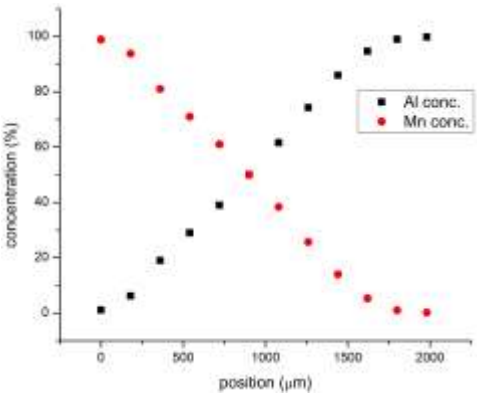

Figure 2(b) *EDS concentration profile of the sample in 2(a). The transition extends to 1500μm, and the concentration range is 0-100% for both (Al, Mn) components.*

Grain boundary characterization based on diffraction data

Á.K. Kiss, and J.L. Lábár

In materials science and its applications it is important to reveal the correlation between the technique of fabrication and the resulting structure, as well as between the structure and the properties of the materials. This is why the proper characterization of a manufactured material is inevitable. Two newly developed techniques are presented here, which facilitate the investigation of polycrystalline materials with transmission electron microscope (TEM) in terms of grain boundary characterization.

Both methods are based on computer supported measurements, which are capable of displaying either a grain boundary network or dislocations (or both) and additionally determining the orientation of grain boundary (GB) planes (i.e. determining their indices expressed in the coordinate systems of either neighbouring grains). Every step of the method (data acquisition and evaluation) is automated therefore it may serve as

a basis of sample-characterization as far as distribution of grain-boundary planes is concerned.

The novelty is that additional information from the sample is obtained in addition to the ones provided by orientation maps. (Orientation mapping was carried out by the ASTAR tool installed on the TEM.) Two different mathematical algorithms (non-negative matrix factorization, NMF and the calculation of cross correlation) are applied to the same diffraction dataset, which is originally acquired for orientation mapping – without the need of any further measurements. With the help of the first algorithm, the width of the projection of a GB i.e. the overlapping area between the neighbouring grains can be detected and quantified automatically (Fig. 1).

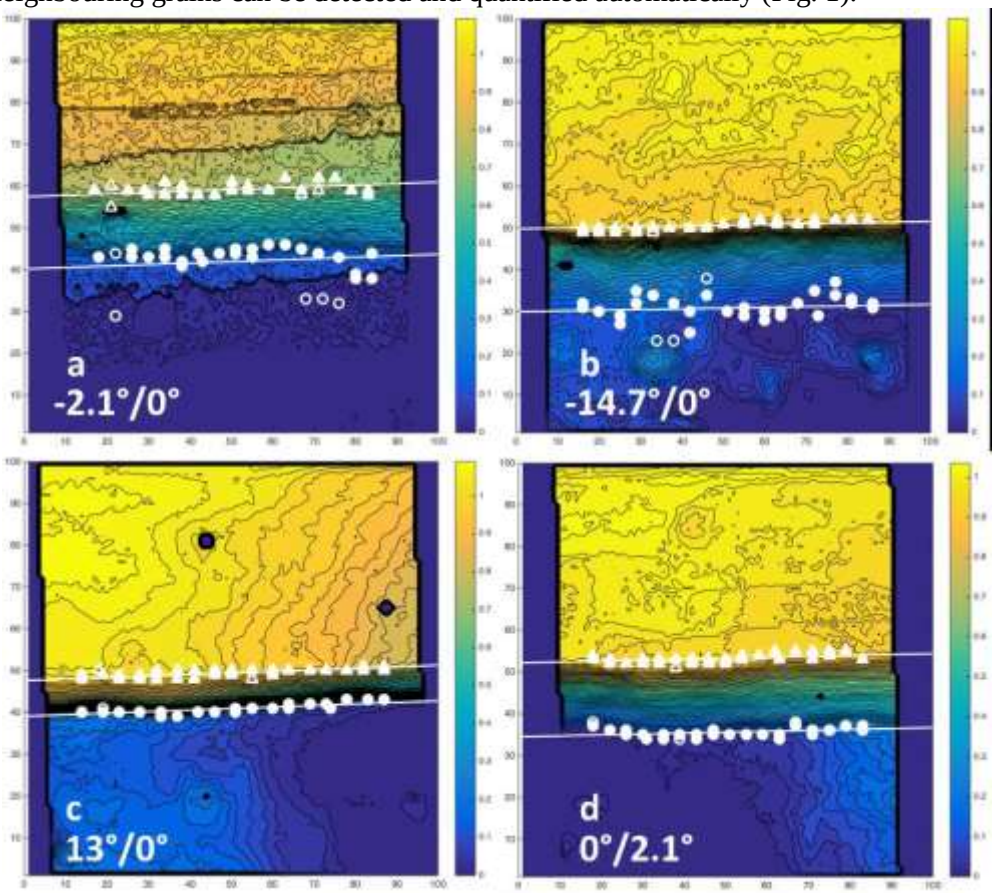

Figure 1 *The same part of a GB in silicon thin film is shown here. The diffractions coming from the local neighborhood of the GB were evaluated by NMF at different tilt positions. The extent of the upper grain is identified with the shades of yellow on the contour level representations; the projection of the overlapping area (tilted GB-plane) can be clearly recognised between the marked lines.*

This operation predicts the possibility of characterizing TEM samples with respect to the GB-plane distribution, in contrast of those methods, where only the misorientation between grains and perhaps the lateral direction of the GBs are taken into account [Á.K. Kiss, J.L. Lábár: Determining projections of grain boundaries from diffraction data in the TEM, submitted to Microscopy and Microanalysis (2016)]. The other mathematical tool – namely the calculation of the cross-correlation – is capable of providing qualitative new information from the area of interest in the sample. The calculation of cross correlation seems to be effective to express the similarity or dissimilarity of two diffraction patterns, thus the correlation coefficients are sensitive to all features which may alter the diffraction signal. The correlation coefficients are calculated between subsequent diffractions (both through rows and columns) and they are displayed in a grayscale map: it has turned out, that the grains, GBs, overlapping areas and even dislocations can be displayed efficiently with the help of the coefficients (Fig. 2). This technique works with nanometer-resolution and seems to be more efficient than (virtual) bright- and dark field imaging [Á.K. Kiss, E.F. Rauch, J.L. Lábár: Highlighting material structure with transmission electron diffraction correlation coefficient maps, Ultramicroscopy 163, (2016) pp.31–37].

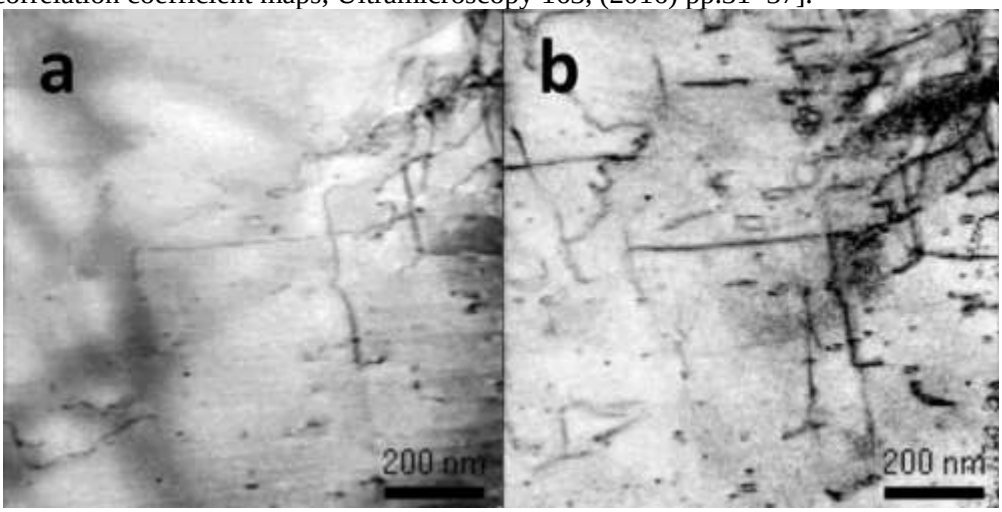

Figure 2 *Virtual bright-field image (**a**) and cross-correlation coefficient map (**b**) of the same part of a deformed steel sample. The dislocations are displayed more efficiently in the latter case. (Edgar F. Rauch is acknowledged for this figure.)*

Nanobiosensorics „Lendület" Research Group

Head: Robert HORVÁTH, Ph.D., Senior Research Fellow

Research Staff

- Robert HORVATH, Ph.D.
- Sándor KURUNCZI, Ph.D.
- Inna SZÉKÁCS, Ph.D.

Ph.D. students / Diploma workers

- Enikő FARKAS, M.Sc./Ph.D. student
- Boglárka KOVÁCS, Ph.D. student
- Judit NÁDOR, Ph.D. student

Ph.D. students / Diploma workers

- Norbert ORGOVÁN, Ph.D. student
- Dániel PATKÓ, Ph.D. student
- Beatrix PÉTER, Ph.D. student
- András SAFTICS, Ph.D. student
- Rita UNGAI-SALÁNKI, Ph.D. student
- Dávid CSIKAI, B.Sc. student
- Enikő FORGÁCS, B.Sc. student
- Gabriella GÁL, M.Sc. student
- Aurél PRÓSZ, B. Sc. student
- Barbara TÜRK, B.Sc. student

The Nanobiosensorics Group was established in 2012 in the framework of the "Lendület" programme of the Hungarian Academy of Sciences. The "Lendület programme" funds young researchers in Hungary aiming at the establishment of their own independent research groups. The research profile of the Nanobiosensorics Group is the development and application of label-free optical biosensors, the mathematical modeling of the relevant biological and biophysical processes. Building on their broad national and international collaborative network the group conducts research in the fields of instrument development, monitoring of cell secreted extracellular vesicles, development of protein-based functional coatings, adhesion studies on human cancer and immune cells, and theoretical modeling.

In 2014, the application for an ERC Consolidator Grant by the head of the research group received qualification category "A (fully meets the ERC excellence criteria and should be funded if sufficient funds are available)" after the interview in Brussels, but the funding line did not reach this proposal due to budgetary constraints. However, using this achievement he could successfully apply for funding from NKFIH in the framework of the ERC_HU call.

Hydrogel film fabrication for biosensing

(Lendület Program, Bolyai Research Scholarship)

A. Saftics, S. Kurunczi, N.Q. Khánh, A. Sulyok, and R. Horváth

Hydrogel interface layers play an important role in the field of biosensors, especially for label-free techniques. The 3D network of carbohydrate hydrogel dextran proved to be advantageous for the enhanced immobilization capacity and for the reduced non-specific binding of the sensor surface. We have been developing tailor-made dextranized surfaces on different substrates.

Recently we have prepared carboxymethylated dextran (CMD) from native dextran in our lab. Then this CMD (with Mw = 100 and 500 kDa) was used for ultrathin surface coatings. Grafting methods based on covalent coupling to aminosilane- and epoxysilane-functionalized surfaces were applied to obtain thin CMD layers. The carboxyl moiety of the CMD was coupled to the aminated surface by EDC-NHS reagents, while CMD coupling through epoxysilane molecules was performed without any additional reagents. The surface layer investigation following the grafting procedures included x-ray photoelectron spectroscopy (XPS), attenuated total reflection infrared spectroscopy (ATR-IR), spectroscopic ellipsometry, atomic force microscopy (AFM) and optical waveguide lightmode spectroscopy (OWLS). The in situ OWLS method was suitable to devise the structure of the interfacial dextran layers by the evaluation of the optogeometrical parameters. Our results suggested an anisotropic layer that can be seen in Fig 1. The developed methodologies allowed to design and fabricate nanometer scale ultrathin CMD layers with well-controlled surface structure, which are very difficult to characterize in aqueous environments using present instrumentation and highly hydrated surface layers.

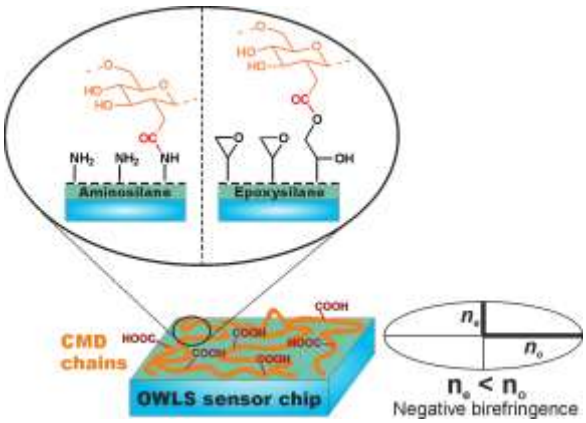

Figure 1 *Schematic illustrations of the CMD grafting chemistries and the supposed structure of the CMD chains on the OWLS sensor chip. The negative birefringence of the layer suggested lain down chains on the surface.*

[A. Saftics, S. Kurunczi, Z. Szekrényes, K. Kamarás, N.Q. Khánh A. Sulyok, S. Bősze, R. Horvath: Fabrication and characterization of ultrathin dextran layers: time dependent nanostructure in aqueous environments revealed by OWLS, submitted manuscript]

Label-free profiling of cell adhesion: Determination of the dissociation constant for native cell membrane adhesion receptor-ligand interaction

("Lendület" grant LP2012-26/2012 of HAS)

N. Orgován, B. Péter, Sz. Bősze (ELTE, Budapest), Jeremy J. Ramsden (Cranfield University, UK), B. Szabó (ELTE, Budapest), and R. Horváth

Cellular adhesion is essential to life. Cells usually establish an anchorage with the extracellular matrix or neighboring cells in the tissue using cell adhesion receptors embedded in the cell membrane, such as integrins, cadherins, selectins, syndecans, and the immunglobulin superfamily of adhesion receptors. Since nowadays many modern drugs intervene at the level of cellular adhesion, there is an ever-increasing demand for techniques that enable the effects of such drugs to be screened in a straightforward and reliable way which moreover produce highly informative (e.g., multiparameter and/or kinetic) data.

Traditional methods for measuring cellular adhesion, including phase-contrast microscopy or mechanical assays, where the adhered cells are subjected to a fluid flow, are cumbersome and hence generally unsuitable for high throughput needed in drug discovery, and kinetic monitoring with high temporal resolution and high signal-to-noise ratio. In contrast, surface-sensitive label-free biosensors are inherently capable of generating good-quality kinetic data. Evanescent field-based label-free optical biosensors including resonant waveguide grating (RWG or Epic) biosensors are considered to be especially straightforward means to monitor cell adhesion, since they can in situ detect refractive index changes in the 100–200 nm thick layer closest to the sensor surface, where the anchorage between the cell and its substratum takes place. Moreover, the probing depth of these biosensors can be fine-tuned through waveguide structure design, so dynamic information from various depths can be simultaneously collected using multimode waveguides, potentially permitting the monitoring of changes inside the cell or in its nucleus triggered by surface adhesion.

In this protocol we described how the adhesion kinetics of living cells on a surface coated with integrin ligands can be characterized in detail. We use an optical biosensor, an Epic BenchTop (BT) system to monitor cell adhesion with unprecedented quality in a high-throughput way. The biosensor data recorded at various ligand densities are used to determine the dissociation constant, so the binding between the RGD ligand and its adhesion receptors embedded in their native cell membrane is characterized in a label-free and perturbation-free manner (Fig. 1) . Of note, the present protocol is equally applicable for other types of ligands and adhesion receptors and can also be used to measure the effects of drugs interfering with cell adhesion [Label-Free Biosensor Methods in Drug Discovery (Methods in Pharmacology and Toxicology, 2015), Springer (Ed. Ye Fang), pp.233-252].

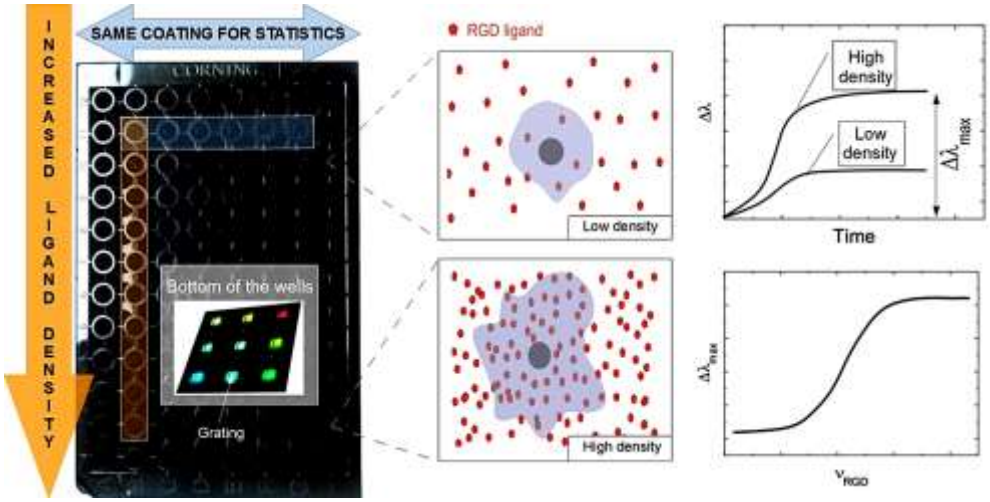

Figure 1 *Monitoring the adhesion kinetics of cells with an Epic biosensor on different ligand densities enables the dissociation constant characterizing the interaction of native cell membrane receptors and their ligands to be determined.*

Incubator proof miniaturized Holomonitor to in situ monitor cancer cells exposed to green tea polyphenol and preosteoblast cells adhering on nanostructured titanate surfaces: validity of the measured parameters and their corrections

("Lendület" grant LP2012-26/2012 of HAS)

B. Péter, J. Nádor, K. Juhász, Á. Dobos, L. Kőrösi (Enviroinvest Ltd., Pécs, Hungary), I. Székács, D. Patkó, and R. Horváth

In 2015 we published two successful applications of holographic microscopy to monitor cancer cell motility, migration, motility speed, and to examine the spreading of preosteoblast cells on a nanostructured titanate coating [104]. The M4 Holomonitor, applied in this study, has a small size, and it is feasible to be put directly into a humidified cell culture incubator. This technique is completely noninvasive and label-free, therefore, nothing disturbs the cells during their movements. A special mechanical stage was also developed in order to position the sample into that range of the optical arrangement where digital autofocusing works with high reproducibility and precision. With the help of this novel development, we could perform two successful measurements demonstrating the capabilities of our novel arrangement. In our first study, it is demonstrated that the movement of HeLa cells was temperately reduced after the addition of polyphenol EGCg. This phenomenon could be monitored in a completely noninvasive and label-free manner.

With this experiment, we proved that our recently developed sample stage is an excellent tool for observing cell dynamical changes and monitoring the effects of chemical substances on living cells. In another experiment, the Holomonitor M4 was used to study cellular adhesion and spreading on nanostructured titanate coatings. A novel arrangement was developed to measure live cell behavior on spin-coated surfaces. We recorded the adhesion and spreading processes of the cells in real time. From the recorded data, we concluded that the averaged cell thickness and area detected by the instrument saturate after 30 min. These results are clearly contradictive to previous investigations where the preosteoblast adhesion on these nanostructured surfaces was monitored by an optical biosensor. Based on these findings, we concluded that under certain thicknesses, relatively large parts of the cells (parts of the thin lamellipodium) slick into the background surface due to the limited vertical resolution of the optical arrangement (Fig. 2). We determined the time-dependent corrected single-cell contact area and averaged thickness by the assumption that the cell volume is constant during the adhesion process. Our new correction method for estimation of the undetected parts of lamellipodia resulted in more precise evaluations supported by earlier biosensor kinetic data [104].

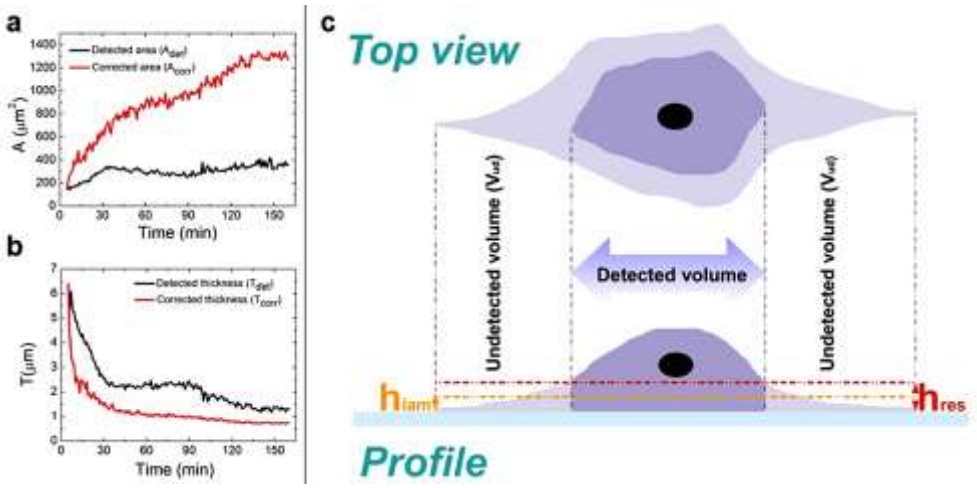

Figure 1 *(a): The detected and corrected data of the preosteoblast cells, (b): the area, and (c): the thickness curves. Sometimes the lamellipodia, the very thin parts of the cells, cannot be sensed perfectly by the instrument.*

Biophysical characteristics of proteins and living cells exposed to the green tea polyphenol epigallocatecin-3-gallate (EGCg): Review of recent advances from molecular mechanisms to nanomedicine and clinical trials

("Lendület" grant LP2012-26/2012 of HAS)

B. Péter, Sz. Bősze (ELTE, Budapest), and R. Horváth

Traditionally, tea was drunk to eliminate toxins, to improve blood flow and resistance to diseases, so its habitual consumption has long been associated with health benefits. Among natural compounds and traditional Chinese medicines, the green tea polyphenol epigallocatechin gallate (EGCg) is one of the most studied active substance. Tea catechins, especially (-)-EGCg, have been shown to have various health benefits, for example anti-metastasis, anti-cardiovascular, anti-cancer, anti-inflammatory and antioxidant effects (Fig. 1). In 2015 we focused on the molecular

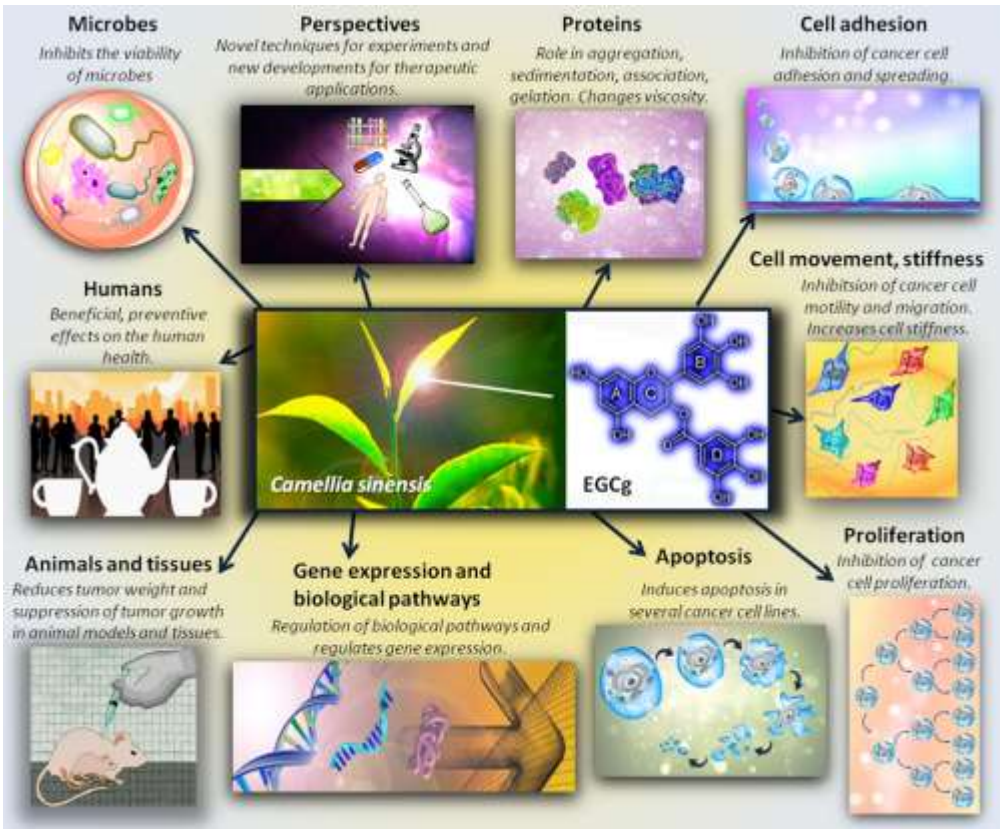

Figure 1 *Diversified effects of EGCg.*

scale interactions between proteins and EGCg with special focus on its limited stability and antioxidant properties, the observed biophysical effects of EGCg on

various cell lines and cultures. The alteration of cell adhesion, motility, migration, stiffness, apoptosis, proliferation, as wells as the different impacts on normal and cancer cells are all summarised in our prospective review article [Beatrix Péter, Szilvia Bősze, Róbert Horváth: Biophysical characteristics of proteins and living cells exposed to the green tea polyphenol epigallocatecin-3-gallate (EGCg): Review of recent advances from molecular mechanisms to nanomedicine and clinical trials]. We also handled the works performed using animal models, microbes and clinical trials. Novel ways to develop its utilization as therapeutic purposes in the future are discussed too, for instance, using nanoparticles and green tea polyphenols together to cure illnesses, and the combination of EGCg and anticancer compounds to intensify their effects. In this review we summarize the experiments and results of the past few years. The limitations of the employed experimental models and the criticisms on the interpretation of the obtained experimental data are summarized as well. We also point out some inaccuracies in the literature.

Automated single cell isolation from suspension with computer vision

("Lendület" grant LP2012-26/2012 of HAS, Bolyai Scholarship, MedInProt)

R. Ungai-Salánki[1,2,3], T. Gerecsei[3], P. Fürjes[4], N. Orgován[2,3], N. Sándor[5], E. Holczer[4], R. Horváth[2], and B. Szabó[2,3,6]

[1]Doctoral School of Molecular- and Nanotechnologies, PE, Veszprém, Hungary
[2]Nanobiosensorics Group, MTA EK MFA, Budapest, Hungary
[3]Department of Biological Physics, ELTE, Budapest, Hungary
[4]MEMS Laboratory, MTA EK MFA, Budapest, Hungary
[5]MTA-ELTE Immunology Research Group, Budapest, Hungary
[6]CellSorter Company for Innovations, Budapest, Hungary

Existing single cell isolation robots can manipulate only surface attached cells seriously limiting the fields of their application for single cell handling. Although naturally adherent cells can be spontaneously immobilized on the surface, the adhesion force needs to be tuned either biochemically or by surface modifications optimized to the cell type. Otherwise the too strongly adhered cells are picked up at an expense of damaging the cell. We developed a computer vision-based robot applying a motorized microscope and micropipette to recognize and gently isolate intact individual cells for subsequent analysis, e.g., DNA/RNA sequencing in 1-2 nanolitres from suspension without immobilizing cells on the surface of the Petri dish [R. Ungai-Salánki, T. Gerecsei, P. Fürjes, N. Orgován, N. Sándor, E. Holczer, R. Horváth, B. Szabó: Automated single cell isolation from suspension with computer vision, accepted for publication in Scientific Reports]. To minimize fluid convection cells were kept in a thin (~100 μm) layer of buffer or culture medium covered by oil. It can retrieve rare cells, needs minimal sample preparation, and can be applied for virtually any tissue cell type. Combination of 1 μm positioning precision, adaptive

cell targeting and below 1 nl liquid handling precision resulted in an unprecedented accuracy and efficiency in robotic single cell isolation. We applied a 3D printer to build miniature multi-well plates into the Petri dish. Single cells were injected either into the wells of a miniature plate with a sorting speed of 3 cells/min or into standard PCR tubes with 2 cells/min. We could isolate labeled cells also from dense cultures containing ~1,000 times more unlabeled cells by the successive application of the sorting process. We compared the efficiency of our method to that of single cell entrapment in microwells and subsequent sorting with the automated micropipette: the recovery rate of single cells was greatly improved. We expect that image-based automated single cell manipulation will become an everyday technique of molecular cell biology.

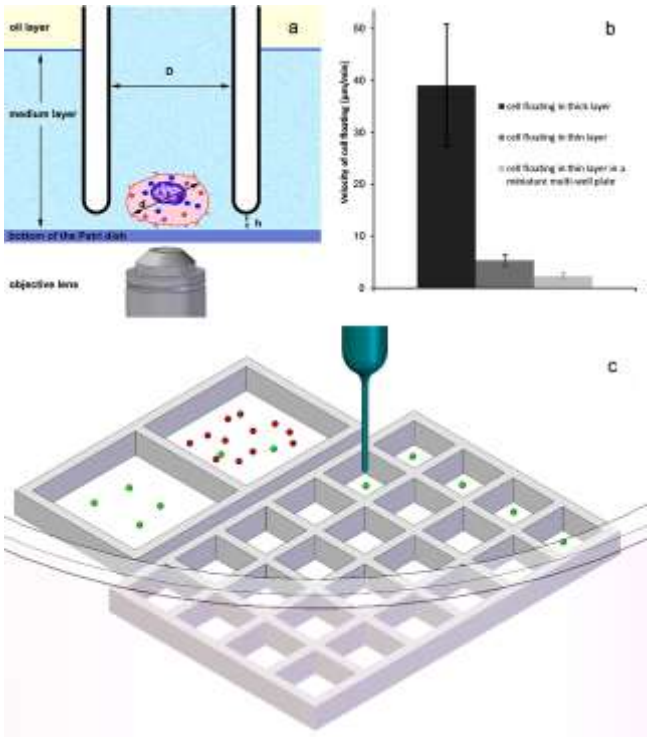

Figure 1 *Automated micropipette for single cell isolation from a thin layer of suspension. Panel a shows the concept of cell sorting. Cells are detected by computer vision. Cell suspension confined into a thin ~100 µm layer of culture medium or buffer covered with oil to avoid the convection-driven floating of cells. The glass micropipette with an inner diameter of D= 30 µm approaches the surface of the dish to a distance of h= 5 µm. Targeted cell is picked up by a slight vacuum connected to the micropipette and controlled by a high speed fluid valve. Inhibitory effect of cell confinement into a thin layer on cell floating is shown in b. Wells of the miniature plate (shown in c) printed into the Petri dish further decreased convection.*

Monitoring of cellular toxicity assessment of agrochemicals by using label-free optical biosensor technique

("Lendület" grant LP2012-26/2012 of HAS, OTKA K109865)

I. Székács, D. Patkó, R. Horváth, and A. Székács[1]

[1]Agro-Environmental Research Institute, National Agricultural Research and Innovation Centre, Budapest, Hungary

In 2015 we continued our work on the application of digital holographic microscopy to cytotoxicology studies. This technology has been successfully applied by our research group for the first time in the world for in vitro cytotoxicity investigations, and occurs to be a promising tool in reducing animal experimentation in toxicology. Digital laser holographic transmission microscopy is a label-free, non-invasive, non-destructive and non-phototoxic method allowing both qualitative and quantitative high resolution measurements of living cells over time. Thus, it offers a highly sensitive and versatile method to study cell morphology parameters, cellular processes and cell viability, including cytostatic and cytotoxic effects of various xenobiotics of chemical or microbiological origin cells are exposed to. In our study on a widely used agrochemical, the herbicide preparation Roundup, currently being criticized for its potential endocrine disrupting effects and carcinogenicity, we evidenced cytostatic and cytotoxic effects of the preparation at concentrations even 200-fold below agricultural administration levels [129,130,140]. Cell morphology parameters, like cell area, thickness and volume, can be very useful when monitoring the effects of different treatments. The toxic effect of Roundup at the concentration 20-fold below agricultural application was seen in 10 minutes, cells take rounded shapes due to cytoskeletal response, and become detached from surfaces they had adhered to (Fig. 1). Consequently a time-dependent decrease in cell area and an increase in maximum thickness of the cells were seen in response to treatment. The above cytotoxic effects have also been evidenced by our group using the rapid and

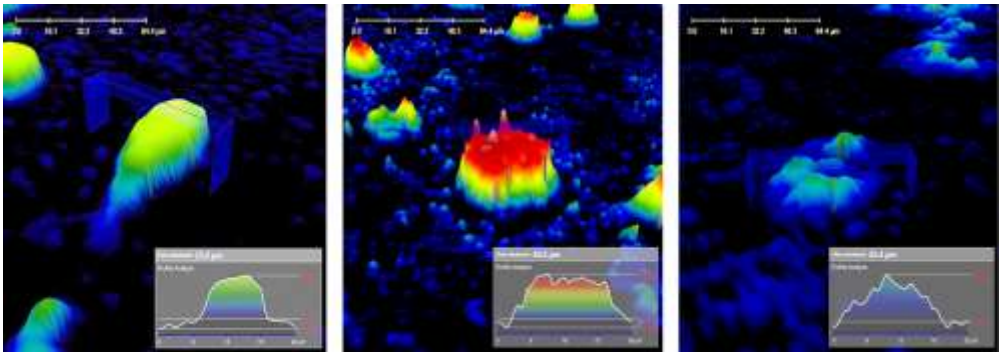

Figure 1 *Time-dependent morphological changes of cells exposed to Roundup (0.1%), detected by phase contrast holographic microscopy. Images were captured every five minutes from the beginning of treatment with Roundup (0 min). After a few minutes of treatment the cells become round, then turn uneven and later break apart.*

high throughput optical biosensor technique, Epic BT. The main advantage of this sensor is that it applies parallel multiple optical waveguide sensoric detection (e.g. on 384-well microplates) of given analytes or surface molecular processes using resonant waveguide grating. This allows rapid parallel analysis of many samples. With the Epic BT method we expand our study of Roundup, as well as its active ingredient glyphosate and adjuvant polyethoxylated tallowamine (POEA) on preosteoblastic cell line MC3T3-E1, as glyphosate has been indicated to inhibit bone development in rats.

The dynamics of living cell adhesion on nanostructured genetically engineered molecular layers revealed by label-free optical biosensors

("Lendület" grant LP2012-26/2012 of HAS, OTKA K104726)

B. Kovács, D. Patkó, I. Székács, N. Orgován, B. Tóth, F. Vonderviszt, and R. Horváth

Our purpose was to record the kinetics of cancer cell adhesion on layers of genetically engineered protein variants, which are displaying cell adhesive RGD motifs. Wild type protein coatings and synthetic polymer films were used in parallel control experiments. We applied two types of waveguide sensors, optical waveguide light-mode spectroscopy and Epic Benchtop system, to record cell adhesion on the surface. The applied protein is a good target for genetic modifications. We constructed protein variants which can display cell adhesive RGD motif. Specific cell surface receptors (integrins) can recognize and bind these molecules, and trigger cell adhesion.
The experimental results confirmed that the PLL-g-PEG polymer coating prevents cell adhesion, while the cells adhered and spread markedly on the RGD grafted PLL-g-PEG polymer layer. On the layer of the wild type protein negligible adhesion could be detected, contrary to the RGD displaying protein variants where significant cell adhesion was observed (Fig. 1). Our work resulted in fine-tuned surface coatings for basic cellular research and biomedical applications. It highlights the possibilities offered by label-free technologies in cell biological research and development.

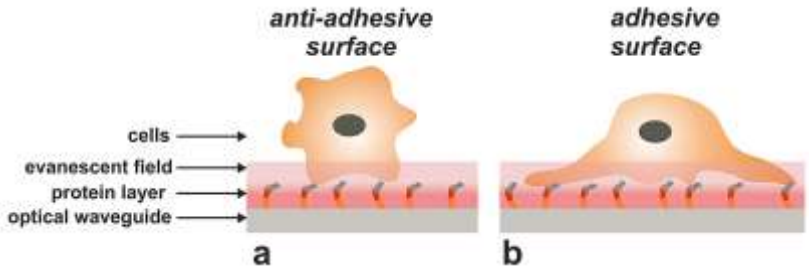

Figure 1 *Schematic representation of anti-adhesive and adhesive surface coating induced cell behavior. a: Wild type protein surface coating hinders cell adhesion on the sensor surface. b: RGD displaying protein surface coating induces cell adhesion and spreading.*

Complex Systems Department

Head: György SZABÓ, D.Sc., scientific advisor

Research Staff

- István BORSOS
- Imre EÖRDÖGH
- Zoltán JUHÁSZ, Ph.D.
- Géza ÓDOR, Ph.D.
- Károly SZÁSZ, engineer
- Attila SZOLNOKI, D.Sc.

Ph.D. students / Diploma workers

- Levente VARGA, Ph.D. student
- Balázs KIRÁLY, Ph.D. student
- Kristóf HÓDSÁGI, student

The main field of research of the Complex Systems group is the statistical physical analysis of non-equilibrium systems mostly centred around many-agent evolutionary game theoretic models, like investigating processes maintaining honest behaviour, e.g. the effects of punishment, evolutionary dynamics and interconnection on the level of cooperation. Among the innovations is the introduction of individual differences causing the players to „re-evaluate" their income, e.g. by amplifying the acceptance of the neighbour's opinion. Another topic is the role of cyclic interactions supporting the maintenance of multi-strategy states (biodiversity) in spatial models.

We have studied the decomposition of symmetric matrix games into four elementary interactions. The coordination games have been extended by additional neutral strategies preserving the order-disorder phase transition when the noise is increased, which is characteristic of the Ising models.

The statistical physical investigation of dynamic processes on random graphs can be materially used in brain research and in the interpretation of social and biological phenomena. This emphasises the study of slow processes (Griffiths phase) on hierarchic and modular networks. Our numerical investigations showed power-law behaviour, which is typical of critical transitions in interconnection systems characteristic of the neural cells of the brain. We have continued the numerical investigation of surface growth in cooperation with German researchers.

Earlier analysis of folk music has been continued and connected to numerical analysis of genetic and linguistic relatedness. The distribution of haplogroups inherited matrilineally has been studied together with geneticists. Our experts have participated in the R&D project "Introducing cognitive methods to improve protection against vehicle collisions", using their experience in software development for image processing.

Does knowing the opponent's strategy guarantee optimal play?

(OTKA K-101490)

A. Szolnoki, and M. Perc

Knowing the strategy of an opponent in a competitive environment conveys obvious evolutionary advantages. But information is costly, and being informed may not necessarily offset the additional cost. By using the methods of statistical physics we have studied [138] a spatial social dilemma game in which beside cooperator (C) and defector (D) strategies we also introduced "informed" strategies: the latter are those who invest extra efforts to explore the aim of neighbours and behave accordingly. In particular, IC players refuse to be exploited by defectors, while ID players avoid being punished when encountering other defectors. We suppose that being informed conveys an advantage to ID players compared to D players. The simplest way to ensure this is to still punish defectors if they meet an ID player.

As a result, we could identify elementary relations between the four competing strategies in the governing food web, which revealed the existence of two three-strategy defensive alliances. We have shown that a direct evolutionary advantage of a strategy within a defensive alliance can be compensated by the other alliance through a faster internal rotation of its strategies. Thus, even though in the food web the informed defectors are superior to unconditional defectors, the alliance whose defense relies on the weaker strategy can still prevail. We have demonstrated that the competition between a direct food-web-based evolutionary advantage and an evolutionary advantage that is rooted in the spatio-temporal dynamics of a defensive alliance gives rise to a re-entrant phase transition. In-between the two stable phases that form the re-entrant pair, we have also identified a very narrow region of coexistence of both defensive alliances, which emerges as a consequence of a delicate equilibrium of the two competing mechanisms.

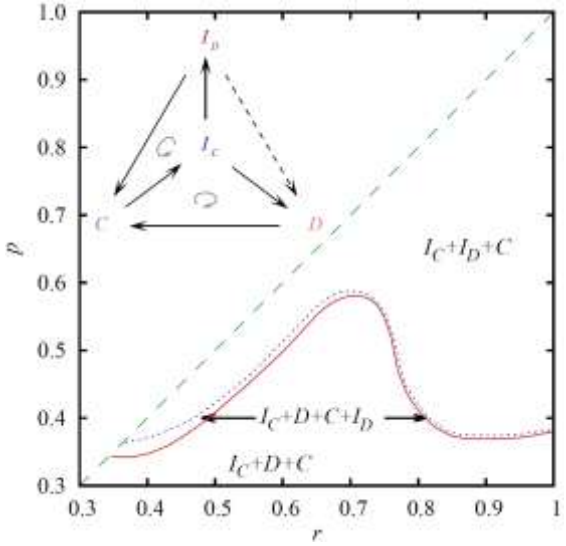

Figure 1 *Full r−p phase diagram, as obtained at a specific cost value. Solid red line denotes continuous phase transitions from the very narrow but stable I_C+D+C+I_D phase to the stable I_C+D+C phase, while the dotted blue line denotes re-entrant continuous phase transitions to the stable I_C+I_D+C phase. Dashed green line is the p < r border.*

Inset in the left-up corner shows the direction of invasion between the competing strategies (see arrows).

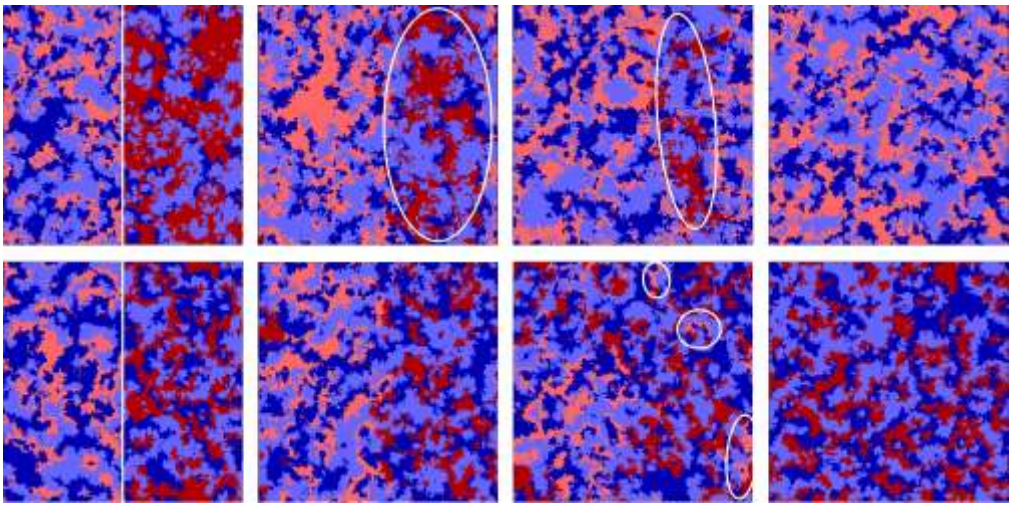

Figure 2 *Snapshots of pattern formation, as obtained for r = 0.65 (top row) and r = 0.95 (bottom row) starting from a prepared initial state. During the relaxation period, each half of the lattice contained the strategies of one triplet only. After the characteristic patterns evolved (leftmost panels), the separating white wall was removed and the two defensive alliances started to compete with each other. In the top row, the (I_C+D+C) triplet (dark blue, light blue, and light red, overall lighter), gradually compresses the (I_C +I_D+C) triplet (dark blue, light blue, and dark red, overall darker). The typical size of the shrinking alliance is encircled with a white ellipse. The snapshots were taken after different iteration steps from left to right. In the bottom row, the (I_C+I_D+C) triplet gradually gets dominant because I_D players are superior to D players. Accordingly, the domains of the (I_C+D+C) triplet (white ellipses) vanish over time.*

Eurasian mtDNA analysis with a new iterative rank-correlation method

(OTKA K-81954)

Z. Juhász, T. Fehér, E. Németh, and H. Pamjav

We have analysed 27-dimensional mtDNA haplogroup distributions of 174 Eurasian, North-African and American populations to describe the haplogroup distributions of populations as composites of certain hypothetic ancient core populations immediately or indirectly determining the migration processes in Eurasia [58]. To identify these core populations, a new iterative algorithm determines the clusters of the 27 studied haplogroups having strong rank-correlations. Combined with our Self Organising Cloud algorithm this allowed us to determine geographically, historically and linguistically interpretable clusters of our dataset having a very specific structure defying classification. Figure 1 shows the rank correlations, where the distances driving the MDS algorithm were calculated as 1-rank correlation for all pairs of Hg-s. Three disjoint “correlating haplogroup clusters” (CHgC) are clearly identified:

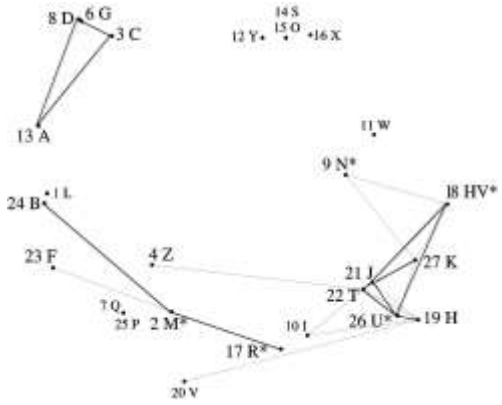

Figure 1 *MDS graph of the correlations between 27 MTDNA haplogroups in Eurasia an America. Thin and thick edges indicate correlations over 0.67 and 0.74 respectively.*

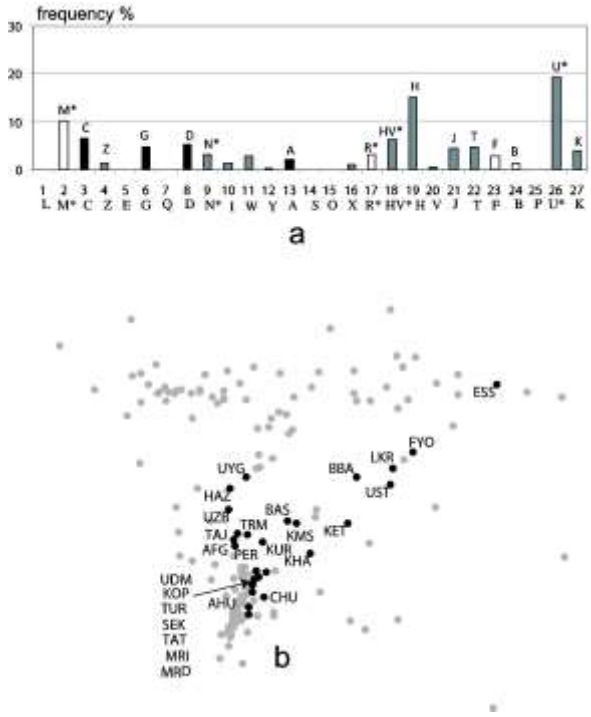

Figure 2 *The main haplogroup distribution of a composite cluster obtained by the Self Organising Cloud algorithm (a), and the location of the related populations in the general MDS-map of the 174 Hg distributions (b).*

Siberian, Western and Eastern components are denoted by black, grey and white columns. Ancient Bronze-age distributions of the Andronovo culture are BBA (Baraba Steppe), LKR (Late Krotovo), UST (Ustinovo), FYO (Fyodorovo). Recent descendants – UYG (Uygur), UZB (Uzbek), KOP (Komi), TUR (Turkish), SEK (Székely), TAT (Tatar), MRI (Mari), MRD (Mordvin) are mainly Uralic and Altaic speaking populations.

The relatively large number of ancient DNA samples provided an invaluable tool for comparing ancient population movements with the location of living populations. Comparing the ancient data of the Andronovo and the Kurgans areas to recent distributions led us to conclude that current East and Central European populations may consist of a Western substrate arising from the Near Eastern Neolithic stock and a Siberian-Western composite population arising from the Andronovo area. The close relations of recent and ancient haplogroup distributions of these areas also make it probable that Uralic and Altaic languages could have played a significant maternal role in the Andronovo culture, and Uralic-speakers in the Kurgans culture.

Griffiths phases and localization in hierarchical modular networks

(OTKA T77629)

Géza Ódor, R. Dickman, and Gergely Ódor

We have studied variants of hierarchical modular network models suggested by Kaiser and Hilgetag [Front. in Neuroinform., 4 (2010) 8] to model functional brain connectivity, using extensive simulations and quenched mean-field theory (QMF), focusing on structures with a connection probability that decays exponentially with the level index [91]. Such networks can be embedded in two-dimensional Euclidean space. We explored the dynamic behavior of the contact process (CP) and threshold models on networks of this kind, including hierarchical trees. While in the small-world networks originally proposed to model brain connectivity, the topological heterogeneities are not strong enough to induce deviations from mean-field behavior, we showed that a Griffiths Phase (GP) can emerge under reduced connection probabilities, approaching the percolation threshold. In this case the topological dimension of the networks is finite, and extended regions of bursty, power-law dynamics are observed. Localization in the steady state was shown via QMF. We investigated the effects of link asymmetry and coupling disorder and showed that localization can occur even in highly connected small-world networks in case of link disorder.

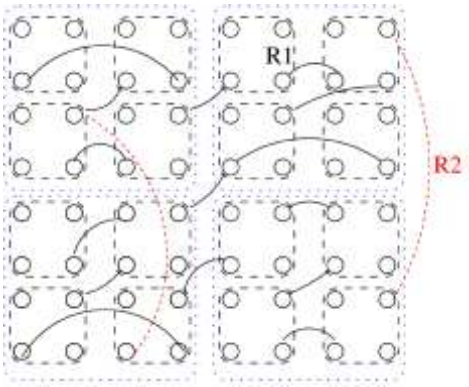

Figure 1 *Two lowest levels of the HMN2d hierarchical network construction. Dashed lines frame bottom level nodes, which are fully connected there, dotted lines frame the nodes of the next level. The solid lines denoted R1 are randomly chosen connections among the bottom level modules, ensuring single connectedness of the network, while those denoted R2 provide random connections on the next level. Links can be directed.*

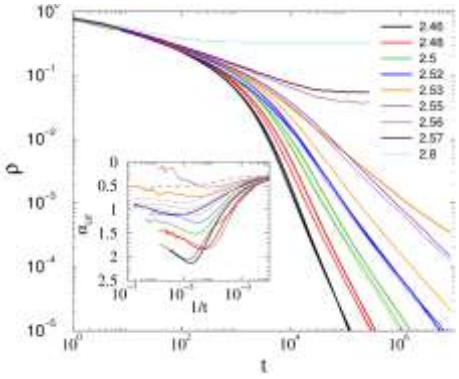

Figure 2 *CP on asymmetric HMN2d networks with average node degree k~4: decay of activity for activation rates (λ) values as indicated. System sizes: l_{max}=8, 9, 10 levels (thin, medium, and thick lines, respectively). Size-independent power laws are observed for 2.45<λ<2.53. Inset: local slopes of the curves in the main plot. In the GP the effective decay exponent α_{eff} tends to non-universal values, in addition with logarithmic corrections.*

MFA Seminar Talks

2015.01.07 **Gergely MÁRTON**
(Semmelweis University, Budapest, Hungary): *"Development and characterisation of novel microelectrode arrays for neurophysiology"*

2015.02.28 **Zoltán HAJNAL**
(MTA EK MFA, Budapest, Hungary): *"Közelítő módszerek az atomi és molekuláris modellezésben"*

2015.02.04 **Dániel PATKÓ**
(MTA EK MFA, Budapest, Hungary): *"Nagyérzékenységű jelölésmentes bioszenzorika"*

2015.03.05 **Péter VANCSÓ**
(MTA EK MFA, Budapest, Hungary): *"Töltésterjedés grafén nanoszerkezetekben"*

2015.03.31 **Carl FRANCK**
(Cornell University, USA): *"Surprises in Unicellular Eucariotic Sensing"*

2015.05.06 **MTA közgyűlés**

2015.05.13 **Béla PÉCZ**
(MTA EK MFA, Budapest, Hungary): *"GaN heterostructures with diamond and graphene for high power applications"*

2015.05.20 **Aryasomayajulu SUBRAHMANYAM**
(ITT Madras, Chennai, India): *"Hospital Acquired Infection (HAI): what can be done by a material scientist?"*

2015.05.27 **Sándor KUGLER**
(BME, Physics Institute, Budapest, Hungary): *"Fascinating amorphous semiconductors"*

2015.06.03 **Péter BARNA**
(MTA EK MFA, Budapest, Hungary): *"A vékonyrétegkutatás koncepciója 60 év távlatából"*

2015.06.10 **György Zoltán RADNÓCZI**
(MTA EK MFA, Budapest, Hungary): *"Amorf Si Ni indukálta kristályosodása"*

2015.06.17	**Peter LOBOTKA** (ELU SAV, Bratislava, Slovakia): *"Fabrication of metallic nanoparticles in ionic liquid"*
2015.08.31- -2015.09.01	**Nobuo TANAKA** (EcoTopia Science Institute, Nagoya University, Japan): *"HREM - 2-days seminar/course"*
2015.10.14	**Zsolt Endre HORVÁTH** (MTA EK MFA, Budapest, Hungary): *"Vezető polimer kompozitok"*
2015.10.21	**Miklós KELLERMAYER** (Semmelweis University, Budapest, Hungary): *"Modern mikroszkópos eljárások egyedi molekulák vizsgálatára"*
2015.10.28	**Nikolett OLÁH** (MTA EK MFA, Budapest, Hungary): *"Bioinert Ti-C nanokompozit fejlesztése orvosi implantátumok felületi tulajdonságainak javítása céljából"*
2015.11.05	**Hiroshi AMANO** (Nagoya University, Japan): *"Progress in III-nitride nanodevices"*
2015.11.11	**Szabolcs CSONKA** (BME, Budapest, Hungary): *"Kvantum dotok felfüggesztett grafénban"*
2015.11.18	**Pavel B. SOROKIN** (Russia): *"New specific properties of 2D films"*
2015.12.02	**Ákos Koppány KISS** (MTA EK MFA, Budapest, Hungary): *"Szemcsehatárok transzmissziós elektronmikroszkópos vizsgálati módszereinek fejlesztése"*
2015.12.08	**Peter SAMUELY** (*UEF SAV, Kosice, Slovakia*): *"The Kosice Centre of Low Temperature Physics"*
2015.12.08	**Pavol SZABÓ** (*UEF SAV, Kosice, Slovakia*): *"Superconductivity near transition to insulating state in molybdenum carbide"*

Research and Development Partners, Foreign Visitors

AMANO, Hiroshi *(Nagoya University, Japan)*
ANTIPINA, Liubov Yu. *(Russia)*
ARAKAWA, Hanae *(Japan)*
ASLAMACI, Abdullah *(INOVENSO Ltd., Turkey)*
BENES, Roman *(Anton Paar, Graz, Austria)*
BEREKMÉRI, Evelin *(Romania)*
BEROZ, Masud *(ComponentZEE LLC , USA)*
BOSI, Matteo *(IMEM-CNR, Parma, Italy)*
BREUER, Stefan *(Technische Universität Darmstadt, Germany)*
BRUNO, Friedhelm *(Germany)*
CARBONI, Alberto *(Italy)*
CHAPELIER, Claude *(France)*
COTTIER, Kaspar *(Creoptix GmbH, Wädenswil, Switzerland)*
CSIKAI Dávid *(Romania)*
DARMIL, Guillaume *(France)*
DAS, Partha Pratim *(India)*
DING, Zejun *(China)*
DRAGANITS, Gerhard *(Zeiss, Austria)*
FARBER, Paul *(Robert Bosch Kft., Germany)*
FIEDLER, Christian *(Agilent, Germany)*
FRANK, Carl Peter *(USA)*
GASTNER, Michael Thorsten *(Germany)*
GILMORE, Mark *(UK)*
HERBERT, Damnik Niklas *(Germany)*
HUNT, Steven *(FEI, UK)*
HWANG Chanyong *(Korean Research Institute of Standards and Science, Daejon, South Korea)*
ISHIHARA, Sotomi *(Toyama National College, Toyama, Japan)*
KAENDERS, Wilhelm *(Toptica AG, Germany)*
KELLING, Jeffrey *(HZDR, Dresden, Germany)*
KOMÁN Zsolt *(Romania)*
KUMAR, Srivastawa Pawan *(India)*
KUNZO, Pavol *(ELU SAV, Slovakia)*
KUROKAWA, K. *(Tateyama Kagaku, Japan)*
LATHUS, Guillaume *(France)*
LOBOTKA, Peter *(ELU SAV, Bratislava, Slovakia)*
MANGANIELLO, Adam *(USA)*
MANUSCO, James F. *(USA)*
McWILLIAMS, Christopher John *(UK)*
NAGY Ádám *(Slovakia)*
NAWRAT, Zbigniew *(Poland)*
NAZIRIZADEH, Yousef *(Germany)*

NÉMET Anikó *(Serbia)*
NERGAARD, Per Olav *(Norway)*
NEWMAN, David *(UK)*
NUTSCH, Andreas *(Fraunhofer IISB, Germany)*
O'DONNELL, James *(France)*
ORBÁN Szabolcs *(Romania)*
ORBÁNOVÁ, Ágnesa *(Slovakia)*
PINTO, Fabrizio *(USA)*
RAMSDEN, Jeremy *(UK)*
ROHR, Kamil *(Poland)*
SCHATZ, Oliver *(Robert Bosch Kft., Germany)*
SCHÖNENBERGER, Christian *(Switzerland)*
SOROKIN, Pavel B. *(Russia)*
SPIGA, Fabio *(Italy)*
STEINRÜCK, Hans-Peter *(Germany)*
SUBRAHMANYAM, Aryasomayajulu *(ITT Madras, Chennai, India)*
SZABÓ, Pavol *(UEF SAV, Slovakia)*
TADA, Kazihuro *(National Institute for Technology, Toyama, Japan)*
TAKAGI, Toshiyuki *(Tohoku University, Sendai, Japan)*
TANAKA, Nobuo *(EcoTopia Science Institute, Nagoya University, Japan)*
TERAYAMA, H. *(Tateyama Kagaku, Japan)*
TRIVUN, Dusko *(Bosnia and Hercegovina)*
UZUNER, Talha *(INOVENSO Ltd., Turkey)*
VANAJA, Aryasomayajula *(India)*
VARGA Levente *(Romania)*
VÁVRA, Jan *(JPK Instruments AG, Checz Republik)*
WATANUKI, Osamu *(Tateyama Kagaku, Japan)*
XU, Huan *(China)*

MFA Publications in 2015

1. **Agócs E**, Bodermann B, Burger S, Dai G, Endres J, Hansen PE, Nielsen L, Madsen MH, Heidenreich S, Krumrey M, Loechel B, Probst J, Scholze F, Soltwisch V, Wurm M: "Scatterometry reference standards to improve tool matching and traceability in lithographical nanomanufacturing", *Progress in Biomedical Optics and Imaging (Proc of SPIE) 9556: Paper 955610, p.12 (2015),* DOI:10.1117/12.2190409
2. **Albert E**, Albouy PA, Ayral A, Basa P, Csík G, Nagy N, Roualdés S, Rouessac V, Sáfrán G, Suhajda Á, Zolnai Zs, Hórvölgyi Z: "Antibacterial properties of Ag-TiO_2 composite sol-gel coatings", *RSC Advances 5:(73) pp.59070-59081 p.11 (2015)*
3. **Albert E**, Basa P, Deák A, Németh Á, Osváth Z, Sáfrán G, Zolnai Zs, Hórvölgyi Z, Nagy N: "Introducing nanoscaled surface morphology and percolation barrier network into mesoporous silica coatings", *RSC Advances 5:(74) pp.60041-60053 (2015)*
4. **Albert E**, Cotolan N, Nagy N, Sáfrán G, Szabó G, Mureşan LM, Hórvölgyi Z: "Mesoporous silica coatings with improved corrosion protection properties", *Microporous and Mesoporous Materials 206 pp.102-113 (2015)*
5. **An H**, Wang J, Szívós J, Harumoto T, Sannomiya T, Muraishi S, Sáfrán G, Nakamura Y, Shi J: "Perpendicular coercivity enhancement of CoPt/TiN films by nitrogen incorporation during deposition", *J Appl Phys 118:(20) Paper 203907 p.4 (2015)*
6. **Anaya J**, Rossi S, Alomari M, Kohn E, Tóth L, Pécz B, Kuball M: "Thermal conductivity of ultrathin nano-crystalline diamond films determined by Raman thermography assisted by silicon nanowires", *Appl Phys Lett 106:(22) Paper 223101 p.5 (2015)*
7. **Anooz BS**, Petrik P, Schmidbauer M, Remmele T, Schwarzkopf J: "Refractive index and interband transitions in strain modified $NaNbO_3$ thin films grown by MOCVD", *J Physics D - Applied Physics 48:(38) Paper 385303 p.9 (2015)*
8. **Babenko V**, Murdock AT, Koós AA, Britton J, Crossley A, Holdway P, Moffat J, Huang J, Alexander-Webber JA, Nicholas RJ, Grobert N: "Rapid epitaxy-free graphene synthesis on silicidated polycrystalline platinum", *Nature Communications 6: Paper 7536 p.8 (2015)*
9. **Balázsi Cs**, Tapasztó O, Balázsi K: "Structural Investigation of Biogenic Calcium Phosphate Based Composites Prepared by Electrospinning", In: *Ágnes Kittel, Pécz B (Eds.), 12th Multinational Congress on Microscopy: MCM 2015., Eger, Hungary, 20150823-28, Budapest: Akadémiai Kiadó, pp.523-524 (2015)*
10. **Balázsi K,** Balázsi Cs: "Biogenic Hydroxyapatite Based Implant Materials", In: *Thakur VK, Kessler MR (Eds.), Green Biorenewable Biocomposites: From Knowledge to Industrial Applications, Waretown: Apple Academic Press Ltd., pp.27-57 (2015)*
11. **Balázsi K**, Barkóczy P, Bársony I, Czvikovszky T, Gyulai J, Hohol R, Janó V, Kaptay Gy, Kocsis-Baán M, Kónya I, Kuzsella L, Lendvai J, Szabó PJ, Tóth Lá, Verő B, Zsámbók D (Eds.): *Országos Anyagtudományi Konferenciasorozat 1997-2015, Jubileumi Kiadvány: Anyagtudomány, anyagvizsgálat, anyaginformatika, Balatonalmádi, Hungary, 20151011-13, Budapest: Magyar Anyagtudományi Egyesület, (2015), (ISBN:978-963-12-3494-7)*
12. **Balázsi K**: "Hypoallergenic Ceramic Implant Materials: Preparation and Properties", In: *Ágnes Kittel, Pécz B (Eds.), 12th Multinational Congress on Microscopy: MCM 2015, Eger, Hungary, 20150823-28, Budapest: Akadémiai Kiadó, pp.137-139 (2015)*

13. **Barna PB**: "Pócza tanár úr - születésének 100. évfordulóján", *Fizikai Szemle 65:(11) pp.372-376 (2015)*
14. **Bársony I**: "A céltudatosság jutalma (A 2014-es fizikai Nobel-díjról)", *Fizikai Szemle 65:(1) pp.33-35 (2015)*
15. **Bársony I**: "Paradigmaváltás az ezredforduló anyagkutatásában", In: Balázsi K, Barkóczy P, Bársony I, Czvikovszky T, Gyulai J, Hohol R, Janó V, Kaptay Gy, Kocsis-Baán M, Kónya I, Kuzsella L, Lendvai J, Szabó PJ, Tóth Lá, Verő B, Zsámbók D (Eds.), *Országos Anyagtudományi Konferenciasorozat 1997-2015, Jubileumi Kiadvány: Anyagtudomány, anyagvizsgálat, anyaginformatika, Balatonalmádi, Hungary, 20151011-13, Budapest: Magyar Anyagtudományi Egyesület, pp.124-133 (2015), (ISBN:978-963-12-3494-7)*
16. **Battistig G**: "Introduction: REM7 - 2014", *Radiation Effects and Defects in Solids 170:(3) pp.153-154 (2015)*
17. **Beke D**, Szekrényes Zs, Czigány Zs, Kamarás K, Gali Ádám: "Dominant luminescence is not due to quantum confinement in molecular-sized silicon carbide nanocrystals", *Nanoscale 7:(25) pp.10982-10988 (2015)*
18. **Bódis E**, Tapasztó O, Zoltán K, Fazekas P, Klébert Sz, Keszler AM, Balázsi K, Szépvölgyi J: "Spark plasma sintering of Si_3N_4/multilayer graphene composites", *Open Chemistry 13:(1) pp.484-489 (2015)*
19. **Bohner B**, Schuszter G, Nakanishi H, Zámbó D, Deák A, Horváth D, Tóth Á, Lagzi I: "Self-Assembly of Charged Nanoparticles by an Autocatalytic Reaction Front", *Langmuir 31:(44) pp.12019-12024 (2015)*
20. **Bulusheva LG**, Okotrub AV, Fedoseeva YuV, Kurenya AG, Asanov IP, Vilkov OY, Koós AA, Grobert N: "Controlling pyridinic, pyrrolic, graphitic, and molecular nitrogen in multi-wall carbon nanotubes using precursors with different N/C ratios in aerosol assisted chemical vapor deposition", *Physical Chemistry Chemical Physics 17:(37) pp.23741-23747 (2015)*
21. **Chandrappan J**, Murray M, Kakkar T, Petrik P, Agócs E, Zolnai Zs, Steenson DP, Jha A, Jose G: "Target dependent femtosecond laser plasma implantation dynamics in enabling silica for high density erbium doping", *Scientific Reports 5: Paper 14037 p.8 (2015)*
22. **Chandrappan J**, Murray M, Petrik P, Agócs E, Zolnai Zs, Tempez A, Legendre S, Steenson DP, Jha A, Jose G: "Doping silica beyond limits with laser plasma for active photonic materials", *Optical Materials Express 5:(12) pp.2849-2861 p.12 (2015)*
23. **Chen X**, Szolnoki A, Perc M: "Competition and cooperation among different punishing strategies in the spatial public goods game", *Phys Rev E Stat Nonlin 92:(1) Paper 012819 p.6 (2015)*
24. **Chubarov M**, Pedersen H, Högberg H, Czigány Zs, Garbrecht M, Henry A: "Polytype pure sp2-BN thin films as dictated by the substrate crystal structure", *Chemistry of Materials 27:(5) pp.1640-1645 p.6 (2015)*
25. **Chubarov M**, Pedersen H, Högberg H, Garbrecht M, Czigány Zs, Andersson SG, Henry A: "Chemical Vapor Deposition of Boron Nitride Thin Films on SiC", *Materials Science Forum 821-823: pp.990-994 (2015)*
26. **Chubarov M**, Pedersen H, Högberg H, Henry A, Czigány Zs: "Initial stages of growth and the influence of temperature during chemical vapor deposition of sp2-BN films", *J*

Vacuum Science and Technology A-Vacuum Surfaces and Films 33:(6) Paper 061520 p.6 (2015)

27. **Cora I**, Dódony I, Tóth L, Kiss KÁ: "Study of Si-containing pyrite (FeS_2)", In: *Ágnes Kittel, Pécz B (Eds.), 12th Multinational Congress on Microscopy: MCM 2015, Eger, Hungary, 20150823-28, Budapest: Akadémiai Kiadó, pp.275-276, p.2 (ISBN:978-963-05-9653-4) (2015)*
28. **Cota WFC**, Ferreira SC, Ódor G: "Griffiths effects of the susceptible-infected-susceptible epidemic model on random power-law networks", *(2015),* arXiv:1512.05274
29. **Craciun D**, Socol G, Cristea DV, Stoicanescu M, Olah N, Balazs K, Stefan N, Lambers E, Craciun V: "Mechanical properties of pulsed laser deposited nanocrystalline SiC films", *Appl Surf Sci 336: pp.391-395. (2015)*
30. **Daróczi CsS** (Eds.): "MTA EK MFA Yearbook 2014", *Budapest: MTA MFA, 2015. 144p. (2015)*
31. **Datz D**, Gasparics A, Vértesy G: "Study of the Fluxset Magnetic Probe Speed-Sensitivity Developed for Detection of Magnetic Nanoparticles in Surgery", *J Electrical Eng 66:(1) pp.57-60 (2015)*
32. **Deschler F**, Riedel D, Deák A, Ecker B, Hauff EV, Como ED: "Imaging of morphological changes and phase segregation in doped polymeric semiconductors", *Synthetic Metals 199: pp.381-387 (2015)*
33. **Dillon FC**, Moghal J, Koós AA, Lozano JG, Miranda L, Porwal H, Reece MJ, Grobert N: "Ceramic composites from mesoporous silica coated multi-wall carbon nanotubes", *Microporous and Mesoporous Materials 217: pp.159-166 (2015)*
34. **Dobrik G**: "Szén alapú nanoarchitektúrák kialakítása és jellemzése pásztázószondás módszerekkel", *127p. (PhD) (2015)*
35. **Dódony E**, Radnóczi GyZ, Pécz B, Stoemenos J, Vouroutzis N, Frangis N: "Investigating MILC Processes in Extreme Conditions", In: *Ágnes Kittel, Pécz B (Eds.), 12th Multinational Congress on Microscopy: MCM 2015., Eger, Hungary, 20150823-28, Budapest: Akadémiai Kiadó, pp.250-252 (2015)*
36. **Fekete B**, Kasl J, Jandova D, Jóni B, Trampus P, Misják F: "Low cycle thermomechanical fatigue of reactor steels: microstructural and fractographic", *Materials Science and Engineering: A Publication of the University of Miskolc 640: pp.357-374 (2015)*
37. **Fekete Z**, Németh A, Márton G, Ulbert I, Pongrácz A: "Experimental study on the mechanical interaction between silicon neural microprobes and rat dura mater during insertion", *J Mater Sci-Materials Medicine 26:(2) Paper 70 p.21 (2015)*
38. **Fekete Z**: "Recent advances in silicon-based neural microelectrodes and microsystems: a review", *Sensors Actuators B Chemical 215: pp.300-315 (2015)*
39. **Fekete Z**: "Technology of ultralong deep brain fluidic microelectrodes combined with etching-before-grinding", *Microsystem Technologies 21:(2) pp.341-344 (2015)*
40. **Fogarassy Zs**: "Fizikai és kémiai módszerekkel gőzfázisból leválasztott szerkezetek kialakítása és jellemzése", *117p. (PhD) (2015)*
41. **Fried M**, Major Cs, Juhász Gy, Petrik P, Horváth Z: "Expanded beam speetro-ellipsometry for big area on-line monitoring", *Proc of SPIE - Int Soc Optical Eng 9525: Paper 95251S p.12 (2015)*

42. **Frigeri C**, Serényi M, Szekrényes Z, Kamarás K, Csik A, Khánh NQ: "Effect of heat treatments on the properties of hydrogenated amorphous silicon for PV and PVT applications", *Solar Energy 119: pp.225-232 (2015)*
43. **Fürjes P**, Holczer EG, Tóth E, Iván K, Fekete Z, Bernier D, Dortu F, Giannone D: "PDMS microfluidics developed for polymer based photonic biosensors", *Microsystem Technologies 21:(3) pp.581-590 (2015)*
44. **Galkin NG**, Galkin KN, Goroshko DL, Chernev IM, Shevlyagin AV, Dózsa L, Osváth Z, Pécz B: "Non-doped and doped Mg stannide films on Si(111) substrates: Formation, optical, and electrical properties", *Jap J Appl Phys 54:(7) Paper 07JC06 p.9 (2015)*
45. **Galkin NG**, Goroshko DL, Galkin KN, Shevlyagin A, Chernev IM, Maslov AM, Dotsenko SA, Subbotin EY, Dózsa L, Osváth Z, Pécz B, Kudrawiec R, Misiewicz J: "Semiconducting Mg_2Sn and Mg_2Ge nanolayers on Si(111) substrates: formation, structure and properties", In: *V E Borisenko, S V Gaponenko, V S Gurin, C H Kam (Eds.), Physics, Chemistry and Applications of Nanostructures: Proc Int Conference Nanomeeting, Minsk, Belorussia, 20150526-29, Minsk: World Scientific, pp.128-131 (2015)*
46. **Gastner MT**, Ódor G: "The topology of large Open Connectome networks for the human brain", *(2015),* arXiv:1512.01197
47. **Gergely-Fülöp E**, Nagy N, Deák A: "Langmuir-Blodgett films of gold nanorods with different silica shell thicknesses", *Period Polytechn Chem Eng 59:(2) pp.104-110 Paper 7596 (2015)*
48. **Gergelyi D**, Földesy P, Zarándy Á: "Scalable, Low-Noise Architecture for Integrated Terahertz Imagers", *J Infrared Millimeter and Terahertz Waves 36:(6) pp.520-536 p.17 (2015)*
49. **Goroshko D**, Chusovitin E, Bezbabniy D, Dózsa L, Pécz B, Galkin N: "Formation and Thermoelectric Properties of $Si/CrSi_2/Si(001)$ Heterostructures with Stressed Chromium Disilicide Nanocrystallites", *Electronic Materials Letters 11:(3) pp.424-428 (2015)*
50. **Gubicza J**, Hegedűs Z, Lábár JL, Kauffmann A, Freudenberger J, Sarma VS: "Solute redistribution during annealing of a cold rolled Cu-Ag alloy", *J Alloys and Compounds 623: pp.96-103 (2015)*
51. **Gurbán S**, Kotis L, Pongrácz A, Sulyok A, Tóth AL, E Vázsonyi, Menyhárd M: "The chemical resistance of nano-sized SiC rich composite coating", *Surface and Coatings Technology 261: pp.195-200 (2015)*
52. **Gyulai J**: "Funkcionális anyagok - 2000 +15+...", In: Balázsi K, Barkóczy P, Bársony I, Czvikovszky T, Gyulai J, Hohol R, Janó V, Kaptay Gy, Kocsis-Baán M, Kónya I, Kuzsella L, Lendvai J, Szabó PJ, Tóth Lá, Verő B, Zsámbók D (Eds.), *Országos Anyagtudományi Konferenciasorozat 1997-2015, Jubileumi Kiadvány: Anyagtudomány, anyagvizsgálat, anyaginformatika, Balatonalmádi, Hungary, 20151011-13, Budapest: Magyar Anyagtudományi Egyesület, pp.116-123 (2015), (ISBN:978-963-12-3494-7)*
53. **Horváth R**, Gardener H, Ramsden J: "Apparent self-accelerating alternating assembly of semiconductor nanoparticles and polymers", *Appl Phys Lett 107:(4) Paper 041604 p.7 (2015)*
54. **Horváth ZJ**: "Transfer logic gates with electrical and optical inputs for large area electronics", *J Electrical Eng 66:(4) pp.235-237 (2015)*

55. **Horváth ZsJ**: "Logic gates and circuits with electrical and optical inputs for thin film and organic electronics", In: *J Vajda, I Jamnický (Eds.), Proc 21st Int Conference on Applied Physics of Condensed Matter: APCOM 2015, Strbske Pleso, Slovakia, 20150624-26, Bratislava: Slovenská Technická Univerzita v Bratislave, pp.295-298 (2005)*

56. **Jarvas G**, Szigeti M, Hajba L, Fürjes P, Guttman A: "Computational Fluid Dynamics-Based Design of a Microfabricated Cell Capture Device", *J Chromatographic Sci 53:(3) pp.411-416 p.6 (2015)*

57. **Juhász Z**, Fehér T, Bárány G, Zalán A, Németh E, Pádár Z, Pamjav H: "New clustering methods for population comparison on paternal lineages", *Molecular Genetics and Genomics 290:(2) pp.767-784 (2015)*, DOI:10.1007/s00438-014-0949-7

58. **Juhász Z**, Fehér T, Németh E, Pamjav H (2015): "mtDNA analysis of 174 Eurasian populations using a new iterative rank correlation method", *Molecular Genetics and Genomics: 291 (1) pp.493-509 (2015),* DOI:10.1007/s00438-015-1084-9

59. **Juhász, Z**: “A Search for Structural Similarities of Oral Musical Traditions in Eurasia and America Using the Self Organizing Cloud Algorithm”, *Journal of New Music Research: 44 (3) (2015)*

60. **Kárpáti T**, Pap AE, Gy Radnóczi, B Beke, Bársony I, Fürjes P: "Reliable aluminum contact formation by electrostatic bonding", *J Micromechanics and Microengineering 25:(7) Paper 075009 p.8 (2015)*

61. **Kiss ÁK**, Edgar F Rauch, Pécz B, Szívós J, Lábár JL: "A Tool for Local Thickness Determination and Grain Boundary Characterization by CTEM and HRTEM Techniques", *Microscopy and Microanalysis 21:(2) pp.422-435 (2015)*

62. **Klébert Sz**, Balázsi Cs, Balázsi K, Bódis E, Fazekas P, Keszler AM, Szépvölgyi J, Zoltán K: "Spark plasma sintering of graphene reinforced hydroxyapatite composites", *Ceramics International 41:(3 (Part A)) pp.3647-3652 (2015)*

63. **Klein A**, Szabó V, Kovacs M, Patkó D, Toth B, Vonderviszt F: "Xylan-Degrading Catalytic Flagellar Nanorods", *Molecular Biotechnology 57:(9) pp.814-819 (2015)*

64. **Kolonits T**, Jenei P, Tóth BG, Czigány Zs, Gubicza J, Bakonyi I, Péter L: "TEM Investigation of Grain and Defect Structure in Electrodeposited Nanocrystalline Nickel", In: Ágnes Kittel, Pécz B (Eds.), *12th Multinational Congress on Microscopy: MCM 2015, Eger, Hungary, 20150823-28, Budapest: Akadémiai Kiadó, pp.456-458 (2015)*

65. **Kovács A**, Duchamp M, Dunin-Borkowski RE, Yakimova R, Neumann PL, Behmenburg H Foltynski B, Giesen C, Heuken M, Pécz B: "Graphoepitaxy of High-Quality GaN Layers on Graphene/6H-SiC", *Advanced Materials Interfaces 2:(2) Paper 1400230 p.6 (2015)*

66. **Kovács A**, Pécz B, Duchamp M, Yakimova R, Neumann PL, Behmenburg H, Foltynski B, Giesen C, Heuken M, Dunin-Borkowski RE: "High Quality Gallium Nitride Heterostructures Grown on Graphene", In: *Ágnes Kittel, Pécz B (Eds.) 12th Multinational Congress on Microscopy: MCM 2015, Eger, Hungary, 20150823-28, Budapest: Akadémiai Kiadó, pp.146-148 (2015)*

67. **Kovács B**, Orgován N, Patkó D, Székács I, Tóth B, Vonderviszt F, Horváth R: "Genetikailag módosított protein rétegeken élő sejtek adhéziójának nyomon követése jelölésmentes optikai bioszenzorokkal", In: *45. Membrán-Transzport konferencia, Sümeg, Hungary, 20150519-22, Sümeg: pp.83-83 (2015)*

68. **Kovács B**, Orgován N, Patkó D, Székács I, Tóth B, Vonderviszt F, Horváth R: "The dynamics of living cell adhesion on nanostructured genetically engineered molecular layers revealed by label-free optical biosensors", In: *Richard Luxton (Eds.), 4th Int Conference on Bio-sensing Technology, Lisbon, Portugal, 20150510-13, Akadémiai Kiadó; Elsevier Science Publishers, 2015. p. online. p.1 (2015)*

69. **Kovács-Kis V**, T. Shumilova, Zs. Czigány, V. Masaitis: "HRTEM study of Popigai impact diamond: nanodiamond in amorphous carbon matrix", In: *Ágnes Kittel, Pécz B (Eds.), 12th Multinational Congress on Microscopy: MCM 2015, Eger, Hungary, 20150823-28, Budapest: Akadémiai Kiadó, pp.58-59 (2015)*

70. **Kozma P**, Janosov M, Petrik P: "Optikai bioérzékelés", *Magyar Tudomány 2015:(10) pp.1171-1179 (2015)*

71. **Kuball M**, Pomeroy JW, Calvo JA, Sun H, Simon RB, Francis D, Faili F, Twitchen D, Rossi S, Alomari M, Kohn E, Tóth L, Pécz B: "Novel thermal management of GaN electronics - diamond substrates", In: ASME (Eds.), *InterPACK/ICNMM 2015, San Francisco, USA, 20150706-09, San Francisco: American Socety of Mechanical Engineers (ASME), Paper 48145 p.5 (2015)*

72. **Kurucz I**, Péter B, Erdei A, Horváth R: "A novel, label-free technique to monitor the integrate cellular response of immunocompetent cells", *4th European Congress of Immunology (ECI) konferencia", poster (2015)*

73. **Kvashnin DG**, Vancsó P, Antipina LY, Márk GI, Biró LP, Sorokin PB, Chernozatonskii LA: "Bilayered semiconductor graphene nanostructures with periodically arranged hexagonal holes", *Nano Research 8:(4) pp.1250-1258 (2015)*

74. **Lábár JL**, Kovács-Kis V: "Short range order in amorphous and nanocrystalline material", In: Ágnes Kittel, Pécz B (Eds.), *12th Multinational Congress on Microscopy: MCM 2015, Eger, Hungary, 20150823-28, Budapest: Akadémiai Kiadó, pp.88-90 (2015)*

75. **Lázár I**, Szilagyi A, Sáfrán G, Szegedi A, Stichleutner S, Lázár K: "Iron oxyhydroxide aerogels and xerogels by controlled hydrolysis of $FeCl_3 \bullet 6H_2O$ in organic solvents: stages of formation", *RSC Advances 5:(89) pp.72716-72727 (2015)*

76. **Lohner T**, Serényi M, Petrik P: "Characterization of sputtered aluminum oxide films using spectroscopic ellipsometry", *Int J New Horizons in Physics 2:(1) pp.1-4 (2015)*

77. **Lugomer S**, Zolnai Zs, Tóth AL, Deák A, Nagy N: "Ar^+ ion irradiation-induced reorganization of colloidal silica nanoparticles in Langmuir-Blodgett monolayers", *Thin Solid Films 574: pp.136-145 (2015)*

78. **Magda GZ**, Pető J, Dobrik G, Hwang C, Biró LP, Tapasztó L: "Exfoliation of large-area transition metal chalcogenide single layers", *Scientific Reports 5: Paper 14714 p.5 (2015)*

79. **Márton G**, Kiss M, Orbán G, Pongrácz A, Ulbert I: "A polymer-based spiky microelectrode array for electrocorticography", *Microsystem Technologies 21:(3) pp.619-624 p.6 (2015)*

80. **Márton G**, Orbán G, Kiss M, Fiath R, Pongrácz A, : "A Multimodal, SU-8-Platinum - Polyimide Microelectrode Array for Chronic In Vivo Neurophysiology", *Plos One 10:(12) Paper e0145307 p.16 (2015)*

81. **Merkel DG**, Bessas D, Zolnai Zs, Rüffer R, Chumakov AI, Paddubrouskaya H, Van Haesendonck C, Nagy N, Tóth AL, Deák A: "Evolution of magnetism on a curved nano-surface", *Nanoscale 7:(30) pp.12878-12887 (2015)*

82. **Meysami SS**, Koós AA, Dillon F, Madhuri Dutta, Grobert N: "Aerosol-assisted chemical vapour deposition synthesis of multi-wall carbon nanotubes: III. Towards upscaling", *Carbon 88: pp.148-156 (2015)*

83. **Misják F**, Nagy KH, P J Szabó, Radnóczi Gy: "Effect of Mn Alloying on the Internal and Surface Structure of Cu Thin Films Designed for Interconnect Applications", In: *Dr T S Sudarshan, Prof Petri Vuoristo, Dr Heli Koivuluoto (Eds.), Surface Modification Technologies XXVIII, Tampere, Finnland, 20140616-18, Chennai: Valardocs, pp.627-634 (2015)*

84. **Molnár G**, Dózsa L, Erdélyi R, Vértesy Z, Osváth Z: "Morphological and electrical properties of self-assembled iron silicidenanoparticles on Si(001) and Si(111) substrates", *Appl Surf Sci 357: pp.573-582 p.10 (2015)*

85. **Nádor J**, Kalas B, Agócs E, Kozma P, Kőrösi L, Székács I, Fried M, Horváth R, Petrik P: "High-sensitivity in situ Kretschmann ellipsometry of protein adsorption and cellular adhesion on titania nanostructures", *4th International Conference on Bio-Sensing Technology, Lisbon, Portugal, 20150510-13, poster presentation (2015)*

86. **Nax HH**, Perc M, Szolnoki A, Helbing D: "Stability of cooperation under image scoring in group interactions", Scientific Reports 5: Paper 12145 p.7 (2015)

87. **Nemcsics Á**: "Quantum Dots Prepared by Droplet Epitaxial Method", in: *Stavrou VN (Eds.), Nanotechnology and Nanomaterials, Quantum Dots - Theory and Applications, Chapter 5, InTech Publ., pp.119-149 (2015), (ISBN:978-953-51-2155-8)*

88. **Németh K**, Balázsi K, Laczik B: "Egyenáramú magnetronos porlasztás fizikai folyamatainak modellezése matematikai módszerekkel", *Anyagok Világa 13:(1) pp.98-124 (2015)*

89. **Németh M**, Schay Z, Srankó D, Károlyi J, Sáfrán G, Sajó I, Horváth A: "Impregnated Ni/ZrO_2 and Pt/ZrO_2 catalysts in dry reforming of methane: Activity tests in excess methane and mechanistic studies with labeled 13CO2", *Appl Catal A-Gen 504: pp.608-620 (2015)*

90. **Neuróhr K**, Péter L, Pogány L, Rafaja D, Csik A, Vad K, Molnár G, Bakonyi I: "Influence of Ag additive to the spacer layer on the structure and giant magnetoresistance of electrodeposited Co/Cu multilayers", *J Electrochemical Society 162:(8) pp.D331-D340 (2015)*

91. **Ódor G**, Dickman R, Ódor Ge: "Griffiths phases and localization in hierarchical modular networks", *Scientific Reports 5: Paper 14451 p.16 (2015),* DOI:10.1038/srep14451

92. **Olah N**, Carta D, Kónya Z: "Vízből történő nehézfém eltávolítás szén nanocsövekkel és mezopórusos amorf szilícium-dioxiddal", *Anyagok Világa 12:(1) pp.41-57 (2015)*

93. **Oláh N**, Fogarassy Zs, Mónika Furkó, Balázsi Cs, Balázsi K: "Sputtered nanocrystalline ceramic TiC / amorphous C thin films as potential materials for medical applications", *Ceramics International 41:(4) pp.5863-5871 (2015)*

94. **Oláh N**, Veres M, Sulyok A, Fogarassy Zs, George Kaptay, Balázsi K: "Structural Characterization of TiC-Based Thin Films by TEM and HREM", In: *Ágnes Kittel, Pécz B (Eds.), 12th Multinational Congress on Microscopy: MCM 2015, Eger, Hungary, 20150823-28, Budapest: Akadémiai Kiadó, pp.148-150 (2015)*

95. **Orgován N**, Péter B, Bősze Sz, Ramsden JJ, Szabó B, Horváth R: "Label-Free Profiling of Cell Adhesion: Determination of the Dissociation Constant for Native Cell Membrane

Adhesion Receptor-Ligand Interaction", In: *Fang Y (Eds.), Label-Free Biosensor Methods in Drug Discovery, New York: Humana Press, pp.327-338 p.11 (2015)*

96. **Osváth Z**, Deák A, Kertész K, Molnár Gy, G Vértesy, Zámbó D, Hwang C, Biró LP: "The structure and properties of graphene on gold nanoparticles", *Nanoscale 7:(12) pp.5503-5509 (2015)*
97. **Otieno G**, Koós AA, Dillon F, Yahya NA, Dancer CEJ, Hughes GM, Grobert N, Todd RI: "Stiffness, strength and interwall sliding in aligned and continuous multi-walled carbon nanotube/glass composite microcantilevers", *Acta Materialia 100: pp.118-125 (2015)*
98. **Patkó D**, Kovács B, Gál G, Klein Á, Kurunczi S, Vonderviszt F, Horváth R: "Baktériumok jelölésmentes vizsgálata interferometrikus optikai bioszenzorral", *(2015)*
99. **Patkó D**: "Nagyérzékenységű jelölésmentes bioszenzorika: optikai, mikrofluidikai fejlesztések a fehérjék, baktériumok és extracelluláris vezikulák felületi kitapadásainak detektálásához", *Pannon Egyetem, Veszprém, 79p. (PhD) (2015)*
100. **Pécz B**, Tóth L, Tsiakatouras G, Adikimenakis A, Kovács A, Duchamp M, Dunin-Borkowski RE, Yakimova R, Neumann PL, Behmenburg H, Foltynski B, Giesen C, Heuken M, Georgakilas A: "GaN heterostructures with diamond and graphene", *Semiconductor Sci Techn 30:(11) Paper 114001 p.6 (2015)*
101. **Pécz B**: "Fiat lux. Legyen világosság! - mondta a Nobel-díj Bizottság", *Természet Világa 146:(2) pp.50-52 (2015)*
102. **Pécz B**: "Fiat Lux. Legyen világosság! - mondta a Nobel-díj Bizottság", *Természet Világa 146:(2. különszám) pp.18-20 (2015)*
103. **Perc M**, Szolnoki A: "A double-edged sword: Benefits and pitfalls of heterogeneous punishment in evolutionary inspection games", *Scientific Reports 5: Paper 11027 p.11 (2015)*
104. **Péter B**, Nádor J, Juhász K, Dobos Á, Körösi L, Székács I, Patkó D, Horváth R: "Incubator proof miniaturized Holomonitor to in situ monitor cancer cells exposed to green tea polyphenol and preosteoblast cells adhering on nanostructured titanate surfaces: validity of the measured parameters and their corrections", *J Biomedical Optics 20:(6) Paper 067002 p.10 (2015)*
105. **Péter B**, Székács I, Ungai-Salánki R, Orgován N, Bősze Sz, Horváth R: "Label-free investigations of the effect of green tea polyphenols on the dynamics of living cells", *4th International Conference on Bio-Sensing Technology (2015)*
106. **Péter B**, Székács I, Ungai-Salánki R, Orgován N, Bősze Sz, Horváth R: "EGCG élő sejtek adhéziós dinamikájára és mozgására gyakorolt hatásának vizsgálata jelölésmentes technikákkal", *pp.89-89, MBFT Konferencia 2015, poster (2015)*
107. **Péter B**, Székács I, Ungai-Salánki R, Orgován N, Bősze Sz, Horváth R: "Zöld tea polifenolok élő sejtek adhéziós dinamikájára gyakorolt hatásának jelölésmentes vizsgálata", In: *45. Membrán-Transzport konferencia, Sümeg, Hungary, 20150519-22, Sümeg: pp.98-98 p.1 (2015)*
108. **Petrik P**, Agócs E, Kalas B, Kozma P, Fodor B, Nador J, Major Cs, Fried M: "Multiple angle of incidence, spectroscopic, plasmon-enhanced, internal reflection ellipsometry for the characterization of solid-liquid interface processes", *Proc of SPIE - Int Soc Optical Eng 9529: Paper 95290W (2015)*

109. **Petrik P**, Fodor B, Agócs E, Kozma P, Nador J, Kumar N, Endres J, Juhász Gy, Major Cs, Pereira SF, Lohner T, Urbach HP, Bodermann B, Fried M: "Methods for optical modeling and cross-checking in ellipsometry and scatterometry", *Proc of SPIE - Int Soc Optical Eng 9526: Paper 95260S p.11 (2015)*

110. **Petrik P**, Kumar N, Fried M, Fodor B, Juhász Gy, Pereira SF, Burger S, Urbach HP: "Fourier ellipsometry - An ellipsometric approach to Fourier scatterometry", *J European Optical Society-Rapid Publications 10: Paper 15002 p.5 (2015)*

111. **Piszter G**, Kertész K, Bálint Zs, Biró LP: "Matematikai pontossággal látnak a lepkék", *Természet Világa 146:(3) pp.112-115 (2015)*

112. **Putz AM**, Horváth ZE, Gonter K, Almásy L: "One-pot synthesis and characterization of nano-size silver chloride", *Digest J Nanomaterials and Biostructures 10:(1) pp.89-94 (2015)*

113. **Radnóczi Gy**: "The Effect of a Second Component on Thin Film Structure Development", In: *T Minea (Eds.), Magnetron Ion Processes and Arc Technologies European Conference: MIATEC-2015, Paris, France, 20151208-11, Paris: Société Francaise du Vide, pp.80-83 p.3 (2015)*

114. **Radnóczi GyZ**, E Dodony, Battistig G, Vouroutzis N, Stoemenos J, Frangis N, A Kovács, Pécz B: "Electron microscopy study of Ni induced crystallization in amorphous Si thin films", In: *Stergios Logothetidis, Argirios Laskarakis, Christoforos Gravalidis (Eds.), Int Conf Exhib Nanotechnologies & Organic Electronics (Nanotexnology 2014): AIP Conference Proc, Thessaloniki, Greece, 20140705-12, Thessaloniki: AIP Publishing, pp.31-37 (2015)*

115. **Rajasekaran N**, Mani J, Tóth BG, Molnár G, Mohan S, Péter L, Bakonyi I: "Giant Magnetoresistance and Structure of Electrodeposited Co/Cu Multilayers: The Influence of Layer Thicknesses and Cu Deposition Potential", J E*lectrochemical Society 162:(6) pp.D204-D212 (2015)*

116. **Sáfrán G**, Szász N, Sáfrán E: "Two-In-one sample preparation for plan-VIew TEM", *Microscopy Research and Technique 78:(7) pp.599-602 (2015)*

117. **Sáfrán G**, Szívós J, Németh M, Horváth A: "Phase Mapping of Thin Mn-Al Layers by Combinatorial TEM", In: *Ágnes Kittel, Pécz B (Eds.), 12th Multinational Congress on Microscopy: MCM 2015, Eger, Hungary, 20150823-28, Budapest: Akadémiai Kiadó, pp.559-560 (2015)*

118. **Sipos P**, Choi C, Németh T, Zajzon N, Kovács-Kis V: "Mobility and speciation of potentially toxic metals in the total suspended particulate matter in Budapest, Hungary", In: *Fajciková K, Cvecková V, Zvarová I, Rapant S (Eds.), 31st SEGH 2015 Int Conf of the Society for Environmental Geochemistry and Health: Book of Abstracts, Bratislava, Slovakia, 20150622-26, Bratislava: State Geological Institute of Dionyz Stur, p.7. p.1 (2015)*

119. **Sipos P**, Kovács-Kis V, Németh T, Balázs R: "Direct observation of sorption capacity of individual soil mineral particles and their association", In: *Goldschmidt 2015 25th Anniversary Abstracts, Praha, Czech Republik, 20150816-21, p.2909. p.1 (2015)*

120. **Sipos P**, Németh T, Kovács-Kis V: "Complex mineralogical study of metal sorption onto soil mineral phases", In: *Fajcíková K, Cvecková V, Zvarová I, Rapant S (Eds.), 31st SEGH 2015 Int Conf of the Society for Environmental Geochemistry and Health: Book of*

Abstracts, Bratislava, Slovakia, 20150622-26, Bratislava: State Geological Institute of Dionyz Stur, p.62. p.1 (2015)

121. **Sophia PJ**, Attolini G, Bosi M, Buffagni E, Ferrari C, Frigeri C, Vad K, Csik A, Takáts V, Zolnai Zs, Arivuoli D: "Influence of surface roughness on interdiffusion processes in InGaP/Ge heteroepitaxial thin films", *ECS J Solid State Science and Technology 4:(3) pp.P53-P56 (2015)*
122. **Sun H**, Pomeroy JW, Anaya J, Simon RB, Francis D, Faili F, Twitchen D, Rossi S, Alomari M, Kohn E, Tóth L, Pécz B, Kuball M: "Diamond substrates for novel thermal management of GaN transistors", In: *De Beers Diamond Conference, Warwick, UK, 20150706-09, University of Warwick, Paper in press. p.1 (2015)*
123. **Süle P**, Kaptás D, Bujdosó L, Horváth ZE, Nakanishi A, Balogh J: "Chemical mixing at "al on Fe" and "fe on Al" interfaces", *J Appl Phys 118:(13) Paper 135305 (2015)*
124. **Süle P**, Szendrő M, G. Magda, C. Hwang, L. Tapasztó: "Nanomesh type graphene superlattice on Au(111) substrate", *Nano Letters 15:(12) pp.8295-8299 (2015)*
125. **Süle P**, Szendrő M: "Time-lapsed graphene moiré superlattice on Cu(111)", *Modelling and Simulation in Materials Science and Engineering 23:(2) Paper 025001 p.25 (2015)*
126. **Szabó B**, A Borbíró, Fürjes P: "Lab-on-a-chip rendszerek a betegágy melletti diagnosztikában", *Orvosi Hetilap 156:(52) pp.2096-2102 (2015)*
127. **Szabó G**, Bodó KS, Allen B, Nowak MA: "Four classes of interactions for evolutionary games", *Phys Rev E Stat Nonlin 92:(2) Paper 022820 p.9 (2015)*
128. **Szabó G**, Szolnoki A: "Congestion phenomena caused by matching pennies in evolutionary games", *Phys Rev E Stat Nonlin 91:(3) Paper 032110 p.6 (2015)*
129. **Székács I**, Patkó D, Horváth R, Székács András: " Jelölésmentes holografikus mikroszkópia alkalmazása sejttoxicitás-vizsgálatokban ", *A Magyar Biofizikai Társaság XXV. Kongresszusa, 20150825-28, Budapest, poster presentation (2015)*
130. **Székács I**, Patkó D, Horváth R, Székács András: "Holografikus mikroszkópia alkalmazása sejttoxicitás-vizsgálatokban", In: *45. Membrán-Transzport konferencia, Sümeg, Hungary, 20150519-22, Sümeg: pp.107-107 (2015)*
131. **Székács I**: "Optical Waveguide Light-Mode Spectroscopy for Ion Channel Profiling: OWLS Sensor for Ion Channel Profi ling", In: *Fang Y (Eds.), Label-Free Biosensor Methods in Drug Discovery., New York: Humana Press, pp.155-165 (2015)*
132. **Szilágyi E**, Bányász I, Kótai E, Németh A, Major Cs, Fried M, Battistig G: "Determination of migration of ion-implanted Ar and Zn in silica by backscattering spectrometry", *Radiation Effects and Defects in Solids 170:(3) pp.229-237 (2015)*
133. **Szívós J**, M Serényi, Gergely-Fülöp E, Sáfrán G: "Fabrication of Nanopatterns in a-AlOx Thin Films by a Single Laser Pulse", In: *Berecz T, Májlinger K, Orbulov IN, Szabó PJ (Eds.), Materials Science, Testing and Informatics VII : Selected, peer reviewed papers from the 9th Hungarian Conference on Materials Science, 20131013-15, Balatonkenese, Hungary, Balatonkenese, Hungary, 201310-13-15, Zürich: Trans Tech Publications, pp.259-264, Materials Science Forum, 812 (2015)*
134. **Szívós J**, Serényi M, Gergely-Fülöp E, Lohner T, Sáfrán G: "UV Laser Nanopatterning of Pt Thin Films", In: *Ágnes Kittel, Pécz B (Eds.), 12th Multinational Congress on Microscopy: MCM 2015, Eger, Hungary, 20150823-28, Budapest: Akadémiai Kiadó, pp.478-479 (2015)*

135. **Szolnoki A**, Chen X: "Benefits of tolerance in public goods games", *Phys Rev E Stat Nonlin 92:(4) Paper 042813 p.9 (2015)*
136. **Szolnoki A**, Perc M: "Antisocial pool rewarding does not deter public cooperation", *Proc Royal Society B-Biological Sciences 282:(1816) Paper 20151975 p.8 (2015)*
137. **Szolnoki A**, Perc M: "Conformity enhances network reciprocity in evolutionary social dilemmas", *J R Soc Interface 12:(103) Paper 20141299 p.8 (2015)*
138. **Szolnoki A**, Perc M: "Reentrant phase transitions and defensive alliances in social dilemmas with informed strategies", *Europhys Letters 110:(3) Paper 38003 p.6 (2015),* DOI:10.1209/0295-5075/110/38003
139. **Szolnoki A**, Perc M: "Vortices determine the dynamics of biodiversity in cyclical interactions with protection spillovers", *New J Physics 16: Paper 113033 p.11 (2015)*
140. **Takács E**, Székács I, Madarász E, Darvas B, Horváth R, Székács A: "Glyphosate hatóanyagú növényvédő szer in vitro toxicitása emlőssejtvonalakon", *VIII. Magyar Sejtanalitikai Konferencia, 20150528-30, Budapest, poster presentation (2015)*
141. **Takács M**, Dücső Cs, Pap AE: "Fine-tuning of gas sensitivity by modification of nano-crystalline WO_3 layer morphology", *Sensors Actuators B Chemical 221: pp.281-289 Paper 18658 p.9 (2015)*
142. **Takács M**, Zámbó D, Deák A, Pap AE, Bársony I: "Gas sensitivity enhancement of WO_3 nano-rods by gold nanoparticles", *Procedia Eng 120: pp.1128-1131 (2015)*
143. **Talkenberg F**, Illhardt S, Radnóczi GyZ, Pécz B, Schmidl G, Schleusener A, Dikhanbayev K, Mussabek G, Gudovskikh A, Sivakov V: "Atomic layer deposition precursor step repetition and surface plasma pretreatment influence on semiconductor-insulator-semiconductor heterojunction solar cell", *J Vacuum Science and Technology A-Vacuum Surfaces and Films 33:(4) Paper 041101 p.10 (2015)*
144. **Tapasztó O**, Tapasztó L, Balázsi Cs, Puchy V, Dusza J, Horváth ZE, Balázsi K: "Orientation of Graphene Nanoplatelets in Silicon Nitride Nanocomposites", In: *Ágnes Kittel, Pécz B (Eds.), 12th Multinational Congress on Microscopy: MCM 2015, Eger, Hungary, 20150823-28, Budapest: Akadémiai Kiadó, pp.539-540 (2015)*
145. **Tian Q**, Takács E, Krakovsky I, Horváth ZE, Rosta L, Almásy L: "Study on the Microstructure of Polyester Polyurethane Irradiated in Air and Water", *PolymerS 7: pp.1755-1766 (2015)*
146. **Tomás I**, Kovárík O, Kadlecová J, Vértesy G: "Optimization of fatigue damage indication in ferromagnetic low carbon steel", *Measurement Science & Technology 26:(9) Paper 095603 (2015)*
147. **Tóth EL**, Holczer EG, Kristóf I, Fürjes P: "Optimized Simulation and Validation of Particle Advection in Asymmetric Staggered Herringbone Type Micromixers", *Micromachines 6:(1) pp.136-150 (2015)*
148. **Tóth L**, Pécz B, Rossi S, Alomari M, Kohn E, Anaya J, Kuball M: "TEM Study of Nanocrystalline Diamond Films", In: *Ágnes Kittel, Pécz B (Eds.), 12th Multinational Congress on Microscopy: MCM 2015, Eger, Hungary, 20150823-28, Budapest: Akadémiai Kiadó, pp.562-564 (2015)*
149. **Ungai-Salánki R**, Gerecsei T, Fürjes P, Orgován N, Sándor N, Eszter Holczer, Horváth R, Szabó B: "Automated single cell isolation from suspension with computer vision", *VIII. Magyar Sejtanalitikai Konferencia, poster (2015)*

150. **Ungai-Salánki R**, Gerecsei T, Hős Cs, Orgován N, Sándor N, Bajtay Zs, Erdei A, Horváth R, Szabó B: "Egyedi sejtek automatizált válogatása és manipulálása mikroszkópon", *Microtrade Tudományos Szimpózium 2015, Budapest, MTA-TTK, oral presentation (2015)*

151. **Ungai-Salánki R**, Hős Cs, Orgován N, Sándor N, Bajtay Zs, Erdei A, Horváth R, Szabó B: "Egyedi sejtek adhéziós vizsgálata számítógép- vezérelt mikropipettával", *pp.25-25, A Magyar Biofizikai Társaság XXV. kongresszusa, oral presentation (2015)*

152. **Ungai-Salánki R**, Sándor N, Horváth R, Szabó B: "High-throughput image based single cell isolation", *Microscopy and Analysis 2015:(16) pp.10-13 p.6 (2015)*

153. **Ungai-Salánki R**, Szabó I, Orgován N, Székács I, Szabó B, Bősze Sz, Horváth R: "Effect of FNIII14 and C8 peptides on tumor cell adhesion: studied by a high-throughput label-free optical biosensor", *4th International Conference on Bio-Sensing Technology, poster (2015),*

154. **Vancsó P**: "Töltésterjedés grafén nanorendszerekben", *ELTE, Budapest, 117p. (PhD) (2015),* DOI:10.15476/ELTE.2015.136

155. **Vértesy G**, Uchimoto T, Takagi T, Tomás I, Kage H: "Nondestructive characterization of flake graphite cast iron by magnetic adaptive testing", *NDT & E International 74: pp.8-14 (2015)*

156. **Vértesy G**, Uchimoto T, Takagi T, Tomás I: "Correlation between ultrasonic velocity and magnetic adaptive testing in flake graphite cast iron", *J Electrical Eng 66: pp.174-177 (2015)*

157. **Vukov J**, Varga L, Allen B, Nowak MA, Szabó Gy: "Payoff components and their effects in a spatial three-strategy evolutionary social dilemma", *Phys Rev E Stat Nonlin 92:(1) Paper 012813 p.9 (2015)*

158. **Wang Z**, Wang L, Szolnoki A, Perc M: "Evolutionary games on multilayer networks: a colloquium", *European Physical Journal B 88:(5) Paper 124 p.15 (2015)*

159. **Watanabe K**, Nagata T, Wakayama Y, Sekiguchi T, Erdélyi R, Volk J: "Band-Gap Deformation Potential and Elasticity Limit of Semiconductor Free-Standing Nanorods Characterized in Situ by Scanning Electron Microscope-Cathodoluminescence Nanospectroscopy", *ACS Nano 9:(3) pp.2989-3001 p.13 (2015)*

160. **Zámbó D**, Radnóczi GyZ, Deák A: "Preparation of compact nanoparticle clusters from polyethylene glycol-coated gold nanoparticles by fine-tuning colloidal interactions", *Langmuir 31:(9) pp.2662-2668 (2015)*

161. **Zolnai Zs**, Toporkov M, Volk J, Demchenko DO, Okur S, Szabó Z, Özgür Ü, Morkoc H, Avrutin V, Kótai E: "Nondestructive atomic compositional analysis of BeMgZnO quaternary alloys using ion beam analytical techniques", *Appl Surf Sci 327: pp.43-50 (2015)*